

HEAT STRESS AND ISCHEMIA/REPERFUSION CAUSE OXIDATIVE STRESS
VIA NADPH OXIDASE IN HYPOTHALAMIC NEURONS

Except where reference is made to the work of others, the work described in this dissertation is my own or was done in collaboration with my advisory committee. This dissertation does not include proprietary or classified information.

Colin Brian Rogers

Certificate of Approval:

Elaine S. Coleman
Associate Professor
Anatomy, Physiology and
Pharmacology

Dean D. Schwartz, Chair
Associate Professor
Anatomy, Physiology and
Pharmacology

Holly R. Ellis
Associate Professor
Chemistry and Biochemistry

Robert J. Kemppainen
Professor
Anatomy, Physiology and
Pharmacology

George T. Flowers
Dean
Graduate School

HEAT STRESS AND ISCHEMIA/REPERFUSION CAUSE OXIDATIVE STRESS
VIA NADPH OXIDASE IN HYPOTHALAMIC NEURONS

Colin Brian Rogers

A Dissertation
Submitted to
the Graduate Faculty of
Auburn University
in Partial Fulfillment of the
Requirement for the
Degree of
Doctor of Philosophy.

Auburn, Alabama
May 9th, 2009

HEAT STRESS AND ISCHEMIA/REPERFUSION CAUSE OXIDATIVE STRESS
VIA NADPH OXIDASE IN HYPOTHALAMIC NEURONS

Colin Brian Rogers

Permission is granted to Auburn University to make copies of this dissertation, upon request of individuals or institutions at their expense. The author reserves all publication rights.

Signature of Author

Date of graduation

VITA

Colin Brian Rogers, son of Brian Arnott Rogers and Janice Elaine Rogers, was born April 20th, 1980 in Mount Airy, Maryland. He graduated from South Carroll High School with honors in 1998. He attended Auburn University in Auburn, Alabama for four years and graduated with a Bachelor of Science in Molecular Biology in December, 2002. In the spring of 2003, he began working as a research assistant II in the Department of Anatomy, Physiology and Pharmacology, Auburn University under Dr. Dean Schwartz. In fall 2004 he joined the Department of Anatomy, Physiology and Pharmacology in the College of Veterinary Medicine as a graduate teaching assistant under the guidance of his mentor, Dr. Dean Schwartz. In fall of 2006 he was elected vice-president of the College of Veterinary Medicine Graduate Student Club.

DISSERTATION ABSTRACT
HEAT STRESS AND ISCHEMIA/REPERFUSION CAUSE OXIDATIVE STRESS
VIA NADPH OXIDASE IN HYPOTHALAMIC NEURONS

Colin Brian Rogers

Doctor of Philosophy, May 9th, 2009
(B.S., Auburn University, Auburn, AL, 2002)

191 Typed Pages

Directed by Dean D. Schwartz

Ischemia/reperfusion-related injuries are associated with a wide range of diverse disorders including but not limited to aging, heat stroke, diabetes and Alzheimer's disease. Ischemia/reperfusion is known to cause oxidative stress through the generation of reactive oxygen species (ROS) and the resulting oxidative stress is thought to be a contributing factor in the progression of these neurological disorders [345]. In addition to ischemia/reperfusion injury, oxidative stress has also been reported to occur in response to heat stress in the brain and is thought to be one of the main contributors to the progression of heat-related illnesses [353]. In the present study, we examined whether simulated ischemia/reperfusion and mild heat stress increases ROS generation through similar mechanisms in cultured hypothalamic cells. Hypothalamus IVB cells were grown

under normal culture conditions and either heat stressed at 43°C for 15 minutes followed by 15 minutes recovery or exposed to simulated ischemia/reperfusion by incubation for 1 hour in ischemic media in the absence of oxygen followed by 2 hours incubation in normal oxygenated media (reperfusion). Heat stress caused a significant increase in HSP70 and HO-1 gene expression as measured by real time RT-PCR. Heat stress also caused an increase in cytoplasmic HO-1 protein expression and nuclear translocation of HSF-1 as measured by western blot. Heat stress and simulated ischemia/reperfusion also increased ROS generation as measured by the fluorescent indicator carboxy-H₂DCFDA. The increase in ROS was attenuated by pretreatment with the NOX inhibitor apocynin and the PKC inhibitors Gö6976 and Ro-31-8220. To further investigate the generation of ROS, we measured NOX activity using chemiluminescence. Similar to what was seen with ROS generation, both mild heat stress and simulated ischemia/reperfusion increased NOX activity and these effects were blocked by apocynin, DPI, Gö6976, Ro-31-8220 and calphostin C. Furthermore, using RT-PCR and western blot analysis, NOX4 and PKC α were found to be expressed in IVB cells. These results suggest that both heat stress and simulated ischemia/reperfusion cause oxidative stress through PKC α -mediated NOX4 activation in hypothalamic IVB cells.

ACKNOWLEDGEMENTS

I would like to express my gratitude to those in Auburn University's College of Veterinary Medicine, its Dean Dr. Timothy Boosinger, the Associate Dean of research Dr. Carl Pinkert, as well as those in the Department of Anatomy, Physiology and Pharmacology and its Department Head Dr. Edward Morrison for the opportunity to attend graduate school at Auburn University. I express my deepest appreciation for my mentor and major advisor, Dr. Dean Schwartz, for his support and guidance. Without him, none of this would have been possible. I would also like to thank the members of my committee, Dr. Robert J. Kemppainen, Dr. Elaine S. Coleman, and Dr. Holly Ellis for all their help planning and executing this project. For their assistance in the laboratory and friendship during this work, I would like to thank Dr. Heather Edwards, Dr. Pete Christopherson, Dr. Eric Plaisance, Dr. Deepa Bedi, Dr. Naglaa El-Orabi, Zhechuan Fan, Sudhir Ahluwalia, Kathy O'Donnell and Barbara Steele. I would also like to thank Dr. Jim Sartin, Dr. Ya-Xiong Tao, Dr. Tim Braden, Dr. Robert Judd, Dr. Barbara Kemppainen, Dr. Larry Myers, Debbie Allgood, Hattie Alvis, Diane Smith, Dorothy Spain, Kathy O'Donnell, Barbara Steele and Mary Lloyd for all their help and support. I would also like to express my appreciation to my family, my mother Janice Rogers, my father Brian Rogers, my second mom Pat Schmidt and her husband Roland Schmidt, my late grandmother Eula Rogers, my late grandfather Sydney Rogers, my stepmother Ellen Sue Brockett and my stepbrothers Ben and Alex Lyon for all their love and support.

Style manual or journal used: Brain Research

Computer software used: Microsoft Word, Endnote, Microsoft Excel, SAS,
and Adobe Photoshop.

TABLE OF CONTENTS

LIST OF TABLES.....	x
LIST OF FIGURES.....	xi
INTRODUCTION.....	1
LITERATURE REVIEW.....	10
MATERIALS.....	54
METHODS.....	57
RESULTS.....	88
DISCUSSION.....	131
CONCLUSION.....	147
REFERENCES.....	148
APPENDICES.....	175

LIST OF TABLES

Table 1. Hypothalamic hormones and their biological functions.....	41
Table 2. Gene Specific Primers for PCR.....	64
Table 3. PKC Inhibitors.....	72

LIST OF FIGURES

Figure 1. Proposed Structures of Activated NOX Isoforms.....	17
Figure 2. RNA Integrity Gel.....	61
Figure 3. Effect of heat stress on the expression of HSP70 and HO-1.....	89
Figure 4. Effect of heat stress on HO-1 protein levels.....	91
Figure 5. Effect of heat stress on HSF-1 protein levels in the cytoplasm and nucleus....	93
Figure 6. ROS generation in response to heat stress in IVB cells.....	95
Figure 7. ROS generation in response to I/R in IVB cells.....	97
Figure 8. Apocynin inhibits heat-induced oxidative stress in IVB cells.....	99
Figure 9. Apocynin inhibits I/R-induced oxidative stress in IVB cells.....	101
Figure 10. NOX activity in response to heat stress in IVB cells.....	103
Figure 11. NOX activity in response to I/R in IVB cells.....	105
Figure 12. PCR analysis for NOX in control IVB cells and rat heart.....	108
Figure 13. Western blots for NOX2 and NOX4 in IVB cells and rat brain.....	109
Figure 14. Effect of the PKC inhibitors on heat-induced ROS generation.....	111
Figure 15. Effect of the PKC inhibitors on I/R-induced ROS generation.....	113
Figure 16. Effect of PKC inhibitors on heat-induced NOX activity.....	116
Figure 17. Effect of PKC inhibitors on I/R-induced NOX activity.....	120
Figure 18. Effect of PKC and PI3-kinase inhibitors on NOX activity.....	124
Figure 19. NOX activity in response to PMA in IVB cells.....	127

Figure 20. PKC μ , PKC α , PKC β , PKC δ , PKC ϵ and PKC ζ mRNA expression.....129

Figure 21. Western blot for PKC α , PKC δ , PKC ϵ , PKC γ , PKC ζ and PKC μ130

INTRODUCTION

Stroke is one of the leading causes of morbidity and mortality in the United States and throughout the world [272]. Stroke is commonly characterized as cerebral ischemia caused by a loss of blood flow to the brain due to arterial blockage or associated with cardiac arrest [48]. Risk factors associated with stroke include hypercholesterolemia [11], hypertension [17], hyperhomocysteinemia [34], sedentary life-styles and smoking [272]. Cerebral ischemia is defined as regional tissue hypoxia which becomes aggravated by the bolus return of oxygenated blood following removal of blockage or return of cardiac function, which is referred to as reperfusion injury [6]. Reperfusion injury is also associated with surges of intracellular calcium, free radicals, excitatory amino acids and eicosanoids, leading to ATP depletion, neural apoptosis and microvascular inflammation [55,288]. Recently, oxidative stress has also been reported to be a contributing factor to cell injury following ischemia and reperfusion [6]. Oxidative stress is a general term used to describe the level of oxidant damage in a cell or tissue caused by the generation of reactive oxygen species (ROS) [196]. It has become widely recognized that oxidative stress contributes to the pathology of a number of neurological disorders and is involved in the injury observed following ischemia and reperfusion [345].

In addition to ischemia/reperfusion injury, oxidative stress has also been reported to occur in response to heat stress in the brain and is thought to be one of the main contributors to the progression of heat-related illnesses [353]. Hyperthermia has received considerable attention of late due to increasing incidence of heat-related illnesses involving athletes, the elderly, and soldiers exposed to hot environments and severe heat waves [337]. Increased environmental temperatures are a major problem when accompanied by physical activity and/or dehydration because of the potential for the development of heat stroke [289]. Heat stroke occurs when brain temperatures exceed 105-106°F. At these temperatures the ability of the hypothalamus to coordinate thermoregulation throughout the body is compromised [290]. The decreased ability of the hypothalamus to regulate body temperature can cause greater increases in brain temperature, increases in intracerebral pressure, overall decreases in blood pressure and ultimately multi-organ dysfunction [290]. Even mild hyperthermia that does not result in heat stroke has been reported to cause long term neurological defects including memory loss, personality disorders, and dementia caused by brain lesions [267]. Current treatments for heat-related illnesses are limited and mainly focus on removing the individual from the hot environment and cooling the individual's core body temperature [53]. A better understanding of the mechanisms involved in the generation of ROS associated with heat stress can potentially lead to more effective therapeutic strategies targeted at minimizing heat-related brain injury.

Heat stress and ischemia/reperfusion cause oxidative stress through the generation and accumulation of ROS, which can damage proteins, lipids, molecular machinery and DNA [72,152,197,198,203,275,352,360]. The exact mechanisms of ROS generation are

unclear, but both intra- and extracellular ROS increase with mild heat stress and ischemia/reperfusion [230,345]. Several enzymes have been reported to contribute to the production of ROS in response to various stressors. Cyclooxygenase (COX) and lipoxygenase (LOX) are key ROS-generating enzymes that convert arachidonic acid into either prostaglandins or leukotrienes, respectively, and are involved in the inflammatory and pain responses associated with oxidative stress [322]. Nitric oxide synthase (NOS) catalyzes the conversion of L-arginine and oxygen into citrulline and nitric oxide (NO) [236]. NO can interact with superoxide to produce the highly reactive compound peroxynitrite. To date, three subtypes of NOS have been described. The inducible form of NOS (iNOS) is thought to be involved in inflammation [209]. Endothelial NOS (eNOS) is constitutively expressed and NO production in endothelial cells is involved in vascular tone and platelet aggregation [204]. Neuronal NOS (nNOS) is expressed in nerves and various other cell types and produces NO that is reported to play a role in neurotransmission [201,363]. Lastly, the enzyme xanthine oxidase catalyzes the conversion of hypoxanthine and xanthine to uric acid and generates hydrogen peroxide as a by-product [233]. Xanthine oxidase has been shown to play a role in vascular injury associated with ischemia, inflammatory diseases and chronic heart failure [238]. The role of these enzymes in both ischemia/reperfusion and heat stress induced oxidative stress in the brain is not yet fully understood, but it appears these enzymes are mainly involved in inflammation-mediated cerebrovascular damage associated with ischemia/reperfusion and heat stroke.

The major source of non-enzymatic ROS generation in aerobic cells comes from mitochondrial sources. Cellular respiration occurs through a process called oxidative

phosphorylation in the mitochondria allowing for the generation of energy, in the form of adenosine triphosphate (ATP), via the electron transport chain (ETC) [253]. The ETC transfers electrons through a series of specialized enzyme complexes generating a proton gradient that drives the synthesis of ATP via ATP synthase [194]. Under normal conditions, 1-2% of all oxygen consumed during respiration undergoes single electron reduction by leakage of electrons from quinone pools to form the superoxide radical [237]. Mitochondrial superoxide dismutase (SOD) subsequently converts superoxide into oxygen and hydrogen peroxide which are then converted to water and oxygen by catalase and/or glutathione peroxidase. However, under stress conditions, the number of electrons leaking out of the ETC is enhanced leading to an accumulation of superoxide in the mitochondria and ultimately, mitochondrial dysfunction [187]. Indeed, alterations in mitochondrial function have been reported to be involved in diverse pathological oxidative stress states such as aging and neurodegeneration [99,237]. These increases in ROS are responsible for progressive deterioration of cell structures and continuous damage to mitochondrial DNA over time [99,237].

The current study focuses on yet another ROS generating system. NADPH oxidase (NOX) is a major source of ROS in mammalian cells and was originally identified in neutrophils [92]. NOX is a membrane bound, multisubunit enzyme that transports electrons across biological membranes to molecular oxygen to catalyze the formation of superoxide [346]. Studies suggest NOX-derived ROS may play especially important roles in ROS-sensitive signal transduction cascades, including those critically important for cell proliferation, differentiation, apoptosis and even necrosis because of their rapid generation and degradation [162,317]. NOX has also been suggested to

contribute to ischemia/reperfusion injury associated with lung disease [251], liver injury [193], hypertension [57] and atherosclerosis [58].

To date, little is known about the effects of heat stress on NOX activation and signaling. Studies using the NOX inhibitors apocynin and diphenylene iodonium, suggest NOX is involved in ROS generation in response to heat exposure in neutrophils [202], fibroblasts [60] cardiomyocytes [61] and neuronal cells [68]. Heat-exposure to aged rats has been reported to produce increased levels of ROS in the liver and intestinal epithelial cells that possibly contributes to cellular dysfunction and age-related reductions in heat tolerance [89,152,360]. Although the source(s) of ROS generation was not directly assessed in this study, the authors suggested that mitochondria or a ROS-generating enzyme such as NOX was responsible for the heat-induced ROS generation. Recently, heat shock-induced ROS generated from NOX was reported to cause an increase in the expression of matrix metalloproteinases (MMPs) via the mitogen activated protein kinase (MAPK) pathway in skin cells [286]. MMPs are enzymes involved in the proteolysis of extracellular matrix proteins and are suggested to play a role in the development of skin aging exposed to ionizing radiation [59]. In prostate tumor cells exposed to heat, a NOX-induced increase in ROS generation was found to increase the expression of p-glycoprotein and hypoxia inducible factor-1 (HIF-1 α) through the p38 MAPK pathway, which is involved in protection from apoptosis [286,332]. These investigations suggest that heat-induced NOX activation and the resulting ROS generation may act as a key signaling event involved in initiating protective mechanisms against potentially lethal heat exposure.

In the brain, NOX has been identified as the source of ROS generation in response to lipopolysaccharide (LPS)-induced fever in rats [262]. Treatment with the NOX inhibitor, apocynin, protected against the LPS-induced neuron injury associated with neurovascular inflammation [183]. ROS generated from NOX are also found to increase permeability and damage of the blood brain barrier that occur following a stroke [147]. A major role of NOX-derived ROS in cerebral vasculature is attributed to structural and functional changes associated with ROS accumulation that can lead to neuronal damage [65]. In the hippocampus, NOX-derived superoxide is thought to play a role in regulating memory and emotion by controlling synaptic transmission [162]. However, increased accumulation of NOX-derived ROS following cerebral ischemia/reperfusion is an important underlying cause for neuronal injury leading to delayed neuronal death (DND) [330]. Studies performed using the NOX inhibitor apocynin, were reported to protect neurons against global cerebral ischemia/reperfusion-induced oxidative stress injury in the hippocampus [330]. Abramov *et al.* report that in rat hippocampi and cortices exposed to hypoxia, ROS accumulation was attributed to the mitochondria and the ROS-generating enzyme xanthine oxidase, but upon reperfusion in the rat, NOX appeared to be the main source of ROS generation [6]. This suggests a biphasic generation of ROS during ischemia/reperfusion in the brain involving multiple sources.

The activation of NOX has been reported to involve the signaling molecule protein kinase C (PKC), which phosphorylates the p47^{phox} subunit and other subunits of NOX, thereby activating the enzyme [334]. PKC, a family of serine/threonine kinases, is an important enzyme that mediates a wide range of signal transduction processes, such as

differentiation and proliferation [111,341]. The PKC family of enzymes is divided into three groups. The calcium/phospholipid-dependent or conventional PKCs, including PKC α , PKC β and PKC γ ; the calcium-independent or novel PKCs, including PKC δ , PKC ϵ , PKC μ , PKC η and PKC θ ; and the calcium and phospholipid-independent or atypical PKCs, including PKC ζ and PKC λ . It has been reported that the PKC isoforms α , β , δ , ϵ , γ and ζ are expressed in the brain, but the role of each PKC isoform remains to be elucidated [118]. Studies using the PKC δ inhibitor, rottlerin, prevented the increase of ROS generated by NOX in neuronal cells exposed to advanced glycation end (AGE) products associated with a number of neurodegenerative diseases [228]. In the spinal cord, use of the PKC inhibitor, staurosporine, prevented ischemic neuronal injury [199]. In the brain, contrasting reports on the effects of ischemia/reperfusion on PKC activity suggest site-specific and PKC isoform-specific modulation of PKC activity in response to ischemia/reperfusion [46,47,118,164,338]. A role for PKC in activating NOX in the brain has also been shown in response to ganglioside treatment in microglial cells and exposure to zinc in neurons and astrocytes [215,230]. Although studies on the effects of heat stress on PKC activation in the brain are limited [131], heat stress has been shown to activate PKC in the heart [146], Jurkat cells [344], and various other cells in the body [128]. These studies suggest a role for PKC in NOX activation in the brain, which appears to occur in response to a variety of conditions including ischemia/reperfusion and heat stress.

Another group of enzymes that has been shown to play a role in activating NOX by phosphorylating the p47^{phox} subunit and potentially other subunits of NOX are the phosphatidylinositol-3 kinase (PI3 kinase) enzymes [91,350]. PI3 kinase catalyzes the

conversion of phosphatidylinositol 4,5-bisphosphate (PIP₂) to PIP₃, which is involved in the recruitment and activation of the phox homology domains of the NOX subunits [91]. However, the exact mechanism by which PI3 kinase regulates NOX activation other than p47^{phox} phosphorylation in intact cells is still unknown. In the heart, PI3 kinase has been shown to play a role in cardiac protection by initiating the Akt pathway, or cell survival pathway, in response to ischemia/reperfusion [44]. In the brain, PI3 kinase-mediated NOX activation has been shown to occur in response to growth factors and augments neurite differentiation [137,245]. Both heat stress and ischemia/reperfusion have been shown to activate PI3 kinase, yet the link between PI3 kinase activation and NOX activation leading to an increase in ROS accumulation has not been examined [82,333].

As mentioned previously, oxidative stress is a major contributing factor to both ischemia/reperfusion injury and the progression of heat-related illnesses, but the source(s) and mechanisms of ROS generation have not been identified in the brain. More specifically in the hypothalamus, which is a critical region of the brain involved in temperature regulation, hormonal stress response, neurotransmission and homeostasis [19,120,314], the mechanisms of oxidative stress are not yet known. The crucial role of the hypothalamus in regulating the body's ability to respond and adapt to stressful stimuli make it a good candidate for investigating the cellular effects of ischemia/reperfusion and heat stress on NOX activation and signaling. The hypothalamus has been reported to express the gp91^{phox} (NOX2) [149] and p47^{phox} [45] subunits of NOX, as well as NOX1 and NOX3 [67]. One issue that may cause some discrepancies among investigators characterizing NOX expression in the hypothalamus is the fact that the cell populations in the histological sections used in these studies contain not only neurons, but astrocytes and

endothelial cells as well. This could cause invalid characterization of NOX expression levels in hypothalamic tissue sections. To avoid this issue, we utilized a hypothalamic neuronal cell line to investigate NOX expression and activation in this study [150]. Thus, the hypothesis that was tested in this study was that heat stress and ischemia/reperfusion share a common signaling pathway to increase ROS generation via NOX in a hypothalamic neuronal cell line.

LITERATURE REVIEW

Oxidative stress is a general term used to describe the level of oxidant damage in a cell or tissue caused by the generation of reactive oxygen species (ROS). It is widely accepted that oxidative stress contributes to the pathogenesis of numerous disease states including stroke [326], ischemia/reperfusion injury [127], heat-related illnesses [129], atherosclerosis [121], cardiovascular diseases [124], hypertension [356], diabetes mellitus [223], neurodegeneration [246] and aging [50]. Many of these diseases are also associated with impaired antioxidant activity and impaired energy metabolism which further leads to oxidative stress [113]. The implication of oxidative stress as a major component of a multitude of diseases, presents the need to understand the mechanisms by which oxidative stress occurs. Currently, the mechanisms by which oxidative stress occurs is not yet fully understood. A major focus of studying oxidative stress involves exploring the ROS-generating enzymes that produce ROS as by-products of their enzymatic activity. These enzymes include, but are not limited to cyclooxygenase (COX) [322], lipoxygenase (LOX) [322], xanthine oxidase (XO) [233], nitric oxide synthase [209] and NADPH oxidase (NOX) [5]. The ROS produced by these enzymes can overwhelm the cell's endogenous antioxidant system leading to oxidative stress.

ROS are small oxygen-derived molecules including oxygen radicals such as superoxide (O_2^-), hydroxyl (OH), and peroxy (RO_2), and non-radicals such as hydrogen

peroxide (H_2O_2). ROS generation is generally caused by a cascade of reactions that begins with the production of the oxygen radical superoxide [278]. Superoxide rapidly dismutates to hydrogen peroxide either spontaneously or by the antioxidant enzyme, superoxide dismutase (SOD). Hydrogen peroxide can then be converted into water and oxygen by two other antioxidant enzymes, catalase and/or glutathione peroxidase. Other elements in the cascade of ROS generation include the reaction of superoxide with nitric oxide to form peroxynitrite and the iron-catalyzed Fenton reaction which leads to the formation of the hydroxyl radical. When ROS production exceeds the antioxidant system, the accumulation of ROS can become harmful to the cell by interacting with macromolecules including proteins, lipids, carbohydrates, and nucleic acids [152,360]. Through such interactions, ROS may irreversibly destroy or alter the function of the target molecule and have been increasingly identified as major contributors to damage in biological systems.

ROS have also been found to play a beneficial role in the immune system for host defense [306]. The necessity of ROS in the immune system became clear in 1957 when Berendes *et al.* made the link between deficiencies in ROS generation and reduced ability of patients' leukocytes to fight invading pathogens [30]. This rare syndrome, referred to as chronic granulomatous disease (CGD) was recognized in young boys suffering from reoccurring infections and was later attributed to the absence of the cytochrome b_{558} complex in these patients' phagocytes [84]. The cytochrome b_{558} complex is now referred to as NADPH oxidase (NOX) and it is a superoxide-producing enzyme that is found in both phagocytic and nonphagocytic cells. ROS can also play a beneficial role in cell signaling and are considered to be excellent second messengers because of their rapid

formation and degradation. The cell signaling events are termed reduction-oxidation (redox) reactions because they require ROS to regulate a variety of signaling cascades involved in cell growth, differentiation, protection and apoptosis [278]. Reports show that exogenous addition of superoxide or hydrogen peroxide can stimulate cell growth and differentiation in neuronal cells [151], cardiac cells [277], endothelial cells [271], fibroblasts [42], smooth muscle cells [259], and cancer cells [331]. These studies emphasize the importance of ROS as key signaling molecules for normal cell function and presents researchers with numerous questions about the mechanisms behind the generation of ROS.

As mentioned previously, there are many sources of ROS throughout the body. Cyclooxygenase (COX) and lipoxygenase (LOX) are key ROS-generating enzymes that convert arachidonic acid into either prostaglandins or leukotrienes, respectively, and are involved in the inflammatory and pain responses associated with oxidative stress [322]. There are two isoforms of COX, COX1 is constitutively active and COX2 is induced by inflammatory cytokines such as interleukin-1, that can be reduced by a nutritional diet consisting of omega-3 fatty acids [241]. Two omega-3 fatty acids in particular are docosahexaenoic (DHA) and eicosapentaenoic acid (EPA) that compete with arachidonic acid thereby inhibiting COX2 and protect from inflammation and atherosclerosis [207]. The COX and LOX pathways generate biologically active lipids that play important roles in inflammation, cardiovascular disease and tumor progression [255]. Interestingly, the expression of COX2 and LOX varies throughout the progression of various cancers, and thereby they have been shown to regulate a whole host of processes necessary for cancer development [227]. In retinal epithelial cells exposed to

ischemia/reperfusion, COX2 and xanthine oxidase were found to produce ROS that were inhibited by SOD treatment and the COX inhibitor ibuprofen, and thereby decreased inflammatory cell recruitment, vascular permeability and improved retinal perfusion [263]. A study by Tang *et al.* found that by preconditioning cardiac cells with hydrogen peroxide, which increased the expression of COX2 and iNOS, the heart was protected against a subsequent more lethal hydrogen peroxide treatment and this group attributed that protection to COX2 and iNOS [305]. This study supports the idea that COX2 is involved in cardioprotection against myocardial infarction and leads us to believe that COX and LOX are involved in cardiovascular and immune regulation.

One of the most well known ROS-generating enzymes is nitric oxide synthase (NOS). NOS is a crucial enzyme in the body that regulates vascular tone [217], neurotransmission [7] and inflammation [209]. NOS catalyzes the conversion of L-arginine and oxygen into citrulline and nitric oxide (NO) [236]. To date, three subtypes of NOS have been described. The inducible form of NOS (iNOS) is thought to be involved in inflammation [209] and cardioprotection [305]. Endothelial NOS (eNOS) is constitutively expressed in endothelial cells and generated NO is involved in vascular tone and platelet aggregation [204]. Neuronal NOS (nNOS) is expressed in nerves and various other cell types and produces NO that is reported to play a role in neurotransmission and in learning and memory [201,363]. At low levels, NO can act as an antioxidant by increasing glutathione levels in the mitochondria and increasing mitochondrial biogenesis and lipid catabolism [35]. On the other hand, when NO levels are elevated following exposure to cytokines, NO can react with superoxide to produce the harmful peroxynitrite radical that causes neurodegeneration by killing surrounding

neurons [201]. The role of peroxynitrite production in neuronal death is supported by findings in heat stressed rats with elevated levels of peroxynitrite which were reduced by treatment with the antioxidant compound H-290/51 [12]. This study failed to determine the source of superoxide production that combined with NO, suggesting another ROS-generating enzyme is involved in oxidative stress caused by heat exposure.

Xanthine oxidase is another ROS-generating enzyme that catalyzes the conversion of hypoxanthine and xanthine to uric acid and generates hydrogen peroxide as a by-product [233]. Xanthine oxidase has been shown to play a role in vascular injury associated with ischemia, inflammatory diseases and chronic heart failure [238]. Xanthine oxidase also functions in the testes to mediate ROS damage caused by testicular torsion which causes ischemic damage in the testes [168]. Overall the harmful role of xanthine oxidase is thought to be through the formation of hydrogen peroxide as a by-product and not the uric acid which is mainly associated with an inflammatory response similar to COX2, LOX and iNOS.

The major source of non-enzymatic ROS generation in aerobic cells comes from mitochondrial sources, specifically complex I and complex III [57,190]. Cellular respiration occurs through a process called oxidative phosphorylation in the mitochondria allowing for the generation of energy, in the form of adenosine triphosphate (ATP), via the electron transport chain (ETC) [253]. The ETC transfers electrons through a series of specialized enzyme complexes generating a proton gradient that drives the synthesis of ATP via ATP synthase [194]. Under normal conditions, 1-2% of all oxygen consumed during respiration undergoes a single electron reduction by leakage of electrons from quinone pools to form the superoxide radical [237]. Then, mitochondrial superoxide

dismutase (SOD) converts superoxide into hydrogen peroxide which is then converted to water and oxygen by catalase and glutathione peroxidase. However, under stress conditions, the number of electrons leaking out of the ETC is enhanced leading to an increase and accumulation of superoxide in the mitochondria and ultimately, mitochondrial dysfunction [187]. Alterations in mitochondrial function have been reported to be involved in diverse pathological oxidative stress states such as aging and neurodegeneration [99,237]. The mitochondria have also been shown to generate ROS in response to ischemia/reperfusion [6,57,58,114] and heat stress [15,70,144,178,286,337], but the intensity of these stresses appear to be a major factor in mitochondrial ROS generation. These mitochondrial induced increases in ROS are responsible for progressive deterioration of cell structures and continuous damage to mitochondrial DNA over time [99,237]. These studies support the idea that mitochondria are the source of ROS in response to heat stress and ischemia/reperfusion and the mitochondria may be the cause of cell death in response to lethal exposure to heat and ischemia/reperfusion.

The current study focuses on yet another ROS generating system. NADPH oxidase (NOX) is a major source of ROS in mammalian cells and was originally identified in neutrophils [92]. NOX is a membrane bound, multisubunit enzyme that transports electrons across biological membranes to molecular oxygen to catalyze the formation of superoxide [346]. Studies suggest NOX-derived ROS play an important role in ROS-sensitive signal transduction cascades, including those critically important for cell proliferation, differentiation, apoptosis and even necrosis because of their rapid generation and degradation [162,317]. NOX-derived ROS are thought to also play a role in the cellular response to heat stress by regulating the expression of heat responsive

genes [243]. It is suggested that NOX is involved in initiating oxidative-stress sensitive signaling pathways that also regulate heat shock protein (HSP) production and these proteins protect the cell from both heat stress and oxidative stress. NOX has also been suggested to contribute to ischemia/reperfusion injury associated with lung disease [251], liver injury [193], hypertension (57) and atherosclerosis (58). These findings support the involvement of NOX in the two important oxidative stress-causing states; heat stress and ischemia/reperfusion that will be the focus of this review.

The NADPH Oxidase Homologues

Nicotinamide adenine dinucleotide phosphate (NADPH) oxidase (NOX) is a family of ROS-generating enzymes that were first discovered in phagocytes in 1964 by Rossi and Zatti [268]. NOX is a membrane-bound enzyme that transports electrons from NADPH across biological membranes to molecular oxygen, catalyzing the formation of superoxide [346]. The NOX family consists of seven homologues which are appropriately named NOX1-5 and Duox 1-2. Along with a preserved function of ROS generation in all the NOX isoforms, they all have conserved structural properties including a COOH terminus, a NADPH-binding site at the COOH terminus, a FAD-binding region, six conserved transmembrane domains and four highly conserved heme-binding domains [306]. The prototypical NOX is a multisubunit enzyme that consists of two membrane-bound subunits gp91^{phox} (NOX2) and p22^{phox} and up to four cytosolic subunits p47^{phox}, p67^{phox}, p40^{phox} and the small GTPase Rac1 (figure 1) [225]. Upon activation, these subunits combine to form a membrane-bound complex known as NOX.

Each of the homologues and subunits will be individually described in greater detail in this section of the review.

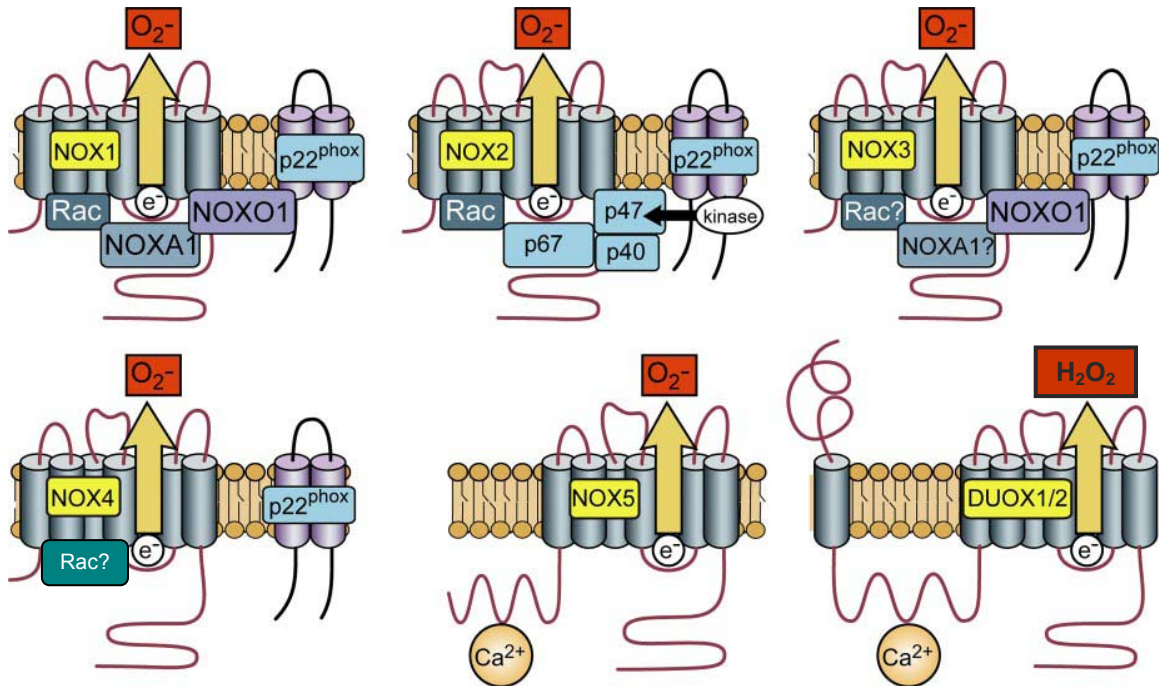


Figure 1. Proposed Structures of Activated NOX Isoforms. The NOX enzymes have similar structures, but differ in their activation mechanisms. NOX1 activation requires p22^{phox}, NOXO1, p47^{phox}, NOXA1 and Rac1. NOX2 (gp91^{phox}) activation requires p22^{phox}, p47^{phox}, p67^{phox}, p40^{phox} and Rac1 as well as p47^{phox} phosphorylation. NOX3 activation requires p22^{phox}, NOXO1, NOXA1 and may require Rac1. NOX4 requires p22^{phox} and may require Rac1 and phosphorylation. NOX5, DUOX 1, and DUOX2 are activated by Ca²⁺ and do not appear to require subunits. Figure modified from Bedard *et al.* 2007.

NOX2

NOX2, also known as gp91^{phox}, is the prototypical NOX and its biochemical features have been extensively studied through the past years [225,266]. The majority of information known about the structural features and topography of all NOX isoforms

were derived from studies on NOX2 in phagocytes and is appropriately termed the phagocytic NOX [138]. To date, sequencing and antibody mapping studies suggest that NOX2 has six transmembrane domains, a cytoplasmic NH₂ terminus and a cytoplasmic COOH terminus [306]. NOX2 in humans is a highly glycosylated protein that has a molecular weight of 91 kilodaltons (kDa) [327]. Activation of NOX2 occurs through a complex series of protein/protein interactions between the gp91^{phox}, p22^{phox}, p47^{phox}, p67^{phox}, p40^{phox} and the small GTPase Rac1 subunits.

The NOX2 protein is thought to be unstable in the absence of the membrane-bound subunit, p22^{phox}, based on studies using phagocytes of p22^{phox}-deficient patients that had no detectable levels of the NOX2 protein [75]. Activation of NOX2 also requires the translocation of the cytosolic factors p47^{phox}, p67^{phox}, p40^{phox} and Rac1 to the gp91^{phox} and p22^{phox} transmembrane complex. Further evidence suggests that full activation of NOX2 requires an additional step involving the phosphorylation of p47^{phox} by protein kinase C (PKC) and/or phosphatidylinositol 3-kinase (PI3 kinase), leading to a conformational change and interaction with p67^{phox} and p22^{phox} [109]. Translocation of p47^{phox} to the membrane is initiated by its phosphorylation, which allows p67^{phox} to dock with gp91^{phox} and p22^{phox} and thereby recruits the small p40^{phox} subunit to the complex [115]. Rac1, a small Rho-GTPase, then interacts with NOX through the direct interaction with gp91^{phox} and p67^{phox} [165,172]. Following assembly, the NOX2 complex is active and generates superoxide via the transfer of an electron from NADPH to oxygen.

NOX2 was first described in neutrophils and macrophages. However, increasing evidence at both the mRNA and protein level show the expression of NOX2 in many nonphagocytic cells, including neurons [280], cardiomyocytes [124], skeletal muscle

cells [142], hepatocytes [260], endothelial cells [145], and hematopoietic stem cells [254]. In smooth muscle cells, NOX2 has been shown to colocalize with the perinuclear cytoskeleton suggesting NOX2 is not only a membrane-bound complex but may have a function in other cellular compartments [186]. Interestingly, NOX2 gene expression is increased by interferon- γ in phagocytes [226], in myofibroblasts after carotid artery injury [302] and in cardiomyocytes after acute myocardial infarction [167]. These studies support the idea that activity and expression of NOX2 can be regulated to alter ROS production in various cell types.

The role of NOX2 in brain function is less clear. In hippocampal neurons, NOX2 has been reported to be localized in the synaptic membranes of nerves and is thought to play a role in superoxide-dependent long-term potentiation and memory function via neuronal plasticity [307]. Evidence also suggests a role of NOX-derived ROS in cognitive function in that mice overexpressing superoxide dismutase (SOD) have impaired memory [309,310]. Learning and memory are impaired in NOX2- and p47^{phox}-deficient mice, as well as in chronic granulomatous disease patients lacking a functional NOX, however the degree of this impairment is mild, suggesting more of a modulatory role of NOX in learning and memory [160,242]. Interestingly, NOX2 found in hippocampal neurons appear to regulate NMDA receptor signaling necessary for normal neurotransmission [242,307]. On the other hand, NOX2 has also been reported to contribute to neurodegeneration by oxidizing amyloid-precursor protein (APP) that is associated with Alzheimer's disease [257]. These studies emphasize the need to clarify the role of NOX2 in normal and abnormal brain function.

NOX1

NOX1 was the first homolog of NOX2 described. NOX1 and NOX2 genes appear to be the result of recent gene duplication because the number and length of their exons are nearly identical [20,298]. NOX1 and NOX2 share a 60% sequence homology and both human and mouse NOX1 genes are located on the X chromosome [20,298]. NOX1 has been found to contain splice variants, one of which lacks exon 11 that encodes for a non-ROS producing form of NOX1 [97]. Studies show a molecular mass of NOX1 in the range of 55–60 kDa suggesting NOX1 is most likely not glycosylated, despite the presence of two glycosylation sites in the extracellular domains [69]. NOX1 is highly expressed in colon epithelium [301] and is also expressed in a variety of other cell types, including neurons [137], vascular smooth muscle cells [173], endothelial cells [163], uterus and prostate [298], placenta [163], and osteoclasts [177]. NOX1 is also expressed in several cell lines, including colon tumor cell lines Caco-2 [66], HT-29 [252] and the pulmonary epithelial cell line A549 [107].

In vascular smooth muscle cells, NOX1 gene expression is induced by platelet-derived growth factor (PDGF), prostaglandin F₂, and angiotensin II [173,298,342]. Studies on the inducible expression of NOX1 in the vascular system suggest an involvement of epidermal growth factor (EGF) receptor transactivation and involvement of ATF-1, PI3-kinase, and PKC [87]. In the brain, NOX1 has been found to negatively regulate neuronal differentiation by suppressing neurite outgrowth [137]. There is also evidence in the brain that suggests NOX1 regulates growth by associating with growth factor receptors and initiating the expression of mitogenic genes by altering the redox state of the cell [278]. NOX1 has been found to be constitutively active in the neurons of

mice, but is contradicted by studies in humans that reported weak constitutive activity and requirement of the PKC activator phorbol-12-myristate-13-acetate (PMA) for full activation [98,303]. NOX1 requires the membrane subunit p22^{phox} for activation and the NOXA1 (activator subunit), NOXO1 (organizer subunit) and Rac1 are also required for the full activation of NOX1 [153,154]. These studies suggest NOX1 is a key enzyme involved in regulating growth and differentiation of neurons and smooth muscle cells.

NOX3

NOX3 was first described in 2000 based on its sequence homology to NOX2, but functional studies were only recently performed revealing a role for NOX3 in the inner ear [157,239]. NOX3 shares 56% amino acid homology with NOX2 and the gene for human NOX3 is located on chromosome 6 [157,239]. Sequence alignment and hydropathy plot analysis predict the overall structure of NOX3 to be very similar to NOX1 and NOX2 [157]. Two different studies led to a defined role of NOX3 in the inner ear. The original study that characterized the role for NOX3 in the inner ear was performed using the "head tilt" mutant mouse that revealed mutations in the NOX3 gene causing vestibular defects [239]. This was the first study to show a functional role of NOX3 in the inner ear that was responsible for the perception of motion and gravity. Another study focused on NOX3 tissue distribution using real time RT-PCR and in situ hybridization. They found high NOX3 expression throughout the inner ear [21] and low levels of NOX3 in the brain [21], fetal spleen and kidney [61,157].

NOX3 is a p22^{phox}-dependent enzyme and its expression appears to stabilize p22^{phox}, which leads to p22^{phox} translocation to the plasma membrane [315,316].

Functional studies suggest p22^{phox} is required for NOX3 activation and truncated p22^{phox} inhibits ROS generation by NOX3 [154,315]. Yet, there remains some controversy over the *in vivo* relevance of p22^{phox} for NOX3 function because no vestibular dysfunction has been reported for p22^{phox}-deficient CGD patients [279]. Expression studies show both p47^{phox} and p67^{phox} are capable of activating NOX3 similar to NOX1 and NOX2, but may not be required for its activation [161]. NOX3 appears to be constitutively active even though the role for a constitutively active NOX in the inner ear still remains unclear.

NOX4

NOX4 was originally identified as a NOX homolog highly expressed in the kidney, and is sometimes referred to as renox (renal oxidase) [96,287]. NOX4 is 39% homologous to NOX2 and the gene for human NOX4 is located on chromosome 11 [105]. NOX4 has a molecular weight of around 75 kDa and/or 65 kDa from both endogenous NOX4 expressing cells, such as smooth muscle cells and endothelial cells as well as in NOX4 transfected endothelial cells [126,135]. The different molecular masses detected and the fact that NOX4 contains four glycosylation sites, suggests that NOX4 is glycosylated [287]. NOX4 mRNA expression has also been detected in neurons [318], osteoclasts [354], endothelial cells [9], smooth muscle cells [83], hematopoietic stem cells [254], fibroblasts [74], keratinocytes [54] and melanoma cells [40]. NOX4 expression in the brain appears to localize in neurons as detected by immunohistochemistry and RT-PCR yet the role of NOX4 in the brain is not yet known [318]. NOX4 expression is induced by a variety of conditions including hypoxia and reoxygenation [299,318], endoplasmic reticulum stress [250], shear stress [134], carotid

artery injury [302], and tumor necrosis factor- α (TNF α) stimulation of smooth muscle [216]. Upregulation of NOX4 expression has been reported in response to angiotensin II and is thought to be involved in the development of hypertension [125]. NOX4 expression can be down-regulated in response to the peroxisome proliferator activated receptor (PPAR)- γ ligands [135], supporting evidence that NOX4 is involved in vascular regulation associated with the Renin-Angiotensin system.

In vascular smooth muscle, NOX4 is found in proximity to focal adhesions [126], but in transfected epithelial cells NOX4 appears to localize near the endoplasmic reticulum (ER) [206,319], which is thought to occur by the accumulation at the site of protein synthesis. In vascular smooth muscle and endothelial cells, NOX4 is located near the perinuclear membrane, suggesting a role in gene expression regulation [126,169]. NOX4 is a p22^{phox}-dependent enzyme and co-localizes with and stabilizes the p22^{phox} subunit [14]. Functional studies suggest a requirement for p22^{phox} in NOX4-dependent ROS generation [154,206]. NOX4 does not appear to require cytosolic subunits for its activity, and it has been shown to be constitutively active [96,206,287]. The requirement of Rac1 or PKC for the activation of NOX4 is not yet clear, but in some endogenous NOX4-expressing cells, a Rac requirement and PKC-dependency have been documented [104,139].

As mentioned above, NOX4 has been suggested to be a constitutively active enzyme; however, not all data favor this concept. NOX4 activation has been shown in response to a variety of stimuli, including lipopolysaccharide in HEK293 cells [244], insulin in adipocytes [200], angiotensin II or high glucose in mesangial cells [104,139], and PMA-stimulated vascular endothelial cells [169]. There is also evidence of the

upregulation of NOX4 expression during a stroke [318]. The authors suggest the increase in NOX4 expression was due to the increase in available oxygen associated with reperfusion following a stroke. However, the authors did not examine NOX4 activity to determine if stroke affected both expression and activity leading to an increase in ROS from NOX4. Angiotensin II and high glucose stimulation are suggested to activate NOX4 through a Rac1-dependent mechanism [104,139], although the requirement for Rac1 in NOX4 activation still remains controversial. Another interesting, yet controversial finding related to NOX4 is its ability to produce hydrogen peroxide rather than superoxide [200]. Studies also suggest this may be due to the rapid conversion of superoxide to hydrogen peroxide by either spontaneous dismutation or by the enzyme superoxide dismutase [206]. These findings lead us to believe that NOX4 is a unique isoform of the NOX family, both structurally and functionally, and can increase ROS production by increased gene expression and increased activity.

NOX5

NOX5 was first described in 2001, by two different groups. Banfi *et al.* described a protein consisting of over 700 amino acids containing a long intracellular NH₂ terminus and a calcium-binding EF-hand domain [61]. Cheng *et al.* predicted a protein of 565 amino acids which lacked the EF-hand domain and had an overall structure similar to NOX1–4 [22]. These predicted protein structures from the two groups are both derived from cDNA and therefore the exact structure of NOX5 has not yet been identified. Based on the requirement of calcium for NOX5 activation, the structure containing the EF-hand domain is the most likely candidate. NOX5 is described as an 85-kDa protein and is

located on chromosome 15 [39]. NOX5 mRNA expression has also been reported in the testis, spleen, lymph nodes, vascular smooth muscle, bone marrow, pancreas, placenta, ovary, uterus, stomach, and in various fetal tissues [22,61,274]. NOX5 does not require p22^{phox} for its activation, as demonstrated by p22^{phox} siRNA studies that decreased the activity of NOX1-NOX4, but not NOX5 [154]. NOX5 does not appear to require cytosolic subunits, similar to NOX4, but activation of NOX5 is mediated by an increase in the cytoplasmic calcium concentration [22,23]. The calcium-binding domain of NOX5 undergoes conformational changes in response to calcium elevations and becomes activated upon the interaction between the calcium-binding region and the catalytic COOH-terminus of the enzyme [22,23]. These findings suggest NOX5 plays a role in calcium-sensing and is a potential mediator of calcium-induced ROS generation.

Duox1 and Duox2

The final two isoforms of NOX are named Duox1 and Duox2 (duox refers to dual oxidase), and are predominately expressed in the thyroid [71,79]. The thyroid gland, located in the neck, is involved in regulating metabolism through the conversion of thyroxine (T4) to triiodothyronine (T3) [218]. The conversion of T4 to T3 is catalyzed by the enzyme thyroid peroxidase in the presence of hydrogen peroxide. The source of hydrogen peroxide was traditionally thought to be thyroid peroxidase, but current studies suggest it is a calcium- and NADPH-dependent enzyme [32]. This concept led investigators to focus on the NOX family of enzymes which led to the discovery of two novel NOX isoforms in the thyroid, called Duox1 and Duox2 [71]. The hydrogen peroxide produced by Duox1 and Duox2 is thought to be directly produced by these

enzymes and not a product of spontaneous dismutation or superoxide dismutase action on superoxide [81,90]. Yet there still remains some controversy over these findings because of the rapid conversion of superoxide to hydrogen peroxide making it hard to confidently say whether Duox1 and 2 only produce hydrogen peroxide or superoxide.

The Duox isoforms are 50% homologous with NOX2, but a truncated form of Duox2 has also been found in rat thyroid cell lines [219]. Both Duox1 and Duox2 have two glycosylation states including a glycosylated form found in the endoplasmic reticulum that is around 180 kDa, and a fully glycosylated form found at the plasma membrane that is around 190 kDa [218]. The peroxidase homology region of Duox2 is suggested to be extremely important to normal thyroid function because mutations in the extracellular domain have been associated with hypothyroidism [323]. They have also been described in airway epithelia [90] and the prostate [328] suggesting they may play a role in epithelial cells other than the thyroid. Duox1 and Duox2 appear to be major regulators for maintaining normal metabolic activity in humans by their requirement for normal thyroid function.

NADPH Oxidase Subunits and Regulatory Proteins

p22^{phox}

The NOX subunit p22^{phox} is closely associated with the gp91^{phox} (NOX2) subunit on the plasma membrane [133]. The gene for human p22^{phox} is located on chromosome 16 and is predicted to have at least two transmembrane domains [110,180]. Evidence suggests two transmembrane domains with both the NH₂-terminus and the COOH-terminus facing toward the cytoplasm [43,138]. The molecular weight of p22^{phox} is 22

kDa [247]. The expression of p22^{phox} is widely distributed in both fetal and adult tissues and in various cell lines [61,248]. Studies show the expression of p22^{phox} increases in vascular tissues in response to angiotensin II [217], streptozotocin-induced diabetes [86], and hypertension [356] revealing a major role in regulating vascular function. The promoter region of p22^{phox} contains consensus sequences for transcription factors including interferon- γ , Elk1, GAGA, and Nuclear Factor- κ B (NF- κ B) suggesting p22^{phox} is highly regulated at the transcriptional level [220].

In phagocytes and endothelial cells, p22^{phox} co-localizes with gp91^{phox} in intracellular storage sites, such as the golgi, and translocates to the membrane upon activation [27,143]. In vascular smooth muscle cells p22^{phox} co-localizes with NOX1 [116] and with NOX1 and NOX4 in transfected vascular smooth muscle cells [14,116]. Currently, it is proposed that gp91^{phox} and the p22^{phox} are stable only as a heterodimer, while the monomers undergo proteasomal degradation [73]. This is supported by studies on NOX2-deficient CGD patients who have no detectable p22^{phox} protein within phagocytes, and p22^{phox}-deficient CGD patients who have no detectable NOX2 protein [248]. Studies using siRNA-mediated p22^{phox} downregulation show decreased function of NOX1-4, but not of NOX5 [39,154] suggesting p22^{phox} is a necessary component for these NOX isoforms.

p47^{phox} and NOXO1

The two NOX subunits p47^{phox} and NOXO1 are recognized as organizer subunits. They are termed organizer subunits based on observations in neutrophils of patients lacking the p47^{phox} subunit in which there was no translocation of the p67^{phox}, p40^{phox},

and Rac1 to form a functional NOX2 complex [231,325]. The genes for human p47^{phox} and NOXO1 are located on chromosomes 7 and 16, respectively [62]. The molecular weights of p47^{phox} and NOXO1 are 47 and 41 kDa, respectively, and are both cytosolic proteins that contain a phox (PX) domain which interacts with membrane phospholipids [303]. They also have two SH3 domains that allow for the interaction with p22^{phox} [180,303]. P47^{phox} has an autoinhibitory domain that prevents the interaction with p22^{phox} until p47^{phox} is phosphorylated and undergoes a conformational change thereby blocking the autoinhibitory domain [181]. The AIR is absent in NOXO1 which may promote constitutive activity in the NOXO1 subunit. NOXO1 and p47^{phox} also contain a COOH-terminal proline-rich region that interacts with SH3 domains in NOXA1 and p67^{phox}, respectively [181].

The expression of p47^{phox} has been reported in neurons [307], hepatocytes [260], lung [10], endothelial cells [145], and vascular smooth muscle [25]. NOXO1 is highly expressed in the colon [20], but also found in other tissues, including testis, small intestine, liver, kidney, pancreas, uterus, and inner ear [62]. Rac1 fails to translocate to the membrane in neutrophils from patients lacking p47^{phox} [80] which provides further evidence for p47^{phox} as an organizer subunit. The autoinhibitory domain of p47^{phox} prevents the association with p22^{phox}, but upon phosphorylation of the autoinhibitory domain of p47^{phox}, a conformational change occurs allowing for the translocation to the plasma membrane and association with the p22^{phox} subunit. In humans, stimulation by the PKC activator PMA is necessary for full activation and p47^{phox} is also thought to be regulated at least in part by PI3-kinase [98,303].

p67^{phox} and NOXA1

The two activator subunits p67^{phox} and NOXA1 were discovered in parallel with the respective organizer subunits (p47^{phox} and NOXO1). These two subunits are called activator subunits because p67^{phox} interacts with p47^{phox} which is thought to activate NOX2 following the translocation of p67^{phox}/p47^{phox}, p40^{phox} and Rac1 to gp91^{phox} and p22^{phox} [258]. Both p67^{phox} and NOXA1 possess NH₂-terminal domains that interact with Rac1 [172] as well. The human p67^{phox} and NOXA1 genes are found on chromosomes 1 and 9, respectively [303]. Although p67^{phox} and NOXA1 share only 28% amino acid identity, their overall domain structure is similar [28]. Their molecular weights are 67 and 51 kDa, respectively, and they are both cytoplasmic proteins. p67^{phox} is expressed in phagocytes, B lymphocytes [106], glomerular, endothelial cells [145], neurons and astrocytes [230]. The expression of p67^{phox} is induced by a variety of stimuli, including zinc exposure in neurons and astrocytes [230], interferon- γ in HL60 cells [182] and angiotensin II in aortic adventitial fibroblasts [240]. p67^{phox} and NOXA1 interact through their COOH-terminal SH3 domain with the proline-rich repeats of p47^{phox} and NOXO1 [110]. Thus, these subunits appear to be necessary for NOX2 activation, but their involvement in the activation of other NOX isoforms is not well documented.

p40^{phox}

p40^{phox} was first detected by coimmunoprecipitation with p47^{phox} and p67^{phox} [339]. p40^{phox} is specific for NOX2 and is suggested to enhance oxidase function, but is not necessary for functional NOX2 in phagocytes [339]. The human p40^{phox} gene is located on chromosome 22 and is a cytosolic protein with a molecular weight of 40 kDa

[80]. The structural domains of p40^{phox} include an SH3 domain, a PX domain, and a PB1 domain [80]. p40^{phox} has been shown to interact with p47^{phox} and p67^{phox} during the activation of NOX2 [265]. The p40^{phox} protein is expressed in phagocytes [339], B lymphocytes [106], hippocampus [307], and vascular smooth muscle [312].

Rac1

The Rho family of GTPases is a subfamily of small G proteins in the Ras superfamily of proteins. The members of the Rho GTPase family have been described as molecular switches that regulate many cellular processes including cell proliferation, apoptosis, cell division, and gene expression [125]. Rac1 (Ras-related C3 botulinum toxin substrate 1) is a member of the Rho GTPase family. The activation of Rac occurs through the exchange of bound guanine diphosphate (GDP) to guanine triphosphate (GTP), which is catalyzed by guanine nucleotide exchange factors (GEFs) [265]. It was reported that Rac1-GTP is necessary for the activation of NOX2 through binding to the p67^{phox} subunit [364]. The Rac1 gene codes for a protein that is around 21 kDa. It is ubiquitously distributed and regulates cell cycle, cell-cell adhesion, motility and differentiation [2]. Rac1 is involved in the activation of NOX1 and NOX2, but its involvement in NOX3 activation is unclear. NOX4 activity appears to be Rac1-independent, although one study using cells endogenously expressing NOX4 implicates a role for Rac1 in NOX4 activation [104]. There are no data suggesting a role for Rac1 in NOX5 or DUOX activation.

NOX Physiology and Pathophysiology

The physiological functions of NOX include host defense [266], cellular signaling [101], posttranslational processing of proteins, regulation of gene expression and cell differentiation [173]. The mechanisms of activation and tissue distribution of the various members of the NOX family are markedly different and still not fully understood. NOX is a major source of ROS in the vascular system, leading to the widespread use of the term vascular NOX [108]. Along with its role in the vascular system, NOX also appears to play a role in the physiology and pathophysiology of the central nervous system (CNS) [51,365]. This role is only now beginning to be investigated. The nervous system accounts for over 20% of all oxygen consumed by the body, and as a result produces large quantities of ROS [77]. The nervous system is particularly sensitive to oxidative stress because of enrichment of polyunsaturated fatty acids in the cell membranes of the various cell types. ROS generation in the CNS has traditionally focused on the pathological effects of mitochondrial ROS production. More recently, studies have begun to unravel the role NOX plays in ROS generation in the nervous system [273].

Astrocytes are glial cells that play an important role in providing regulatory molecules for neurons. They also play an important role in the CNS inflammatory response [329]. In astrocytes, activation of PKC [3,249] or the administration of calcium ionophores has been shown to activate NOX [5]. The type of NOX activated, however, is a matter of contention. Abramov *et al.* reported reduced ROS generation in astrocytes of NOX2-deficient mice, suggesting NOX2 may be the predominant isoform in astrocytes [5]. NOX-derived ROS are thought to play diverse roles in astrocyte function including regulating cell survival via Akt activation [261,355], as well as contributing to

inflammation and oxidative damage of nearby neurons [4]. In glia, the phorbol ester PMA, known activator of PKC, stimulates NOX-derived increases in superoxide production [201]. In oligodendrocytes, neither ROS generation nor expression of NOX have been reported, although these cells appear to respond to ROS generated by neighboring cells [18]. Microglia are macrophage-like cells that produce large amounts of ROS through the phagocyte NADPH oxidase [174,324]. The main function of ROS in microglia appears to be its participation in host defense and the removal of debris from the CNS.

In neurons, the expression of NOX was thought not to occur because of their high susceptibility to oxidative damage. However, over the past few years neuronal expression of NOX4 [318], NOX2 [304] and NOX1 [137] have been reported. The two main functions of NOX in neurons appear to involve regulation of cell fate and modulation of neuronal activity [188]. Induction of neuronal apoptosis in response to serum deprivation or by brain-derived neurotrophic factors appears to be mediated through NOX2-derived ROS generation [158,304]. In PC12 cells, NOX1 negatively regulates NGF-induced neurite outgrowth [137]. This study supports the idea that ROS derived from NOX can modulate neuronal growth and differentiation in the brain. NOX enzymes may also modulate neuronal activity as suggested by studies involving angiotensin II-stimulated neurons [364,365]. Angiotensin II-mediated NOX activation is thought to mediate neuronal chronotropic actions by regulating cardiovascular function and fluid balance [300]. Evidence also suggests a role for NOX-derived ROS in cognitive function where mice overexpressing SOD have impaired memory [309,310]. More specifically, NOX enzymes, particularly NOX2, may be involved in long-term

potentiation and learning [148]. Learning and memory are impaired in NOX2- and p47^{phox}-deficient mice, as well as in CGD patients; however the degree of this impairment is mild, suggesting more of a modulatory role of NOX [160,242]. Interestingly, all elements of the phagocyte NOX are found in hippocampal neurons where NOX is thought to be involved in NMDA receptor signaling necessary for normal neurotransmission [242,307]. These findings lead us to believe that NOX-derived ROS are an important regulator of normal CNS function. However, increased NOX activity may also contribute to pathological conditions such as neurodegeneration and cardiovascular disease.

There is also increasing evidence for a role of microglial NOX2 in inflammatory neurodegeneration, including Alzheimer's disease and Parkinson's disease [64,358]. In the case of Alzheimer's disease, several studies show a role of microglia in amyloid precursor protein (APP)-dependent neurodegeneration [64,246,285]. APP fragments released from neurons activate NOX2 in neighboring microglia cells through a Vav-dependent mechanism [257,340]. Consequent ROS generation by NOX2 in microglia leads to death of neighboring neurons through interactions with their cellular organelles [257]. Several studies suggest similar mechanisms in Parkinson's disease, however, the microglia-activating ligands are less well defined [33,94,95]. A strong argument for a role of NOX2 in Parkinson's disease is shown in experiments with NOX2-deficient mice, that appear to be protected from oxidative stress in a 1-methyl-4-phenyl-1,2,3,6-tetrahydropyridine (MPTP) model of Parkinson's disease [361]. Dementia is a common problem in advanced human immunodeficiency virus (HIV) disease, and microglia activation is thought to be a key element in the development of the disease. The

activation of NOX2 by the HIV-1 negative factor (nef) suggests the involvement of NOX2 in the progression of HIV in humans [51,234]. Overall, the role of NOX in the CNS is complex because NOX is necessary for normal physiological functions in some cases, but can also aid in the progression of many neurodegenerative diseases in other cases. This emphasizes the need to investigate NOX more extensively to truly understand its role in the CNS.

PKC and NOX

Protein kinase C (PKC) represents a family of serine/threonine kinases that are involved in signal transduction and controls numerous cellular processes. All PKCs have a conserved C-terminal domain (substrate binding domain), N-terminal regulatory domain (phosphorylation donor site) and require a lipid phosphatidylserine as a cofactor [24]. Differences in structure and substrate requirements allow for the PKC family to be divided into three groups. The conventional PKCs (α , β_I , β_{II} and γ) are activated by calcium and/or diacylglycerol (DAG); the novel PKCs (δ , ϵ , μ , η and θ) are calcium-independent and activated by DAG; the atypical PKCs (ζ , λ) are calcium-independent and do not respond to DAG either. Evidence suggests that each of the PKC isoforms plays a unique role and are involved in various signaling cascades within all cell types [136].

Since the PKC family is so large, it exhibits the extent to which these proteins are distributed among different tissues, subcellular localization and biochemical properties. Various PKC isoforms can interact with the plasma membrane, golgi, cytoskeleton, mitochondria and nucleus [24]. Phorbol esters are a group of compounds used to activate conventional and novel isoforms of PKC by interacting with the DAG-sensitive region of

these PKCs. The most commonly used phorbol ester is phorbol-12-myristate-13-acetate (PMA), which has been linked to ROS generation through PKC-dependent NOX activation [186].

Oxidative stress can enhance the production of platelets which is a key step in vascular injury associated with atherosclerosis [256]. Polyphenolic compounds such as quercetin and catechin can inhibit ROS generation by inhibiting PKC-dependent NOX which decreases platelet production and reduces vascular injury. In endothelial cells, PKC α , ϵ and ζ activate NADPH oxidase in response to VCAM-1 [1], docosaheanoic (DHA) [207] and in PI3 kinase gamma knockout mice [91], respectively. In fibroblasts, PKC α and δ were found to activate NADPH oxidase in response to WKYMV (W-Tryptophan, K-Lysine, Y-Tyrosine, M-Methionine, V-Valine) and insulin [52,136]. Diabetes is a major risk factor for premature atherosclerosis through oxidative stress. It has also been reported that diabetic PKC β knockout mice had reduced oxidative stress generated from NADPH oxidase which protected renal function [232]. An interesting study showed α -tocopherol, a lipid-soluble antioxidant, inhibits PKC α -dependent NOX, thereby decreasing ROS generated in monocytes, critical for atherogenesis, exposed to hyperglycemia [321].

Hyperthermia and ischemia/reperfusion have been shown to activate PKC and NOX separately, but no one has examined the potential link between PKC activation and NOX activation [146,199,344]. Many of the PKC isoforms are redox-sensitive and can be activated by ROS creating a connection between PKC-dependent ROS generation and ROS-sensitive PKC activation. PKC δ is a redox-sensitive kinase which is involved in apoptosis in response to ROS generation [349]. PKC δ can also cause ROS generation by

phosphorylating the p47^{phox} subunit of NOX [31]. PKC is abundant in neurons and necessary for their survival and function implicating their importance in the brain. PKC plays a role in memory and learning by controlling neuronal plasticity which is likely attributed to ROS generation. Specifically, studies show that lithium-induced memory impairments are due to an impaired function of PKC α , but the mechanism for this impairment is not yet known [159]. In neurons, 6-hydroxydopamine, a neurotoxin that mimics Parkinson's disease, causes oxidative stress through PKC δ leading to neuronal apoptosis [117]. Inhibition of PKC δ prevents the increase of ROS generated by NOX in neuronal cells exposed to advanced glycation end products (AGEs) [228]. PKC α , β _{II} and δ have been reported to activate NOX in microglial cells in response to ganglioside treatment [215] and zinc was reported to activate NOX via PKC in cortical neurons and astrocytes [230].

PI3-Kinase and NOX

The majority of what is known about kinase regulation of NOX comes from studies done in neutrophils. Several kinases other than PKC have been reported to phosphorylate subunits of NOX and regulate its activity including phosphoinositide-3 kinase (PI3 kinase), extracellular regulated kinase (ERK) and p38 mitogen activated protein kinases (MAPK) [350]. The most well documented of the three, is PI3 kinase, which catalyzes the conversion of phosphatidylinositol 4,5-bisphosphate (PIP₂) into PIP₃. PIP₃ then activates phospholipase C (PLC) which is converted to inositol-3-phosphate (IP3) and diacylglycerol (DAG). Conventional and novel PKC are activated by DAG leading to the activation of NOX via phosphorylation of the p47^{phox} subunit [350]. This

presents the possibility that PI3 kinase and PKC are linked in their activation of NOX through DAG formation.

PI3 kinase is activated by various stimuli including ischemia [49], pro-inflammatory cytokines [91,214], endothelin-1 [166] and growth factors [245]. Ischemic preconditioning has been linked to the activation of PI3 kinase to increase hepatic tolerance to ischemia/reperfusion [49]. PI3 kinase is thought to confer neuronal protection through the activation of protein kinase B (PKB or Akt) through activating nuclear factor κ B (NF- κ B) and blocking caspase 3 activation [41]. Other than the few studies in neurons, not much else is known about the role of PI3 kinase and NOX in the brain. Tumor necrosis factor α (TNF- α) mediates PI3 kinase activation through PKC α and PKC ζ which activates NOX2 to generate ROS required for NF- κ B activation and ICAM-1 expression in endothelial cells in inflammation [214]. Platelet-derived growth factor (PDGF) binds to its receptor, activating PI3 kinase which converts PIP2 to PIP3 then binds to the pleckstrin homology domain of NOX1-associated β Pix (Rac-GEF) causing the activation of NOX1 and ROS generation [245]. This shows a clear relationship between PI3 kinase and PKC activation that can activate NOX.

NOX Inhibitors

Diphenylene iodonium

The most commonly used non-specific NOX inhibitor is diphenylene iodonium (DPI). DPI and other diaryl-iodonium compounds irreversibly inactivate the majority of redox-active proteins such as flavoproteins [284]. DPI has been shown to inhibit NOX [304]. DPI is not specific to NOX and has also been shown to inhibit nitric oxide

synthase [295], xanthine oxidase [76] and mitochondrial complex I [189]. DPI has been shown to block apoptosis in neurons exposed to high salt [68] and NGF-starved conditions [304]. Studies using DPI make it hard to narrow down the enzyme responsible for ROS generation in response to an applied stimulus because DPI will block all ROS generating enzymes in the body. Therefore, using DPI along with the other NOX inhibitor apocynin, investigators can better identify that the ROS reduction seen with these inhibitors is due to NOX-derived ROS generation.

Apocynin

The plant-derived phenol 4-hydroxy-3-methoxyacetophenone, apocynin, was first described in the 1990's as a low-affinity inhibitor of the phagocyte respiratory burst [293]. Studies on the effect of the phagocyte NADPH oxidase suggested that apocynin must be metabolized by peroxidases to generate the inhibitory compound and acts by inhibiting the translocation of the cytoplasmic subunits [171]. Apocynin at higher concentrations has been used as an effective NOX4 inhibitor [83,269]. One recent study suggests that apocynin may actually stimulate ROS production in nonphagocytic cells [264]. Yet, another recent study suggests apocynin acts as an antioxidant and should not be considered a NADPH oxidase inhibitor [123]. In a model of global cerebral ischemia-reperfusion injury in the gerbil, apocynin strongly diminishes damage to the hippocampus [330]. Therefore, apocynin reduces ROS generated by NOX, but it may be due to direct inactivation of NOX or by antioxidant properties that bind to ROS. Further studies are necessary to determine the effectiveness and specificity of apocynin to NOX.

Heat Stress Physiology and Pathophysiology

Hyperthermia has recently received considerable attention due to increasing incidents of heat-related illnesses involving athletes, the elderly, and soldiers exposed to hot environments and severe heat waves [337]. Increased environmental temperatures are a major problem when accompanied with physical activity and/or dehydration because of the potential for the development of heat stroke [289]. Heat stroke occurs when brain temperatures exceed 105-106°F because at these temperatures the ability of the hypothalamus to coordinate thermoregulation of the body is compromised [290]. The decreased ability of the hypothalamus to regulate body temperature can cause increases in brain temperature, intracerebral pressure and overall decreases in blood pressure and multi-organ dysfunction [290].

The hypothalamus is the thermoregulator of the body and is involved in sensing changes in body temperature through direct contact with warmed blood and receives signals from spinal cord thermoreceptors. The anterior and preoptic regions of the hypothalamus are suggested to be the main areas of the hypothalamus responsible for eliciting a variety of thermoregulatory responses [37]. These responses include redirecting blood flow to the skin, cutaneous vasodilation, sweating, panting and various behavioral responses leading to increased heat loss [36]. During exposure to high ambient temperatures the skin becomes heated and sends signals through the central nervous system to the hypothalamus which can initiate these heat loss mechanisms [38].

The hypothalamus is also a critical region of the brain that controls the stress response through the activation of the hypothalamic-pituitary-adrenal (HPA) axis [235]. Upon stimulation of the hypothalamus, it secretes a variety of hormones into the

hypophyseal portal system to the anterior pituitary which control a variety of biological actions shown in table 1. This review focuses on the release of corticotrophin releasing hormone (CRH) from the hypothalamus to the pituitary gland. In the anterior pituitary, CRH stimulates the release of adrenocorticotrophic hormone (ACTH) into the peripheral circulation. ACTH acts on the adrenal glands located near the kidneys causing the production of glucocorticoids (cortisol) that can feed back to the hypothalamus to control the production of CRH. The HPA axis controls the immune response by releasing cortisol or corticosterone into the circulation, which can inhibit pro-inflammatory cytokine production, leading to a reduction in inflammation [130]. This is especially important in brain because inflammation can cause brain edema and disruption of the blood brain barrier that can lead to ischemia in neurons [63]. The main roles of inflammation include increased blood flow, increased membrane permeability and repairing damage done by environmental stressors, such as prolonged exposure to extreme heat [352]. Excessive inflammation can also cause edema that leads to the blockage of blood flow, and subsequent ischemia. This shows the importance of the HPA axis in balancing the inflammatory response in the body and more specifically in the brain.

Table 1. Hypothalamic hormones and their biological functions.

Hormone	Pituitary Hormone Release	Biological Functions
Vasopressin or Antidiuretic Hormone (ADH)	Vasopressin or ADH	Water Conservation
Oxytocin	Oxytocin	Uterus Contraction Milk Ejection
Thyrotropin-Releasing Hormone (TRH)	Thyroid-Stimulating Hormone (TSH)	Thyroid Regulation Metabolic Control
Gonadotropin-Releasing Hormone (GnRH)	Follicle-Stimulating Hormone (FSH)	Gonad Regulation
	Lutenizing Hormone (LH)	Gonad Regulation
Growth Hormone-Releasing Hormone (GHRH)	Growth Hormone (GH)	Growth Regulation
		Milk Production
Somatostatin	Inhibits GH and TSH	Growth Regulation Thyroid Regulation
Prolactin-Releasing Hormone (PRH)	Prolactin	Milk Production
Corticotrophin-Releasing Hormone (CRH)	Adrenocorticotrophic Hormone (ACTH)	Adrenal Control

In general, higher temperatures and/or longer exposures to heat increase the risk for problems in CNS functions. The importance of the CNS on the body's response to heat stress is due in part to the role of neurotransmitters including norepinephrine, epinephrine, acetylcholine, dopamine and serotonin [102,103]. These neurotransmitters are involved in transferring thermal information and regulating thermoeffector response [102,103]. The dopaminergic and serotonergic neurons of the hypothalamus have been shown to increase activity in humans exercising in the heat, suggesting they are actively regulating heat and water loss [347,348]. Thus, the thermoregulatory responses to heat stress are biomarkers that can potentially provide more insights into heat stress physiology [179]. The concentration of pro-inflammatory cytokines, such as interleukin-1 (IL-1 β), IL-6 and TNF α strongly correlate with the severity of heat stroke as well [119,212]. These pro-inflammatory cytokine levels become too high under heat stroke in part because of impaired glucocorticoid production and can increase cerebral pressure and edema.

An interesting study done by Niu *et al.* was performed on rats exposed to 43°C heat for 70 minutes until heat stroke was induced [229]. Both heat stroke and control rats were then subjected to a hyperbaric chamber (100% O₂ at 253 kPa for 1 h) to determine if pure oxygen was protective against heat stroke-induced death. The untreated heat stroke rats had an average survival time of around 22 minutes and displayed all the clinical signs of heat stroke including cerebrovascular dysfunction, arterial hypotension, intracranial hypertension, cerebral hypoperfusion, cerebral hypoxia, cerebral ischemia and tissue ischemia/injury in hypothalamus. On the other hand, the heat stroke rats exposed to pure oxygen had increased survival times of 160 minutes and reduced levels of

cerebrovascular and ischemia/reperfusion injury. This study was an interesting representation of heat stroke-induced oxidative stress in the hypothalamus because they extensively examined all parameters for the clinical signs of heat stroke. This study provides insight into the importance of understanding the cellular mechanisms of heat stroke-induced ROS generation leading to this pathological condition.

The majority of studies focused on heat stress in the hypothalamus did not examine the effects at the cellular level and therefore not much is known. However, heat stress is known to cause increased membrane fluidity, protein unfolding and misfolding, oxidative stress, and increased expression of heat shock proteins (HSPs) [243]. Exposure to heat causes the misfolding and unfolding of proteins in the cell that can cause proteins to lose their functionality. This initiates the heat shock response (HSR), which increases HSP gene expression through the phosphorylation and translocation of the transcription factor heat shock factor-1 (HSF-1) [276]. HSF-1 then binds to the heat shock element (HSE) found upstream of the promoter region of all HSPs and promotes their gene expression [343]. HSPs act as molecular chaperones through their binding to misfolded proteins and refolding them to their proper state, ultimately restoring their function [291]. HSPs are highly conserved and ubiquitously expressed and respond to various stressors including ischemia/reperfusion, ethanol and inflammation [141,192,208,221,283]. The ability of HSPs to protect against heat stress and ischemia/reperfusion-induced oxidative stress suggest the oxidative stress component to heat exposure may be a more important factor in the physiology and pathology of heat-related illnesses.

Heat Stress Causes Oxidative Stress

Heat stress has been shown to cause oxidative stress through the production of ROS in the brain, heart, liver and skeletal muscle [275,337]. Oxidative stress is thought to be a major contributor to the progression of heat-related illnesses [353], however the mechanisms are still unknown. Heat stress has been shown to cause ROS generation through the activation of ROS generating systems including NOX [262], NOS [12], and the mitochondria [70]. In the mitochondria, heat stress has been reported to cause disruptions in the electron transport chain that lead to the release of cytochrome c and apoptosis [70]. Bautista *et al.* found that elevated levels of ROS and other free radicals inactivated complex I of the mitochondria and caused mitochondrial dysfunction leading to apoptosis [26]. An interesting study done in yeast, found lethal heat stress of 42°C for one hour elicited mitochondria-derived hydrogen peroxide thereby causing mutations in nuclear DNA [70]. These studies emphasize that lethal heat stress may cause oxidative stress in the mitochondria resulting in ROS that are able to permeate other cellular organelles, such as the nucleus and cause damage to DNA. The majority of studies using lethal heat stress exposures point toward irreparable damage to the mitochondria due to an overwhelming production and accumulation of ROS from the mitochondria [362].

A study performed using heat-exposed rat skeletal muscle found increased ROS generation that caused decreased muscle function and increased muscle fatigue [366]. The authors proposed that NOX may also contribute to ROS generation in the muscle because the muscles are highly vascularized and endothelial NOX may be the source of ROS measured in this study. The authors only speculated on the source of ROS because they did not directly test any of the potential sources and therefore further studies in the

muscle need to be performed to determine the ROS sources. Another study from the same group, following up on their previous findings, utilized inhibitors of both the mitochondria and NOX, but the inhibitors did not reduce heat-induced ROS levels and therefore, they were still unable to identify the source of ROS generation in the diaphragm muscle [367]. This may be due to the fact that ROS are quickly made and quickly degraded making them difficult to measure. Nitric oxide synthase has been shown to contribute to hyperthermia-induced oxidative stress in the brain which leads to edema and increased permeability of the blood brain barrier [282]. However, this study did not explore the role of hyperthermia on the increase in other ROS-generating enzymes and they suggest the role of NO following hyperthermia is mainly involved in decreasing cerebral hypertension.

Heat Stress and NOX

Traditionally heat stress was thought to cause oxidative stress via mitochondrial sources, but recently researchers have suggested NOX may actually be the major source of ROS generation caused by heat stress [275]. In aged rats, heat stress was reported to cause ROS generation in the liver and epithelial cells, but the sources were not examined [360]. This increase in ROS generation is thought to contribute to the age-related decline in heat tolerance through decreases in antioxidant enzymes [89,152,360]. An investigation of infrared exposure, which increases temperature of the skin, was found to cause ROS generation through NOX and xanthine oxidase but ROS production by these enzymes was actually promoted by the mitochondria [286]. These findings are interesting because they are the first to show that infrared exposure to skin causes

multiple sources to generate ROS which activate MMPs and the MAPK pathway that could lead to skin aging and deterioration.

Microglia exposure to lipopolysaccharide (LPS), associated with increases in body temperature, leads to generation of superoxide by NOX2 and nitric oxide by inducible nitric oxide synthase; these react to form peroxynitrite and lead to cell death in neighboring oligodendrocytes [185]. Another group investigating LPS-induced fever in rats also found NOX was the source of ROS generation [262]. Treatment with the NOX inhibitor, apocynin, protected against the LPS-induced neuron injury associated with neurovascular inflammation [183]. Other than fever-induced heat stress in the brain, not much is known about the mechanisms of ROS generation in response to heat stress. More importantly, no one has examined the potential sources of ROS generated in hypothalamic neurons exposed to heat stress. Therefore a major goal of our study was to determine the source(s) of ROS generation in hypothalamic neurons.

Ischemia/Reperfusion Physiology and Pathophysiology

Stroke is commonly characterized as cerebral ischemia caused by a loss of blood flow to the brain due to arterial blockage or loss of blood flow to the brain during cardiac arrest [48]. Cerebral ischemia is defined as regional tissue hypoxia which becomes aggravated by the bolus return of oxygenated blood following removal of blockage or return of cardiac function, which is referred to as reperfusion injury [6]. Reperfusion injury is also associated with surges of intracellular calcium, free radicals, excitatory amino acids and eicosanoids, leading to ATP depletion, neural apoptosis and microvascular inflammation [55,288]. The elderly are at higher risk of cerebral vascular

blockage and as many as 5 million people aged 60 and older died from stroke in 2005, whereas under 1 million people, ages 0 to 59, died from stroke in 2005 [294].

Strokes can be divided into three main types including thrombotic, embolic, and hemorrhagic. The thrombotic stroke is caused by a local reduction of blood flow arising from an atherosclerotic buildup in one of the cerebral blood vessels that eventually become occluded [17]. A reduction of blood flow can arise when an embolus (loose object in the blood) dislodges from the heart or atherosclerotic plaque and travels to the cerebral artery where it occludes blood flow [313]. A hemorrhagic stroke occurs when a cerebral blood vessel ruptures, can occur as a result of hypertension, aneurysm (bulging of a blood vessel) or a congenital arterio-venous malformation [13]. Tissue plasminogen activator (TPA) is a current treatment for thrombotic occlusions because it actually dissolves the blockage [17]. Hemorrhagic strokes are treated by neurosurgically repairing the ruptured blood vessels. The inability of the mature brain to replace large populations of dead neurons can prevent complete restoration of lost function.

Ischemia/reperfusion injury of the central nervous system (CNS) may occur after stroke. CNS ischemia/reperfusion injury is characterized by disruption of the blood-brain barrier [147], resulting in leukocyte transmigration and cerebral edema and increased intracranial pressure that releases various proteases, lipid-derived mediators, and ROS by leukocytes into the brain tissue, irreversibly damaging surrounding cells including neurons [272]. Cerebral ischemia/reperfusion is also associated with hypercortisolism which is caused by increased production of cortisol by the hypothalamus-pituitary-adrenal (HPA) axis, changes in clearance of cortisol and increased sensitivity to cortisol stimulation in the adrenals [235]. Along with hypercortisolism, ACTH levels have been

found to increase following ischemic brain injury and exacerbate ischemic injury to neurons [88]. This evidence was supported by Hsueh *et al.* who examined the HPA activity in rats following ischemia/reperfusion [130]. They found that a 90 minute cerebral artery occlusion followed by reperfusion at various times (0, 4, and 24 hours) increased HPA activity following ischemia, but was suppressed during reperfusion. The investigators suggest that the high levels of ACTH and POMC, both secreted from the pituitary, found during ischemia were changed due to POMC's ability to suppress ACTH release and this was the reason for the decreased HPA activity during reperfusion. Hypercapnia has also been shown to activate the HPA axis, which exerts anti-inflammatory and antioxidant effects by decreasing the production of pro-inflammatory cytokines. Therapeutic hypercapnia is currently being examined as a potential therapy for stroke patients because it is thought that it will promote long term survival following cerebral ischemia/reperfusion injury associated with stroke [288].

Ischemia/Reperfusion Causes Oxidative Stress

Recently, oxidative stress has also been reported to be a contributing factor to cell injury following ischemia and reperfusion [6]. As previously mentioned, oxidative stress is a general term used to describe the level of oxidant damage in a cell or tissue caused by the generation of ROS [196]. It has become widely recognized that oxidative stress contributes to the pathology of a number of neurological disorders and is involved in the injury observed following ischemia and reperfusion [345]. Cerebral ischemia injury to neurons is caused by the blockage of blood flow, hypoxia, ATP depletion and re-oxygenation of the brain during reperfusion [55]. Recently, the pathogenesis of stroke

has been associated with the generation of ROS both during ischemia and reperfusion [272].

ROS have been found to mediate the majority of damage that occurs after transient brain ischemia through surges in NO and superoxide production, reversal of glutamate reuptake at synapses, activation of NMDA receptors, and elevations in intracellular calcium in neurons [195]. As mentioned previously, increases in NO along with increases in superoxide via NOX, xanthine oxidase and the mitochondria combine to form a highly toxic anion, peroxynitrite [155]. Recent studies suggest the toxicity of peroxynitrite is due to its role in causing single-strand breaks in DNA, which activate the DNA repair protein poly-ADP-ribose polymerase (PARP) [272]. This catalyzes the cleavage and thereby the consumption of NAD⁺, which is the source of energy for many vital cellular processes leaving the cell in an energy-depleted state. By administering antioxidants such as superoxide dismutase (SOD) [351] or utilizing SOD-overexpressing cell lines and mice [156,281], researchers have found that ROS levels are reduced and the brain is protected from apoptosis. These studies support the harmful role of ROS generation following ischemic injury in the brain.

Along with ROS generation found during ischemia, reperfusion of ischemic tissues also results in the formation of ROS and is considered by some to be more harmful to the brain than ischemic injury [195]. Reperfusion injury associated with oxidative stress is thought to be due to the bolus amount of glucose-rich and highly oxygenated blood present during reperfusion [336]. In support of the role of oxidative stress during reperfusion, treatment with the synthetic polyphenol, bisphenol, decreases ROS generation and enhances neuronal cell viability following ischemia/reperfusion [78].

The authors of this study also found increases in the gene expression of hypoxia-inducible factor-1 (HIF1), hemeoxygenase-1 (HO-1), glucose transporter-1 (Glut-1), the oxygen sensor neuroglobin (Nb), SOD1, catalase and glutathione peroxidase following ischemia/reperfusion. These genes are associated with protection from oxidative stress and were unable to protect the neuronal cell cultures from ischemia/reperfusion alone. These studies suggest that early gene response is not sufficient to protect from neuronal dysfunction and that by increasing the antioxidant capacity through administering synthetic antioxidants the brain is protected from ischemia/reperfusion-induced ROS generation.

Another recent study examining ischemia/reperfusion in both mice and neuronal cells supports a role for both high glucose and oxygen levels associated with reperfusion-induced oxidative stress injury [297]. The authors show in this study that removing glucose from the media or treatment with the NOX inhibitor, apocynin, during reperfusion, produced a noticeable decrease in superoxide production and prevention of cell death. These same authors also found the same to be true in mice exposed to ischemia/reperfusion suggesting that both NOX and hyperglycemia associated with reperfusion injury are the major cause of neuronal injury following a stroke. These studies support the major role of ROS generation associated with ischemia/reperfusion and show the importance of elucidating the source(s) of ROS produced during reperfusion injury.

Ischemia/Reperfusion and NOX

The sources of the hypoxia-induced ROS are suggested to be mitochondria [281], xanthine oxidase [6], and/or NOX enzymes [122]. In favor of a role of mitochondria, suppression of the mitochondrial cytochrome-c oxidase suppresses hypoxia-induced ROS generation in various cell lines [58,114]. In mouse cortical neurons manganese superoxide dismutase has been reported to protect against hypoxia-mediated oxidative damage predominately produced by the mitochondria [281]. In favor of a role of xanthine oxidase, ROS generation was blocked by the xanthine oxidase inhibitor, oxypurinol during hypoxia in rat hippocampal neurons [6]. In favor of a role of NOX enzymes, studies using primary mouse carotid body chemoreceptor cells demonstrated that moderate hypoxia leads to increased ROS generation that is absent in cells derived from p47^{phox}-deficient mice [122]. These findings make it hard to elucidate the source of ROS generation in response to hypoxia, but they do suggest that the effects of hypoxia in the brain are complex and potentially multifaceted. The focus of our study is on examining the potential ROS-producing enzymes responsible for ROS generation during reperfusion in the brain.

NOX has been suggested to contribute to ischemia/reperfusion injury associated with myocardial infarction, lung disease [251], liver injury [193], hypertension (57) and atherosclerosis (58). Angiogenesis-inducing ROS were found to be generated by NOX2 in endothelial cells [60] and in a model of hind limb ischemia [311], but by NOX1 in tumor models of angiogenesis [16]. A role for NOX following ischemia/reperfusion injury is supported by studies that show stroke size is markedly reduced in NOX2-deficient mice [326], and increased NOX2 expression in diabetic rats that presented signs

of aggravated ischemic brain injury [170]. In a model of global cerebral ischemia-reperfusion injury in the gerbil, apocynin strongly diminishes damage to the hippocampus [330].

ROS generated from NOX are also found to increase permeability and damage of the blood brain barrier that occur following a stroke [147]. A major role of NOX-derived ROS in cerebral vasculature is attributed to structural and functional changes associated with ROS accumulation that can lead to neuronal damage [65]. In the hippocampus, NOX-derived superoxide is thought to play a role in regulating memory and emotion by controlling synaptic transmission [162]. However, increased accumulation of NOX-derived ROS following cerebral ischemia/reperfusion is an important underlying cause for neuronal injury leading to delayed neuronal death (DND) [330]. Studies performed using the NOX inhibitor apocynin, were reported to protect neurons against global cerebral ischemia/reperfusion-induced oxidative stress injury in the hippocampus [330]. Abramov *et al.* supported these findings and reported that in rat hippocampi and cortices exposed to hypoxia, ROS accumulation was attributed to the mitochondria and the ROS-generating enzyme xanthine oxidase, but upon reperfusion in the rat, NOX appeared to be the main source of ROS generation [6]. This suggests a bi-phasic generation of ROS during ischemia/reperfusion in the brain involving multiple sources.

Increased accumulation of ROS following cerebral ischemia-reperfusion is an important underlying cause for neuronal injury leading to delayed neuronal death (DND) and apocynin (NOX inhibitor) treatment has been reported to protect against global cerebral ischemia/reperfusion-induced oxidative stress and injury in the hippocampus [330]. ROS generation has been reported to occur in response to reperfusion or

reoxygenation following global ischemia in rat hippocampal and cortical neurons and has been attributed to NOX, based on the decrease in ROS generation using NOX inhibitors [6]. To date, the effects of ischemia/reperfusion on ROS generation have not been examined in the hypothalamus. Thus, the focus of this study is on elucidating the source and mechanism for ROS generation in response to heat stress and ischemia/reperfusion in the brain.

MATERIALS

Hypothalamus IVB cell line: Rat hypothalamic neuronal cells were obtained as a gift (Kasckow, J., Mulcahney, J.J., et al. *J Neuroendocrinol* 15(5): 521-9, 2003) and used as the neuronal model system.

Cell culture supplies: Dulbecco's Modified Eagle's Medium (DMEM), fetal bovine serum (FBS), Penicillin/streptomycin/amphotericin B reagent, Hanks Balanced Salt Solution with and without calcium and magnesium (HBSS), trypsin, and phosphate buffered saline (PBS) were purchased from Invitrogen Co. (Calsbad, CA). Culture dishes including T-75, 10cm, 6cm, 96 well, as well as cryotubes were purchased from B.D. Falcon Co. (Franklin Lakes, NJ). Conical tubes (15 and 50ml) were purchased from Corning Inc. (Corning, NY). The hypoxic gas packs with oxygen indicators were purchased from Fisher.

NADPH oxidase activity supplies: Nicotinamide adenine dinucleotide phosphate (NADPH), apocynin, lucigenin, G66976, Ro-31-8220, Calphostin C were purchased from Sigma-Aldrich (St. Louis, MO).

Nucleic acid supplies: TRIzol, blue juice gel loading buffer, and MyIQ supermix for qPCR were purchased from Invitrogen. RNeasy mini kit was purchased from Qiagen Inc. (Valencia, CA). Taq polymerase and its corresponding 10X buffer were obtained from Eppendorf Inc. (Westbury, NY). The iScript first strand synthesis kit, IQ supermix for real time RT-PCR, 96-well optical plates and sealing tape were purchased from Bio

Rad laboratories (Hercules, CA). Agarose gel, NorthernMax denaturing gel buffer, MOPS gel running buffer, formaldehyde sample loading dye, RNase and DNase-free water, DEPC- water were purchased from Ambion Inc. (Austin, TX). The all-purpose molecular weight ladder was purchased from Bionexus Inc. (Oakland, CA). Tris-Acetate-EDTA (TAE) buffer, Tris-EDTA (TE) buffer, chloroform were purchased from Fisher Scientific (Pittsburg, PA). Thin walled PCR tubes, 1.5ml, and 2ml tubes were purchased from LabScientific (Livingston, NJ).

Western Blot Supplies: DC protein assay kit, Laemmli buffer, Tris-Glycine-SDS buffer, β -mercaptoethanol, prestained SDS-PAGE broad range molecular weight marker, kaleidoscope prestained molecular weight marker and 12% SDS-PAGE ready gels were all purchased from Bio-Rad laboratories consignment cabinet (Hercules, CA). ECL plus western blotting detection kit and nitrocellulose membranes were purchased from Amersham Biosciences (United Kingdom). Methanol was purchased from Fisher Scientific. Nonfat dry milk was purchased from Fisher Scientific. Rabbit IgG anti-heme oxygenase-1 (HO-1) or anti-heat shock factor-1 (HSF-1) primary antibodies were obtained from Stressgen/AssayDesigns (Ann Arbor, MI). Goat IgG anti-NOX2 (gp91^{phox}) (C-15) and rabbit IgG anti-NOX4 (H-300) primary antibodies, rabbit anti-goat IgG HRP-conjugated secondary antibody and goat anti-rabbit IgG HRP-conjugated secondary antibodies were obtained from Santa Cruz Biotechnology (Santa Cruz, CA). Mouse IgG anti-PKC α , anti-PKC β , anti-PKC γ , anti-PKC δ , anti-PKC ϵ , anti-PKC ζ , anti-PKC μ and anti-lamin A/C primary antibodies were purchased from Transduction Laboratories (Lexington, KY). The NE-PER Nuclear Extraction Kit was purchased from Pierce Biotechnology (Rockford, IL). Image-iT live green ROS detection kit was

purchased from Molecular Probes/Invitrogen. All other chemicals not mentioned were purchased from Sigma-Aldrich-Fluka (St. Louis, MO).

METHODS

1 – Effect of heat stress on heat shock protein gene expression in hypothalamus IVB cells.

1.1 – Cell Culture:

All cell culture techniques were performed under a sterile level 2 biosafety cabinet. The hypothalamus IVB cell line [150] was derived from the hypothalamic neurons of neonatal rat brains and was obtained as a gift from J. J. Mulcahey (School of Medicine, Department of Psychiatry, and Neurosciences Program, University of Cincinnati, OH). IVB cells were frozen and stored in a liquid nitrogen cryotank in freeze media containing 10% dimethyl sulfoxide (DMSO) and were thawed rapidly in a 37°C water bath prior to use to reduce risk of damaging the cells. Cells were then triturated gently into a five milliliter pipette containing warm high glucose (4.5 milligrams/mL) Dulbecco's modified eagles media (DMEM) supplemented with 10% fetal bovine serum, 100 milligrams/mL streptomycin, 100 U/mL penicillin F and 0.25 milligrams/mL amphotericin B. Cell mixture was then transferred to a fifteen milliliter conical tube, brought up to a total volume of ten milliliters in DMEM growth medium, and centrifuged for five minutes at 200 x g at room temperature. Supernatant was aspirated and the cell pellet was resuspended in DMEM growth medium. Cells were plated into a T75 tissue culture flask and grown at 37°C in a cell culture incubator under 95% air and 5% CO₂. Medium was changed after 24 hours. After cell culture was established, medium was

changed every two days and cells were passaged twice a week at 90% confluence. For passage, cells were washed once with Hank's balanced salt solution (HBSS) without calcium and magnesium and trypsinized for five minutes at 37°C in two milliliters of trypsin (0.05% trypsin w/v). Eight milliliters of DMEM growth medium was added to the cells. Cells were then transferred to a 15 milliliter conical tube and centrifuged at 200 x g for five minutes at room temperature. Supernatant was removed and cells were resuspended in ten milliliters of media and counted by trypan blue exclusion using a hemocytometer. Cells were plated at a density of 2.5×10^5 cells/75 cm².

1.1.1 – Heat stress conditions: To examine the effects of a mild heat stress on hypothalamus IVB cells, cells were grown to 80% confluence and incubated in a 37°C (non-heated control) or 43°C (heat-stressed) water bath for fifteen minutes.

1.2 – HSP gene expression:

To determine expression levels of heat shock proteins (HSPs), heat stress was used to induce HSP gene expression. Heat stress causes the initiation of the heat shock response (HSR) that is characterized by increases in HSP gene expression [243]. To test this in the IVB cells, cells were plated at a density of 5.0×10^5 cells/10 cm dish and grown to 80% confluence. Cells were exposed to 43°C for 15 minutes followed by recovery for 1, 2, 4, 8, 12 and 24 hours at 37°C in the cell culture incubator. At each measurement time, the medium was aspirated and one milliliter of TRIzol (Invitrogen, Calsbad, CA) was added to each plate. Plates were scraped into pre-labeled 1.5 milliliter tubes and stored at -80°C until use.

1.3 – RNA isolation from hypothalamus IVB cells:

1.3.1 – Isolation of total RNA: The heat stressed or control IVB cell samples in TRIzol were removed from the -80°C freezer and allowed to equilibrate to room temperature. Rat brains and hearts were used as control tissues. For whole rat brain and rat heart isolations, tissues were excised and quick frozen in liquid nitrogen. For RNA isolation, the tissue was weighed, placed in trizol (1 mL trizol/100 milligrams tissue) and homogenized at maximum speed for thirty seconds using a polytronic tissue homogenizer (Fisher Scientific, Pittsburg, PA). Chloroform (200 microliters/mL trizol) was added to each sample and shaken vigorously for fifteen seconds. The samples were allowed to sit at room temperature for three minutes, and centrifuged at 14,000 x g for fifteen minutes at 4°C. Following centrifugation, the samples were separated into three distinct layers. The lower fraction represents the organic phase and is red in color. The middle fraction, or interphase, is a white fluffy layer containing DNA. The top clear fraction is the aqueous phase that contains total RNA. The top phase was collected carefully from the side, so as not to disturb the other phases. The extracted aqueous phase should be clear, containing no white or organic phases. The aqueous phase was transferred to a new, clean pre-labeled 1.5 milliliter tube. Total RNA was then isolated from the aqueous phase using the RNeasy mini kit (Qiagen Inc., Valencia, CA). The aqueous phase was combined with 350 microliters of 70% ethanol in diethyl pyrocarbonate (DEPC) water, vortexed, transferred into a spin column and placed into a two milliliter collection tube. Samples were centrifuged at 10,000 x g for thirty seconds at room temperature and the flow through was discarded. Samples were washed with 700 microliters of wash buffer, centrifuged at 10,000 x g for thirty seconds and the flow through was discarded again.

To prevent further contamination, the spin column was transferred to a new clean two milliliter collection tube, washed twice with 500 microliters of RPE buffer and centrifugation at 10,000 x g for thirty seconds at room temperature. The collection tube was discarded and replaced with a new pre-labeled 1.5 milliliter tube. Nuclease-free water (50 μ l) was added to the column and incubated at room temperature for five minutes. The tube was centrifuged at 10,000 x g for two minutes and RNA in the flow through was either stored at -80°C or directly used in the following steps.

1.3.2 – RNA purity and concentration analysis: Sample RNA was analyzed spectrophotometrically for concentration and purity. The optical density of RNA samples was determined by UV spectroscopy using SmartSpec plus spectrophotometer (Bio-Rad, Hercules, CA). Sample RNA was diluted 1:100 in 1X TE buffer (10 millimoles/L Tris-HCl, pH 7.5, 1 millimoles/L EDTA), transferred into a clean cuvette and analyzed spectrophotometrically using 1X TE buffer as a blank. An absorbance at 260 nanometers of one is equivalent to 40 micrograms/mL total RNA. Sample RNA concentrations ranged from 0.1 to 1.0 micrograms/mL. Purity was also assessed using the ratio of absorbencies from 260 nanometers and 280 nanometers ($A_{260/280}$). If the $A_{260/280}$ ratio was not greater than or equal to 1.7, the RNA purity was in question and samples were subjected to denaturing agarose gel electrophoresis to further verify RNA integrity.

1.3.3 – RNA integrity assessment: The purity and integrity of sample RNA was determined using denaturing-formaldehyde agarose gel electrophoresis (Mattheus *et al.* 2003). Total RNA (1 microgram) was diluted in three volumes of formaldehyde sample loading dye (1X denaturing gel running buffer, 50% glycerol, 1 millimoles/L EDTA, pH 8.0, 0.25% bromophenol blue and 0.25% xylene cyanol) and heated to 65°C for fifteen

minutes. Samples were then removed, condensed on ice, centrifuged at 1,000 x g for five seconds and loaded on to the denaturing-formaldehyde agarose gel. A 1.0% agarose gel was prepared in NorthernMax denaturing gel buffer (Ambion Inc., Austin, TX) per manufacturers instructions (1X MOPS buffer in DEPC water). The gel was electrophoresed at 130 volts for thirty minutes, removed from chamber and stained for five minutes in DEPC water containing 1X SYBR Gold (Molecular Probes/Invitrogen, Carlsbad, CA). The gel was de-stained in DEPC water for thirty minutes, visualized via UV illumination and an image was obtained using the FluorS imager (Bio-Rad). RNA integrity was determined by visual analysis of the 28S and 18S ribosomal RNA bands (figure 2). Only samples with the 28S band twice as dense as the 18S band were used for further analysis.

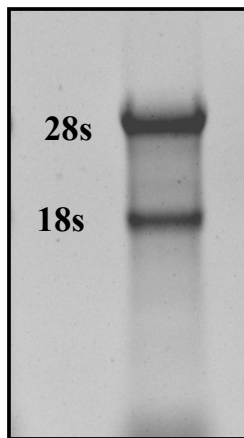


Figure 2. RNA Integrity Gel. The quality of the isolated RNA was assessed following formaldehyde-denaturing agarose gel electrophoresis. This image depicts a representative gel of control RNA isolated from IVB cells. Both ribosomal RNA 18S and 28S bands are clearly visible with the 28S band twice as dense as the 18S band.

1.4 – Evaluation of mRNA expression:

1.4.1 – First strand cDNA synthesis: First strand cDNA was synthesized from total RNA using the iScript first strand synthesis kit (BioRad). Each reaction contained one microgram total RNA, reverse transcriptase buffer, one microliter of reverse transcriptase in a final volume of 20 microliters. The reaction was carried out on a BioRad MyIQ thermocycler under the following conditions: 25°C for five minutes followed by 42°C for thirty minutes then 85°C for five minutes with a final hold at 4°C.

1.4.2 – Real-Time PCR primer design: Primer design is crucial in reproducible and reliable gene expression analysis. Oligonucleotide primers were designed using vector NTI software (Invitrogen, Carlsbad, CA). General guidelines for primer design include a length of 18-24 base pairs, a GC content of 50-60%, a melting temperature (T_m) between 50 and 65°C, no secondary structure, no repeats of G's or C's longer than three base pairs, no G's or C's at ends of primers, no 3' complementarity (also known as primer dimerization), a predicted amplicon of 75-150 base pairs and no secondary structures at the binding sites. All criteria except the secondary structure can be programmed into the primer design tab of Vector NTI. Secondary structure of the gene and the amplicon were assessed using the mfold server provided by Dr. Michael Zuker (<http://bioinfo.math.rpi.edu/~mfold/dna/form1.cgi>). A 75-150 base pair sequence of the gene to be amplified was analyzed for secondary structure shown in appendix A under the following conditions: folding temperature of 60°C, ionic conditions of sodium (50 millimoles/L) and magnesium (3 millimoles/L). The derived secondary structure of the amplicon DNA was then used for further primer design. Primers were designed in regions with no secondary structures. If an area of 75-150 base pairs without secondary

structures was not found, the folding temperature was increased and that new temperature was used for further primer design or another region of the gene was examined and used to design new primers.

The designed primer sequences were BLAST searched for gene specificity. BLAST is a search of all genes stored in the NCBI GenBank database and is available online at www.ncbi.nih.gov/Genbank. If a match was found for a gene other than the gene in which the primers were designed, with an expectation number below 0.01, the primers were discarded and new primers were designed in a different region of the gene. The expectation number is the number of times this match would be expected to occur by chance in a search of the entire database. At least two primer sets for each gene were designed and synthesized by Invitrogen (Carlsbad, CA).

Gene-specific primers were designed for heat shock protein 70 (HSP70) and heme oxygenase-1 (HO-1), as well as the two housekeeping genes, glyceraldehyde 3-phosphate dehydrogenase (GAPDH) and acidic ribosomal phosphoprotein Po (Arbp) (Table 2).

Table 2. Gene Specific Primers for PCR

HO-1 (rat) Accession # NM_012580	sense 5' -CAGGTGTCCAGGGAAGGCTTTAAGC antisense 5' -TTTCGCTCTATCTCCTCTTCCAGGG
HSP70 (rat) Accession # L16764	sense 5' -GTGACCTTCGACATCGACGCCAAC antisense 5' -TGGTGATCTTGTGGCCTTGCC
NOX1 (rat) Accession # NM_053683	sense 5' -CTTCCTCACTGGCTGGGATA antisense 5' -TGACAGCATTTGCGCAGGCT
NOX2 (rat) Accession # AF298656	sense 5' -ATGGGGAAGTGGGCTGTGAAT antisense 5' -TTAGAAGTTTTCTTGTGAA
NOX3 (rat) Accession # NM_001004216	sense 5' -GAGTGGCACCCCTTACCCT antisense 5' -CTAGAAGCTCTCCTTGTGT
NOX4 (rat) Accession # NM_053524	sense 5' -AGTCAAACAGATGGGATA antisense 5' -TGTCATATGAGTTGT
NOX5 (human) Accession # NM_024505	sense 5' -AAGCATACTTGCCCCAGCTG antisense 5' -CAGGCCAATGGCCTTCATGT
Rac1 (rat) Accession # NM_134366	sense 5' -CAGTGAATCTGGGCCTCTGGGACA antisense 5' -GCAGGACTCACAAGGGAAAAGCAA
PKCα (rat) Accession # NM_001105713	sense 5' -TTTACCCGGCCAACGACTCCA antisense 5' -AAATCCGCCCCCTTCTCTGTGT
PKCβ_I (rat) Accession # NM_012713	sense 5' -AGAACGCCGTGGCCGCATCTACAT antisense 5' -TGACAAGCCGTTGGGGTCCATAG
PKCβ_{II} (human) Accession # NM_002738	sense 5' -CCGCATCTACATCCAGGCCACAT antisense 5' -GCTCTACTTTTGGGATCGGGAAT
PKCδ (rat) Accession # NM_133307	sense 5' -TCCCGBAAGCCAGAGACACCAGA antisense 5' -CAGATCGCCCCATTGAGGAAC
PKCϵ (rat) Accession # NM_017171	sense 5' -GCTCTGGCGCGGAAACACCCTTAT antisense 5' -CCATCATCTCGTACATCAGCACGC
PKCζ (rat) Accession # NM_022507	sense 5' -CCCCTTCTGGTTGGCTTACACTC antisense 5' -GCGCCAGCCATCATCTCAAACAT
PKCμ (mouse) Accession # NM_008858	sense 5' -CCCCAACAATTGCAGTGGAGTTAGAAGG antisense 5' -CATCAGGGACACTGGTGGAGAACTCA
GAPDH (rat) Accession # M17701	sense 5' -ATGATTCTACCCACGGCAAG antisense 5' -CTGGAAGATGGTGATGGGTT
Arbp (rat) Accession # NM_007475	sense 5' -AAGCGCGTCCTGGCATTGTCT antisense 5' -CCGCAGGGGGCAGCAGTGGT

1.4.3 – Real-Time PCR: Once primer and RNA quality had been assessed, real-time RT-PCR analysis of HSP70 and HO-1 genes was performed. IVB cells were exposed to 43°C for 15 minutes followed by a recovery time course and RNA isolated at times 1, 2, 4, 8, 12 and 24 hours. Expression of heat shock protein 70 (HSP70) and heme oxygenase-1 (HO-1) as well as the two housekeeping genes glyceraldehyde 3-phosphate dehydrogenase (GAPDH), and acidic ribosomal phosphoprotein Po (Arbp) were measured in duplicate on the myIQ iCycler real-time PCR detection system. No change was detected in housekeeping gene expression. The reaction mixture (concentrations described in section 1.3.3) was as follows: 13 microliters SYBR green supermix, 10 microliters nuclease-free H₂O, 1 microliter of 5 micromoles/L primer mix (both sense and antisense suspended in 1X TE buffer) and 1 microliter experimental cDNA. The thermocycler program was as follows: an initial denaturation at 94°C for 2 min, followed by 35 cycles of 94°C for 15 seconds, 60°C for 30 seconds and 68°C for 1 minute. Each sample was run in duplicate, and a cDNA-free sample (blank) was run with each primer to ensure no DNA contamination.

Next, primer PCR efficiency was determined by real-time PCR using a myIQ iCycler real-time PCR detection system (Bio-Rad). A standard curve was generated using 10-fold dilutions of control cDNA using the newly designed primers (Appendix B). The reaction condition mixture consisted of 1.25 U platinum Taq polymerase, 20 millimoles/L Tris, pH 8.4, 3 millimoles/L MgCl₂, 0.2 moles/L each of the dNTPs, 50 millimoles/L KCl, 1:75,000 dilution of the DNA intercalating dye SYBR green (Platinum SYBR Green Supermix, Invitrogen), and the conditions were as follows: an initial denaturation at 94°C for 2 min, followed by 35 cycles of 94°C for 15 seconds, 60°C for

30 seconds and 68°C for 1 minute followed by a melt curve of 80 cycles starting at 55°C and increasing 0.5°C each cycle. The cycle threshold (Ct) for each dilution was plotted against the dilution and the slope of the line was derived using the formula $E = (10^{-1/\text{slope}}) - 1$. E represents the efficiency of the reaction. Only primers with efficiencies of 80-120% were used for experimentation. In addition, the dilution series provided information regarding the correlation coefficient and only those above 0.995 were used in these experiments.

To ensure no 3' complementarity was present (primer dimerization), a melt curve was also performed (Appendix C). Each primer pair should have only one peak, indicative of one PCR product, and no secondary peak formation at 68-72°C (primer dimers). If these criteria were not met, the primers were discarded.

1.4.4 – Real-Time PCR analysis: Changes in gene expression of the HSP genes HSP70 and HO-1 were calculated relative to the gene expression at time zero. Matched-time non-heated controls were checked prior to these experiments to verify no change in expression levels over time. The modified $\Delta\Delta\text{Ct}$ method as described by Vandesompele et al. [320] was programmed into a Microsoft Excel macro (Bio-Rad) and used for the analysis of gene expression. This method was modified from the $\Delta\Delta\text{Ct}$ method described by Livak and Schmittgen in 2001 and uses complex algorithms that allow for the use of multiple housekeeping genes.

2 – Effect of heat stress on HO-1 protein expression and HSF-1 translocation in hypothalamus IVB cells.

2.1 – Cell Culture:

Hypothalamus IVB cells were plated in ten centimeter dishes and grown to 80% confluence as described in section 1.1, and exposed to 43°C heat stress for fifteen minutes followed by recovery for 1, 2, 4, 8, 12 and 24 hours at 37°C in the cell culture incubator.

2.2 – Preparation of whole cell lysates:

At each measurement time the medium was aspirated, dishes were placed on ice and one milliliter of ice-cold HBSS was added to each plate. Cells were scraped into a pre-chilled 1.5 milliliter microcentrifuge tube, centrifuged at 500 x g for five minutes at 4°C. The supernatant was aspirated and the cell pellet was resuspended in 100 microliters of radioimmunoprecipitation (RIPA) lysis buffer (KH₂PO₄ 10.6 millimoles/L, NaCl 1.5 moles/L, Na₂HPO₄·7H₂O 29.7 millimoles/L, 1% Igepal, 0.5% sodium deoxycholate, 0.1% SDS, supplemented with 100 micrograms/mL PMSF, 50 KIU/mL aprotinin and 100 microliters/mL of sodium orthovanadate), triturated ten times and centrifuged at 10,000 x g at 4°C for fifteen minutes. Supernatant was removed and placed in a pre-chilled 1.5 milliliter microcentrifuge tube and stored at -20°C until western blot analysis.

2.3 – Cytoplasmic and nuclear extractions:

Cytoplasmic and nuclear extracts were isolated by the NE-PER Nuclear Extraction Kit (Pierce Biotechnology, Rockford, IL). Cells were scraped into one

milliliter of HBSS and centrifuged for five minutes at 1,000 x g at room temperature. Cell pellet was then resuspended in 100 microliters of cytoplasmic extraction reagent (CER) I (proprietary recipe supplemented with 100 micrograms/mL PMSF, 50 KIU/mL apoprotin and 100 microliters/mL of sodium orthovanadate); vortexed vigorously for fifteen seconds and incubated on ice for ten minutes. CERII buffer (5.5 microliters) was added, sample vortexed and the cytoplasmic fraction separated from the nuclear by centrifugation at 15,000 x g for five minutes at 4°C. The supernatant (cytoplasm) was separated from the pellet (nucleus) and transferred to a pre-chilled tube. Nuclei were then lysed with the addition of 50 microliters of the Nuclear Extraction Reagent (NER; supplemented with 100 micrograms/mL PMSF, 50 KIU/mL apoprotin and 100 microliters/mL of sodium orthovanadate), followed by four repeats of vortexing and incubation on ice for ten minutes. Samples were centrifuged at 16,000 x g at 4°C for ten minutes and the supernatant was stored at -80°C until use.

2.4 – Determination of protein concentration:

Protein concentration was determined using the DC protein assay (Bio-Rad). A standard curve was generated using bovine serum albumin (BSA) diluted in lysis buffer at concentrations ranging from 0.3 to 1.5 micrograms/microliter. The absorbance was measured at 750 nanometers on a SpectraMax Plus microplate reader (Molecular Devices, Palo Alto, CA). Sample protein concentrations were determined based on the generated standard curve.

2.5 – Western Blot:

Cell lysates or nuclear and cytoplasmic fractions were standardized to fifteen micrograms of protein and boiled in equal volumes of laemmli buffer containing 5% β -mercaptoethanol for five minutes. Samples were separated in a 12% polyacrylamide gel electrophoresis (SDS-PAGE) and transferred electrophoretically to a nitrocellulose membrane. Membranes were blocked at room temperature in 5% milk in 1X TBS-T (20 millimoles/L Tris, 137 millimoles/L NaCl, pH 7.6; and 0.1% Tween 20) for one hour. Membranes were incubated with rabbit IgG anti-heme oxygenase 1 (HO-1) or rabbit IgG anti-HSF-1 primary antibodies (1:1000 dilution, Stressgen/AssayDesigns, Ann Arbor, MI) in 5% milk overnight at 4°C. Membranes were washed three times for five minutes each with 1X TBS-T (5 milliliters), and incubated in 5% milk containing goat anti-rabbit IgG (Stressgen/AssayDesigns, Ann Arbor, MI) conjugated with horseradish peroxidase secondary antibody (1:2,000 dilution) at room temperature for one hour. Membranes were washed again five times for five minutes each with 1X TBS-T (5 milliliters) and immunoreactive bands were detected by chemiluminescence using ECL Plus Western Blotting Detection System (Amersham) on a FluorS Multi Imaging System (BioRad). Each western blot was performed at least twice to account for inter-assay variation.

3 – Reactive oxygen species generated by heat stress and simulated ischemia/reperfusion.

3.1 – Heat stress conditions:

To examine the effects of a mild heat stress on hypothalamus IVB cells, cells were grown to 80% confluence and incubated in a 37°C (non-heated control) or 43°C

(heat-stressed) water bath for fifteen minutes followed by fifteen minutes recovery in a 37°C cell incubator.

3.2 – Simulated ischemia/reperfusion conditions:

To examine the effects of simulated ischemia/reperfusion on hypothalamic IVB cells, cells were grown to 80% confluence and simulated ischemia was introduced by a buffer exchange to an ischemia-mimetic solution (in millimoles/L: 125 NaCl, 8 KCl, 1.2 KH₂PO₄, 1.25 MgSO₄, 6.25 NaHCO₃, 5 sodium lactate, 20 HEPES, pH 6.6). Dishes were then placed in a hypoxic chamber containing hypoxic pouches, which convert available oxygen to carbon dioxide, and equilibrated with 100% N₂. Following one hour of simulated ischemia, reperfusion was initiated by a buffer exchange to warm normoxic reperfusion buffer (in millimoles/L: 110 NaCl, 4.7 KCl, 1.2 KH₂PO₄, 1.25 MgSO₄, 1.2 CaCl₂, 25 NaHCO₃, 15 glucose, 20 HEPES, pH 7.4 and gassed with 95% O₂ and 5% CO₂) for two hours in a 37°C cell culture incubator.

3.3 – Measurement of intracellular reactive oxygen species using microscopy:

Intracellular reactive oxygen species generation (ROS) levels were determined using the Image-it Live Green ROS detection kit (Molecular Probes/Invitrogen). This protocol utilizes the fluorescent probe, 5-,6-carboxy-2',7'-dichlorodihydrofluorescein diacetate (carboxy-H₂DCFDA), a cell permeable dye which enters the cell and is cleaved by cellular esterases to a non-cell permeable non-fluorescent product H₂DCF. H₂DCF is oxidized by ROS to the green fluorescent compound carboxy-DCF that can be detected by fluorescence microscopy (excitation/emission 495/529 nm).

For these experiments IVB cells were plated on electrically charged cover slips in three centimeter dishes (Fisher Scientific, Pittsburg, PA) and grown to 80% confluence. Cells were exposed to heat stress (43°C for fifteen minutes followed by fifteen minutes recovery at 37°C), simulated ischemia/reperfusion (one hour hypoxia followed by two hours reperfusion) or their control conditions as described in 3.1 and 3.2. Following treatments, cells were washed with one milliliter HBSS with calcium and magnesium and labeled with carboxy-H₂DCFDA (25 micromoles/L) in HBSS with calcium and magnesium for thirty minutes at 37°C in the dark. During the last five minutes, nuclei were stained with the blue-fluorescent cell permeable nucleic acid stain Hoeschst 33342 (1 micromoles/L). Cells were washed five times with one milliliter HBSS with calcium and magnesium and coverslips were inverted on glass slides for ROS visualization in a double blind fashion using a 40X magnification at Ex/Em 495/529 nanometers (green) and 350/461 nanometers (blue) on a Nikon 800E fluorescent microscope. Green and blue images were merged and saved as JPEG files. These experiments were repeated at least three times.

3.4 – Effects of apocynin pretreatment on heat- and simulated ischemia/reperfusion-induced ROS generation:

To determine the effect of the NOX inhibitor, apocynin, on ROS production in the hypothalamus IVB cell line, cells were treated with apocynin (300 micromoles/L) or its vehicle for one hour. Cells were then exposed to heat stress, simulated ischemia/reperfusion or control conditions as described above in section 3.1 and 3.2.

ROS generation was measured as described above in section 3.3. These experiments were repeated at least three times.

3.5 – Effects of the protein kinase C inhibitors Gö6976 and Ro-31-8220 on heat- and simulated ischemia/reperfusion-induced ROS generation:

To determine the involvement of protein kinase C (PKC) on ROS generation in response to heat stress and simulated ischemia/reperfusion, the PKC inhibitors Gö6976 (PKC α , PKC β and PKC μ inhibitor) and Ro-31-8220 (PKC α , PKC β , PKC γ and PKC ϵ inhibitor) were used and ROS production was measured in the hypothalamus IVB cell line. These PKC inhibitors are shown on Table 3 with their IC₅₀ values, or half maximal inhibition concentration for each of the PKC isoforms they inhibit. For these experiments, IVB cells were plated on electrically charged coverslips and grown to 80% confluence in DMEM growth media. Medium was changed one day prior to treatments. Cells were then treated with Gö6976 (5 nanomoles/L) and Ro-31-8220 (5 nanomoles/L) or their vehicles in DMEM for one hour before and continuing throughout the exposure of the cells to heat stress, simulated ischemia/reperfusion or control conditions. Following treatments, ROS generation was measured as described above in section 3.3. These experiments were repeated at least three times.

Table 3. PKC Inhibitors

PKC Inhibitor (IC ₅₀ in μ M)	PKC α	PKC β	PKC β_1	PKC β_{II}	PKC γ	PKC δ	PKC ϵ	PKC μ	PKC η	PKC θ
Gö6976	0.002	N/A	0.006	N/A	N/A	N/A	N/A	0.020	N/A	N/A
Ro-31-8220	0.005	N/A	0.024	0.014	0.027	N/A	0.024	N/A	N/A	N/A
Calphostin C	0.050	0.050	0.050	0.050	0.050	0.050	0.050	0.050	0.050	0.050
Rottlerin	30.00	42.00	N/A	N/A	40.00	1.000	100.0	N/A	N/A	N/A

4 – Effect of heat stress and simulated ischemia/reperfusion on NADPH oxidase activity in hypothalamus IVB cells.

4.1 – NADPH oxidase activity:

Hypothalamus IVB cells were plated in six centimeter dishes and grown to 80% confluence as described in section 1.1. NADPH oxidase (NOX) activity was measured in IVB cells using lucigenin-derived chemiluminescence to determine the effects of heat stress and ischemia/reperfusion on NOX activity [190]. Medium was changed one day prior to treatments. Initial experiments were designed to determine the concentration dependent effect of the electron transport chain inhibitor, rotenone (100 nanomoles/L – 1 micromoles/L), and the NOX inhibitor, apocynin (100 nanomoles/L – 1 micromoles/L), on NOX activity. For these experiments, cells were treated one hour before and continuing throughout the experimental period with apocynin (100 nanomoles/L - 1 micromoles/L), diphenylene iodonium (DPI, 1 micromoles/L), rotenone (100 nanomoles/L - 1 micromoles/L) or their vehicle in DMEM growth media and then subjected to either heat stress or simulated ischemia/reperfusion. For the heat stress experiments, cells were placed in either a 37°C (control) water bath for fifteen minutes followed by fifteen minutes at 37°C in a cell culture incubator or a 43°C (heat-stressed) water bath for fifteen minutes followed by fifteen minutes at 37°C in a cell culture incubator. For the simulated ischemia/reperfusion experiments, cells were subjected to 37°C simulated ischemia for one hour followed by two hours of reperfusion at 37°C in a cell culture incubator. Cells were then washed once with phosphate buffered saline (PBS) and dislodged using trypsin (0.05%) for five minutes at 37°C. Krebs' Hepes buffer (KHB) was added (4.5 milliliters) and cells were collected and centrifuged at 200 x g for

five minutes at 4°C. The supernatant was aspirated and cells were resuspended in a final volume of 500 microliters of KHB. Two samples containing 100 microliters each were used for duplicate determination of NOX activity. Each 100 microliter sample was added to 345 microliters of KHB containing lucigenin (6 micromoles/L final concentration) in luminometer cuvettes (Promega, Madison, WI) and read for five minutes in a TD-20/20 Luminometer (Turner Designs, Sunnyvale, CA) to determine background luminescence. To determine stimulated activity, fifty microliters NADPH (100 micromoles/L final concentration) was added and luminescence was measured again for five minutes. NOX activity was expressed as relative light units (RLUs) in the presence of NADPH minus that in the absence of NADPH. Cell number was counted using a hemocytometer for each sample and NOX activity was expressed as RLUs/10⁵ cells. These experiments were repeated at least three times.

4.2 – Effects of the PKC inhibitors Gö6976, Ro-31-8220, Calphostin C and Rottlerin on heat- and simulated ischemia/reperfusion-induced NOX activation:

To determine if PKC was involved in the activation of NOX in response to heat stress and simulated ischemia/reperfusion, the effects of the PKC inhibitors Gö6976, Ro-31-8220, Calphostin C and rottlerin were determined on NOX activity as described above in section 4.1. The PKC inhibitors' selectivity for the various isoforms of PKC is depicted in table 3. For these experiments, hypothalamus IVB cells were grown to 80% confluence in high glucose DMEM supplemented with 10% FBS, 100 milligrams/mL streptomycin, 100 U/mL penicillin F and 0.25 milligrams/mL amphotericin B. Medium was changed one day prior to treatments. Cells were treated for one hour before and

continuing throughout the experiments with Gö6976 (0.5 nanomoles/L - 100 nanomoles/L), Ro-31-8220 (5 nanomoles/L), Calphostin C (0.5 nanomoles/L - 100 nanomoles/L) and rottlerin (1 micromoles/L) in DMEM growth media and cells were subjected to heat stress, simulated ischemia/reperfusion or their control conditions and NOX activity measured. For the heat stress experiments, cell were placed in either a 37°C (control) water bath for fifteen minutes followed by fifteen minutes at 37°C in a cell culture incubator or a 43°C (heat-stressed) water bath for fifteen minutes followed by fifteen minutes at 37°C in a cell culture incubator. For the simulated ischemia/reperfusion experiments, cells were subjected to 37°C simulated ischemia for one hour followed by two hours of reperfusion at 37°C in a cell culture incubator. Following treatments, NOX activity was measured as described above in section 4.1. These experiments were repeated at least three times.

4.3 – Effect of the PI3 kinase inhibitor LY294002 on heat- and simulated ischemia/reperfusion-induced NOX activation:

To determine if phosphoinositol-3-kinase (PI3 kinase) was involved in the activation of NOX in response to heat stress and simulated ischemia/reperfusion, the PI3 kinase inhibitor LY294002 was used and NOX activity was measured as described above in section 4.1. For these experiments, hypothalamus IVB cells were grown to 80% confluence in high glucose DMEM supplemented with 10% FBS, 100 milligrams/mL streptomycin, 100 U/mL penicillin F and 0.25 milligrams/mL amphotericin B. Medium was changed one day prior to treatments. Cells were treated for one hour before and continuing throughout the experiments with LY294002 (10 nanomoles/L) alone or in

combination with calphostin C (50 nanomoles/L) in DMEM growth media and cells were subjected to heat stress, simulated ischemia/reperfusion or their control conditions and NOX activity measured. For the heat stress experiments, cell were placed in either a 37°C (control) water bath for fifteen minutes followed by fifteen minutes at 37°C in a cell culture incubator or a 43°C (heat-stressed) water bath for fifteen minutes followed by fifteen minutes at 37°C in a cell culture incubator. For the simulated ischemia/reperfusion experiments, cells were subjected to 37°C simulated ischemia for one hour followed by two hours of reperfusion at 37°C in a cell culture incubator. Following treatments, NOX activity was measured as described above in section 4.1. These experiments were repeated at least three times.

4.4 – Effect of PMA on NOX activation:

To determine if the NOX activator phorbol-12-myristate-13-acetate (PMA) responds similarly in hypothalamus IVB cells, NOX activity was measured as described above in section 4.1. For these experiments, hypothalamus IVB cells were grown in high glucose DMEM supplemented with 10% FBS, 100 milligrams/mL streptomycin, 100 U/mL penicillin F and 0.25 milligrams/mL amphotericin B to 80% confluence. Medium was changed one day prior to treatments. PMA (20 nanomoles/L) or its vehicle was added to DMEM growth media for thirty minutes and NOX activity was measured as described above in section 4.1. These experiments were repeated three times.

4.5 – Effects of the PKC inhibitors Gö6976, Ro-31-8220 and Calphostin C on PMA-induced NOX activation:

To determine if PMA activated NOX through a PKC mediated pathway, the effect of the PKC inhibitors Gö6976, Ro-31-8220 and Calphostin C were examined on NOX activity as described above in section 4.1. The PKC inhibitors' selectivity for the various isoforms of PKC is depicted in table 3. For these experiments, hypothalamus IVB cells were grown in high glucose DMEM supplemented with 10% FBS, 100 milligrams/mL streptomycin, 100 U/mL penicillin F and 0.25 milligrams/mL amphotericin B to 80% confluence. Medium was changed one day prior to treatments. Cells were treated one hour before and continuing throughout the experimental period with Gö6976 (5 nanomoles/L), Ro-31-8220 (5 nanomoles/L), Calphostin C (50 nanomoles/L) or their vehicle in DMEM growth media. PMA (20 nanomoles/L) was then added to DMEM growth media for thirty minutes and NOX activity was measured as described above in section 4.1. These experiments were repeated three times.

4.6 – Effects of the PI3 kinase inhibitors wortmannin and LY294002 plus Calphostin C on PMA-induced NOX activation:

To determine if phosphoinositol-3-kinase (PI3 kinase) was involved in PMA-induced NOX activation, the effect of the PI3 kinase inhibitor wortmannin (100 nanomoles/L) was examined on NOX activity as described above in section 4.1. For these experiments, hypothalamus IVB cells were grown in high glucose DMEM supplemented with 10% FBS, 100 milligrams/mL streptomycin, 100 U/mL penicillin F and 0.25 milligrams/mL amphotericin B to 80% confluence. Medium was changed one

day prior to treatments. Cells were treated one hour before and continuing throughout the experimental period with wortmannin (100 nanomoles/L) alone or in combination with Calphostin C (50 nanomoles/L) in DMEM growth media. PMA (20 nanomoles/L) was then added to DMEM growth media for thirty minutes and NOX activity was measured as described above in section 4.1. These experiments were repeated three times.

5 – NOX and PKC mRNA expression in control hypothalamus IVB cells.

5.1 – Cell Culture:

Hypothalamus IVB cells were plated in ten centimeter dishes and grown to 80% confluence as described in section 1.1.

5.2 – Polymerase chain reaction:

To determine mRNA expression of the various NOX and PKC isoforms expressed in control hypothalamus IVB cells, PCR was performed on cDNA from IVB cells, rat brain and heart as our reference tissues from section 1.4.1. Gene-specific primers designed for PCR were: gp91phox (NOX2), NOX1, NOX3, NOX4, NOX5, Protein kinase C α (PKC α), PKC β _I, PKC β _{II}, PKC δ , PKC ϵ , PKC ζ , PKC μ , and Rac1 (Table 2).

A standard PCR reaction (1 microliter cDNA, 1 microliter primer mix (5 micromoles/L), 2.5 microliters reaction buffer, 0.5 microliters dNTPs (10 millimoles/L), 0.25 microliters Taq polymerase (1.25 U) and 19.75 microliters ddH₂O) at the designated annealing temperature was performed (1 cycle 2 min @ 95°C; 35 cycles 45 sec @ 95°C, then 45 sec @ 60°C, then one minute @ 72°C; and a final hold at 4°C) using control

cDNA generated from the hypothalamus IVB cells. The PCR product was run on a 1.2% agarose gel, and the number and size of the band(s) were determined. Gel was stained for five minutes in SYBR Gold, destained for thirty minutes in ddH₂O and visualized using a FluorS Multi Imaging System (BioRad).

5.3 – PCR verification:

5.3.1 – Gel extraction: To confirm the mRNA expression data, PCR products from section 5.2 were cloned and sequenced to ensure the correct gene was being identified. Following visualization of NOX2, NOX4 and Rac1 PCR products on a 1.2% agarose gel, bands of appropriate size for these genes were removed using a scalpel and PCR products were extracted using the QIAquick Gel Extraction Kit from Qiagen (Qiagen, Valencia, CA). Bands were weighed and added to three volumes (100 milligrams of gel equals 200 microliters) of binding/solubilization buffer in a sterile microcentrifuge tube. Tubes were incubated in a dry bath for ten minutes at 50°C, vortexing every two minutes, until gel was completely dissolved and color of solution remained yellow. One volume of isopropanol was added, placed in a spin column and centrifuged for one minute at 18,000 x g at room temperature. Flow-through was discarded and binding/solubilization buffer (500 microliters) was added and centrifuged again for one minute at 18,000 x g at room temperature. Discarded flow-through, added wash buffer (750 microliters) and centrifuged for one minute at 18,000 x g at room temperature. Column was placed in a new sterile microcentrifuge tube and elution buffer (30 microliters) was added and centrifuged again for one minute at 18,000 x g at room

temperature. DNA concentration was measured using a spectrophotometer and used immediately for cloning.

5.3.2 – Cloning: NOX2, NOX4 and Rac1 DNA were used from section 5.3.1 to set up a ligation reaction using a TA cloning kit from Invitrogen. A standard ligation reaction contains 10X ligation buffer (1 microliter), pCRII vector (2 microliters), T4 DNA ligase (1 microliter), DNA (14 nanograms) and sterile water to a final volume of ten microliters. Reaction was gently mixed and placed in a thermocycler (BioRad) at 14°C overnight. The ligation product was then used immediately for plasmid transformation.

5.3.3 – Plasmid transformation: Ligation product from section 5.3.2 was used to perform a plasmid transformation using a One Shot Kit from Invitrogen. Vials of INVαF⁺ competent cells were removed from -80°C freezer and centrifuged briefly and thawed on ice. Ligation product (2 microliters) was pipetted into the vial of competent cells and mixed gently with pipette tip. Vials were incubated on ice for thirty minutes, followed by thirty seconds in a 42°C water bath and then placed back on ice. SOC medium was allowed to equilibrate to room temperature and 250 microliters was added to the vial and shaken horizontally for one hour at 225 rpm in a 37°C incubator. Vial was removed and 75 and 175 microliters were spread on two plates with LB agar (10 grams tryptone, 5 grams yeast extract, 10 grams sodium chloride and 15 grams agar in one liter of water) containing X-Gal (40 microliters) and ampicillin (100 micrograms/mL). Plates were placed right side up in foil, to protect X-Gal from light, and allowed to incubate at room temperature for ten minutes. The plates were removed from foil, inverted and allowed to incubate overnight in a 37°C incubator. The next day plates were placed in

4°C refrigerator for two hours to allow for proper color development. This technique is referred to as blue/white screening.

Blue/white screening utilizes X-gal, a colorless modified galactose sugar that is metabolized by β -galactosidase to form an insoluble product which appears blue, and functions as a negative indicator. The hydrolysis of X-gal by the β -galactosidase causes the characteristic blue color in the colonies representing the colonies containing unligated vector. White colonies indicate insertion of target DNA and loss of the cells' ability to hydrolyze X-gal. Bacterial colonies in general are white and a bacterial colony with no vector will also appear white. This is resolved by the presence of an antibiotic, in this case penicillin, in the growth medium and a resistance gene on the vector that allows successfully transformed bacteria to survive despite the presence of the antibiotic.

5.3.4 – Plasmid isolation: To isolate plasmid DNA, ten white colonies containing the target DNA, were removed from plates using sterile wood applicators and placed in five milliliters of LB broth in vent-capped glass culture tubes. The culture tubes were placed in a shaker at 225 rpm and incubated at 37°C overnight. Plasmid DNA was isolated using the Wizard Plus SV Miniprep DNA Purification System (Promega Corporation, Madison, WI). Bacterial cultures (5 milliliters) were placed in 15 milliliter conical tubes and centrifuged at 10,000 x g for ten minutes at room temperature to pellet bacteria. Supernatant was removed and the cells were resuspended in a resuspension buffer (250 microliters; 50 millimoles/L Tris-HCl (pH 7.5), 10 millimoles/L EDTA, 100 microgram/mL RNase A). Cells were lysed in a lysis buffer (250 microliters; 0.2 moles/L NaOH, 1% SDS) and an alkaline protease solution (10 microliters) was added to inactivate endonucleases and other proteins released during bacterial lysis. A

neutralization buffer (350 microliters; 4.09 moles/L guanidine hydrochloride, 0.759 moles/L potassium acetate, 2.12 moles/L glacial acetic acid, pH 4.2) was added, inverted four times and centrifuged at 14,000 x g for ten minutes at room temperature. The supernatant was collected and placed in a spin column and centrifuged at 14,000 x g for one minute at room temperature. The flow-through was discarded and 750 microliters of a wash solution (60% ethanol, 60 millimoles/L potassium acetate, 8.3 millimoles/L Tris-HCl (pH 7.5), 0.04 millimoles/L EDTA (pH 8.0)) was added to the spin column and centrifuged at 14,000 x g for one minute at room temperature, and then repeated. The spin column was again centrifuged at 14,000 x g for two minutes at room temperature to remove all liquid from filtration membrane. The spin column was transferred to a sterile microcentrifuge tube and 100 microliters of sterile water was added. The spin column was centrifuged at 14,000 x g for two minutes at room temperature and the flow-through containing plasmid DNA was placed in a -20°C freezer until needed for restriction digest.

5.3.5 – Restriction digest: Plasmid DNA from section 5.3.4 was used to perform a restriction digest to determine the presence of insert. Restriction digest reaction contained plasmid DNA (31 microliters; 50 nanograms/ μ L), 10X Buffer H (4 microliters) and the restriction enzyme EcoRI (5 microliters; 12 U/ μ L, Promega, Madison, WI). EcoRI was used because the insert is flanked by two EcoRI restriction sites. The reaction was incubated in a 37°C water bath for two hours. The mixture (20 microliters) was added to 10X blue juice (2 microliters), the loading dye, and run on a 1.2% agarose gel. The gel was stained for five minutes in SYBR Gold, destained for thirty minutes in ddH₂O and visualized using a FluorS Multi Imaging System (BioRad). Upon visualization of a band at 150 base pairs, representing the insert of the gene of interest

consistent with the original PCR described in section 5.2, plasmid DNA was quantified using a spectrophotometer and 50 nanograms/ μL was sent to Auburn University Genomics and Sequencing Lab. T7 primers were used for the sequence analysis because they are the primers specific for pCRII vector used in section 5.3.2. Following sequence analysis, the sequences were BLAST searched for gene specificity as described in section 1.4.2.

6 – NOX4 and PKC protein expression in hypothalamus IVB cells:

6.1 – Cell Culture:

Hypothalamus IVB cells were plated in ten centimeter dishes and grown to 80% confluence as described in section 1.1.

6.2 – Preparation of whole cell lysates:

To correlate protein expression with mRNA expression of the various NOX and PKC isoforms in hypothalamus IVB cells, whole cell lysates from control IVB cells and rat brain were isolated. IVB cells were grown to 80% confluence, the medium was aspirated, dishes were placed on ice and one milliliter of ice-cold HBSS was added to each plate. Cells were scraped into a pre-chilled 1.5 milliliter microcentrifuge tube, centrifuged at 500 x g for five minutes at 4°C. The supernatant was aspirated and the cell pellet was resuspended in 100 microliters of radioimmunoprecipitation (RIPA) lysis buffer (KH_2PO_4 10.6 millimoles/L, NaCl 1.5 moles/L, $\text{Na}_2\text{HPO}_4 \cdot 7\text{H}_2\text{O}$ 29.7 millimoles/L, 1% Igepal, 0.5% sodium deoxycholate, 0.1% SDS, supplemented with 100 micrograms/mL PMSF, 50 KIU/mL apoprotin and 100 microliters/mL of sodium

orthovanadate), triturated ten times and centrifuged at 10,000 x g at 4°C for fifteen minutes. The pellet was stored at -20°C until western blot analysis. For control rat brain protein isolation, frozen brain was removed from -80°C freezer, tissue was broken into pieces in a mortar with pestle in liquid nitrogen. The tissue was weighed and homogenized for thirty seconds using a polytronic tissue homogenizer in RIPA buffer (2.4 milliliters RIPA buffer/30 milligrams tissue). Homogenate was incubated on ice for thirty minutes and samples were centrifuged at 14,000 x g for 45 minutes at 4°C. Supernatant was removed and placed in a pre-chilled 1.5 milliliter microcentrifuge tube and stored at -20°C until western blot analysis.

6.3 – Nuclear, cytoplasmic and membrane protein isolation:

To determine the cellular location of NOX4 in control hypothalamus IVB cells and to determine the effects of heat stress and simulated ischemia/reperfusion on PKC translocation; nuclear, cytoplasmic and membrane fractions were isolated using differential centrifugation and NOX4 and PKC immunoreactivity were measured in each fraction. For these experiments, IVB cells were grown to 80% confluence and cells were exposed to heat stress or simulated ischemia/reperfusion as described in section 3.1 and 3.2 respectively. For PMA experiments, cells were treated for thirty minutes with PMA (20 nanomoles/L) in DMEM media in a 37°C cell culture incubator. The medium was then aspirated and the dishes were placed on ice and washed twice with ice-cold PBS. PBS was aspirated, 250 microliters of ice-cold lysis buffer (20 millimoles/L Tris, 2 millimoles/L MgCl₂, 2 millimoles/L EDTA, 10 millimoles/L EGTA, protease inhibitor cocktail (1:200 dilution, Sigma), pH 7.5) was added to one plate from each treatment

group and the plates were scraped into a 1.5 milliliter pre-chilled tube. Tubes were placed in liquid nitrogen for ten seconds and allowed to thaw at room temperature. Lysates were placed in a pre-chilled glass dounce homogenizer and homogenized with ten up and down strokes on ice. The lysate was transferred to a pre-chilled conical tube (15 milliliters) and centrifuged at 500 x g for five minutes at 4°C. Supernatant was placed in a high spin centrifuge tube (12 milliliters) and pellets were resuspended in lysis buffer and served as the nuclear fraction. Samples in the high spin centrifuge tube (12 milliliters) were centrifuged at 75,000 x g for one hour at 9°C. The supernatant was removed and served as the cytoplasmic fraction. The pellet containing the membrane fraction was resuspended in 300 microliters of lysis buffer containing 1% Triton-X, vortexed for fifteen seconds, triturated twenty times and kept on ice for thirty minutes to allow for complete solubilization of the membrane fraction. The nuclear, cytoplasmic and membrane fractions were stored at -80°C until western blot analysis.

6.4 – Determination of protein concentration:

Protein concentration was determined using the DC protein assay (Bio-Rad). A standard curve was generated using bovine serum albumin (BSA) diluted in lysis buffer at concentrations ranging from 0.3 to 1.5 micrograms/ μ L. The absorbance was measured at 750 nanometers on a SpectraMax Plus microplate reader (Molecular Devices, Palo Alto, CA). Sample protein concentrations were determined based on the generated standard curve.

6.5 – Western Blot:

Cell lysates or nuclear, cytoplasmic and membrane fractions were standardized to fifteen micrograms of protein and boiled in equal volumes of laemmli buffer containing 5% β -mercaptoethanol for five minutes. Samples were separated in a 12% polyacrylamide gel electrophoresis (SDS-PAGE) and transferred electrophoretically to a nitrocellulose membrane. Membranes were blocked at room temperature in 5% milk in 1X TBS-T (20 millimoles/L Tris, 137 millimoles/L NaCl, pH 7.6; and 0.1% Tween 20) for one hour. Membranes were incubated with goat IgG anti-NOX2, rabbit IgG anti-Nox4 (1:200 dilution; Santa Cruz Biotechnology, Santa Cruz, CA) or mouse IgG anti-PKC α , anti-PKC β , anti-PKC γ , anti-PKC δ , anti-PKC ϵ , anti-PKC ζ , anti-PKC μ , anti-lamin A/C primary antibodies (Transduction Laboratories, Lexington, KY) in 5% milk overnight at 4°C. Membranes were washed three times for five minutes each with 1X TBS-T (5 milliliters), and incubated in 5% milk containing either rabbit anti-goat, goat anti-rabbit or rabbit anti-mouse IgG (Stressgen/AssayDesigns, Ann Arbor, MI) conjugated with horseradish peroxidase (1:2,000 dilution), respectively, at room temperature for one hour. Membranes were washed again five times for five minutes each with 1X TBS-T (5 milliliters) and immunoreactive bands were detected by chemiluminescence using ECL Plus Western Blotting Detection System (Amersham) on a FluorS Multi Imaging System (BioRad). Each western blot was performed at least twice to account for inter-assay variation.

7 – Statistical analysis:

All data were reported as means \pm standard errors. Differences between treatment groups were analyzed using a One-Way Analysis of Variance (ANOVA). Where significant differences were observed, Student-Neuman-Keuls post-hoc testing was used. All data were analyzed using the Statistical Analysis System (SAS for Windows, version 9.1, SAS Institute, Cary, NC). Significance was accepted at the $P < 0.05$ level.

RESULTS

Effect of heat stress on HSP70 and HO-1 gene expression:

It has been reported that heat stress causes increases in heat shock protein (HSP) gene expression that is associated with the initiation of the heat shock response [291,335]. HSPs act as molecular chaperones through their binding to misfolded proteins and refolding them to their proper state, ultimately restoring their function [291]. Therefore we examined whether the expression of HSP70 and heme oxygenase-1 (HO-1, also termed HSP32) increased after heat stress treatment in IVB cells. IVB cells were exposed to 43°C heat stress for 15 minutes followed by recovery in a 37°C incubator for 1, 2, 4, 8, 12 and 24 hours and RNA was isolated. Basal gene expression of HSP70 and HO-1 did not change in non-heated control cells over a 24 hour period (data not shown). Heat stress caused a significant ($p < 0.05$) increase in both HSP70 and HO-1 gene expression by 1 hour which was the peak for their expression (figure 3). Figure 3 also shows heat stress caused a 19.7 ± 3.45 fold and a 10.5 ± 1.02 fold increase in expression at 1 hour compared to non-heated control cells for HSP70 and HO-1, respectively. By 8 hours and 4 hours, neither HSP70 nor HO-1 expression was significantly different from control. These data suggest that heat stress causes increased transcription of the heat shock genes HSP70 and HO-1.

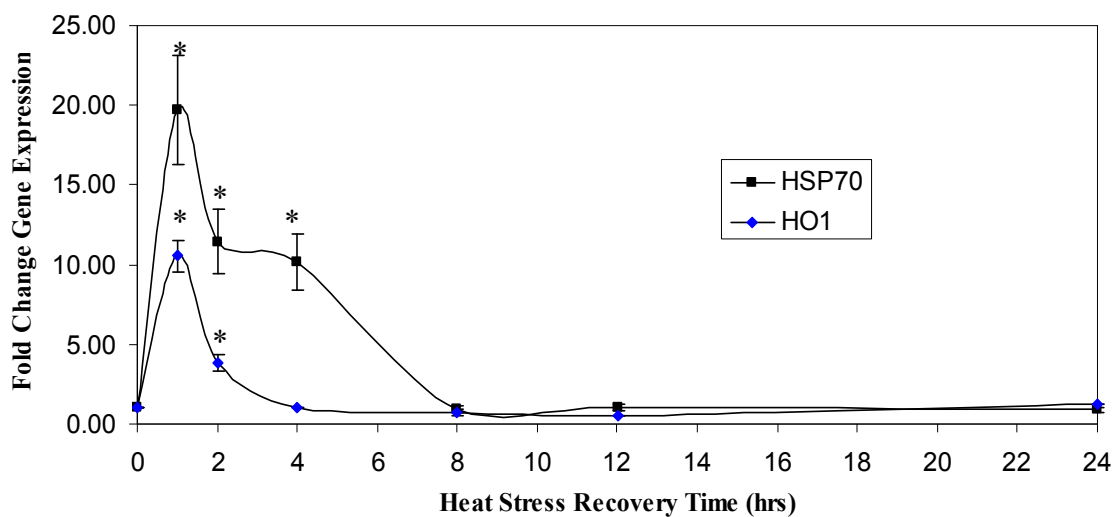


Figure 3. Effect of heat stress on the expression of HSP70 and HO-1. Cells were exposed to 43°C for 15 minutes followed by recovery for up to 24 hours and HSP70 and HO-1 gene expression were measured using real time RT-PCR. Solid square and line indicates HSP70 gene expression. Solid diamond and line indicates HO-1 gene expression. Each data point is normalized to 2 housekeeping genes, glyceraldehyde 3-phosphate dehydrogenase (GAPDH) and acidic ribosomal phosphoprotein Po (Arbp). Error bars represent standard error. * indicates significantly different from non-heated control cells at indicated time ($p < 0.05$). Graph is representative of two independent experiments.

Effect of heat stress on HO-1 protein expression:

The specific role of HO-1 is to catalyze the conversion of free heme to biliverdin, which is converted to the antioxidant bilirubin via biliverdin reductase, and carbon monoxide and iron [132]. The indirect production of the antioxidant bilirubin by HO-1 is protective against oxidative stress and has led to the use of HO-1 as an oxidative stress marker [222]. To verify that HO-1 protein levels increased after heat stress exposure, HO-1 immunoreactivity following heat stress was measured. IVB cells were exposed to 43°C heat stress for 15 minutes followed by recovery in a 37°C incubator for 1, 2, 4, 8, 12 and 24 hours, lysed and normalized for total protein. Basal levels of HO-1 were detected in the lysate of non-heated control cells (figure 4). Figure 4 also shows heat stress increased the expression of HO-1 to 3.5 ± 0.6 fold by 2 hours recovery relative to non-heated control cells. HO-1 levels remained elevated until 24 hours recovery. These data suggest that heat stress increased HO-1 translation in hypothalamus IVB cells.

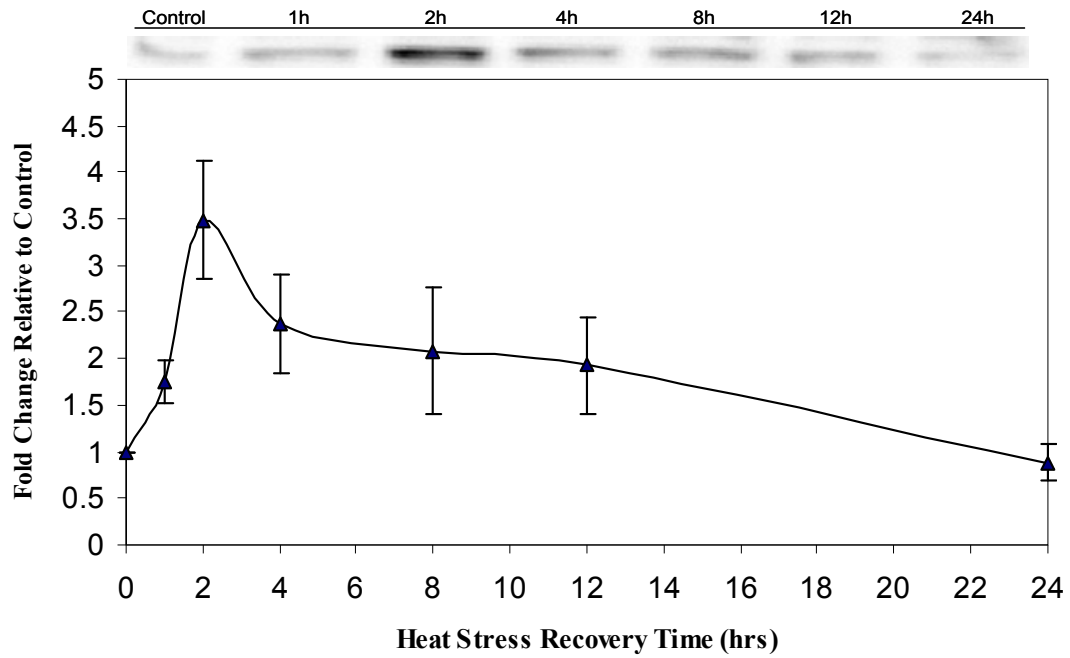


Figure 4. Effect of heat stress on HO-1 protein levels. Cells were exposed to 43°C for 15 minutes followed by recovery for up to 24 hours and HO-1 immunoreactivity was measured using western blot. Western blot is depicted above the graph and is representative of 3 independent experiments. Protein levels were quantified by densitometry. Data is expressed as fold change relative to control.

HSF-1 translocation into the nucleus after heat stress exposure:

The transcription factor heat shock factor-1 (HSF-1) becomes activated and translocates from the cytoplasm to the nucleus in response to heat stress [343]. The activation of HSF-1 is an integral part of the heat shock response that increases the gene expression of HSPs in the nucleus. To determine if exposure of IVB cells to a mild non-lethal heat stress caused HSF-1 translocation from the cytoplasm to the nucleus, cells were exposed to 43°C for 15 minutes followed by recovery at 37°C for 0 to 4 hours and cytoplasmic and nuclear fractions were analyzed for HSF-1 immunoreactivity. HSF-1 immunoreactivity was detected in the cytoplasm and nucleus in non-heated control cells (figure 5). HSF-1 levels increased in the nuclear fraction by 0 hours recovery and remained elevated until 1 hour recovery. HSF-1 levels in the cytoplasmic fraction decreased by 0 hours recovery and remained decreased until 30 minutes recovery and HSF-1 levels increased in the cytoplasm at 1 hour and 4 hours recovery to levels higher than control cells. These data suggest that heat stress increases HSF-1 protein expression and activates HSF-1 causing it to translocate from the cytoplasm to the nucleus thereby initiating HSP70 and HO-1 gene expression. These data also suggest that the mild heat stress used in this study is sufficient to initiate the heat shock response in the IVB cells.

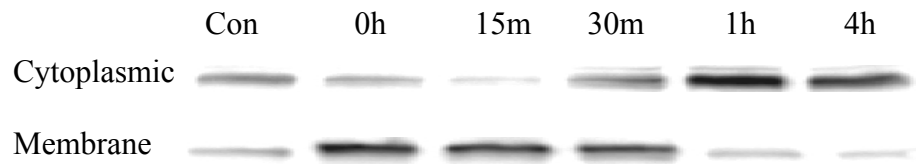


Figure 5. Effect of heat stress on HSF-1 protein levels in the cytoplasm and nucleus. Cells were exposed to 43°C for 15 minutes and HSF-1 immunoreactivity was measured in cytoplasmic and nuclear fractions. Figure is representative of two independent experiments.

Heat stress causes oxidative stress in hypothalamus IVB cells:

It has been reported that heat stress causes oxidative stress by the generation of reactive oxygen species (ROS) in the brain, but the cellular effect of heat stress on hypothalamic neurons has not yet been investigated. One of the main roles of the hypothalamus is to regulate body temperature. The ability of the hypothalamus to regulate body temperature becomes compromised when an individual experiences a heat stroke, which may be attributed to ROS generation and accumulation in hypothalamic neurons. Therefore, we examined whether heat stress caused ROS generation in the hypothalamus IVB cells. IVB cells were grown on charged coverslips and exposed to either 37°C (control) or 43°C (heat stress) for fifteen minutes followed by fifteen minutes recovery in a 37°C cell culture incubator and ROS generation was visualized using fluorescence microscopy. ROS were measured using the Image-it Live Green ROS detection kit (Molecular Probes) which fluoresces green in the presence of ROS. For a positive control, IVB cells were treated with *tert*-butyl hydroperoxide (*t*BHP) (100 µM), a known inducer of ROS, for 90 minutes and ROS generation was measured. In control cells, no green fluorescence was detected and nuclei appeared round with little to no detectable green fluorescence (figure 6a). Treatment of cells for 90 minutes with the positive control *t*BHP (100 µM) caused an increase in green fluorescence throughout the cells suggestive of ROS generation (figure 6b). Likewise, IVB cells exposed to heat stress also displayed green fluorescence throughout the cell (figure 6c). There was also an observed change in cell morphology in response to heat stress and *t*BHP in that cells appeared more rounded compared to control cells.

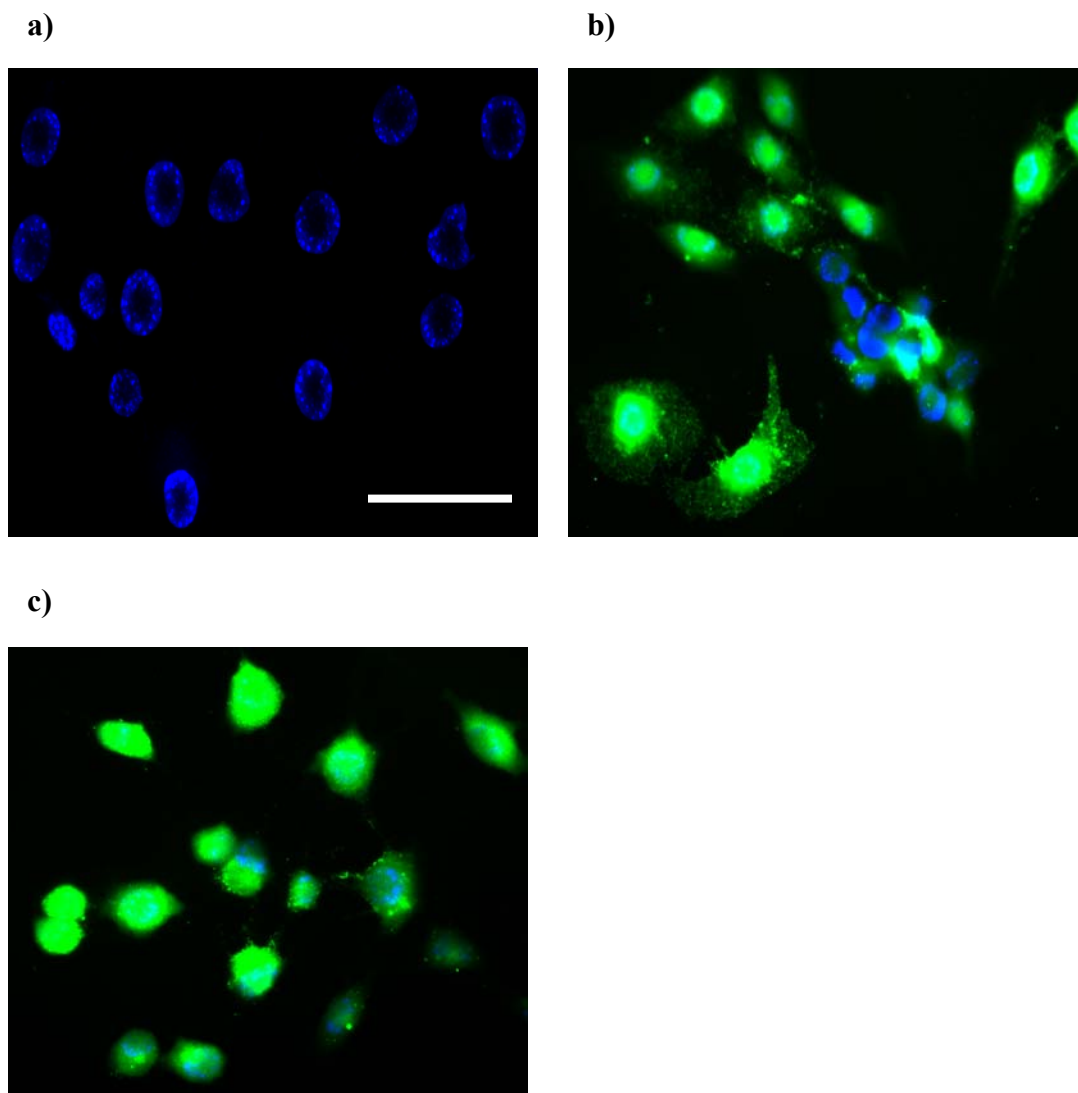


Figure 6. ROS generation in response to heat stress in hypothalamus IVB cells. Cells were double labeled with a Hoescht stain (Excitation/Emission of 350/461 nm), which fluoresces blue inside the nucleus and a carboxy-H₂DCFDA stain (Excitation/Emission of 495/529 nm) which fluoresces green in the presence of ROS. a) Non-heated control cells. b) Cells treated with *t*BHP (100 μ M) as our positive control. c) Cells heated for 15 min at 43°C followed by 15 min recovery at 37°C. Heat stress and *t*BHP caused an increase in ROS indicated by an increase in green fluorescence. All pictures are representative of 3 independent experiments. Scale bar = 35 micrometers.

Simulated ischemia/reperfusion causes oxidative stress in hypothalamus IVB cells:

Next, we wanted to determine if simulated ischemia/reperfusion caused ROS generation in hypothalamic neurons similar to heat stress. Oxidative stress has been linked to neuronal damage following ischemia/reperfusion injury, but ROS generation has not been measured in hypothalamic neurons exposed to ischemia/reperfusion [318]. Therefore, we examined the effect of simulated ischemia/reperfusion on ROS generation in hypothalamus IVB cells. Hypothalamus IVB cells were exposed to one hour simulated ischemia at 37°C followed by two hours reperfusion at 37°C and ROS generation was visualized using fluorescence microscopy. IVB cells exposed to simulated ischemia/reperfusion showed an increase in green fluorescence compared to control cells (figure 7a and 7b). Cells exposed to simulated ischemia/reperfusion also exhibited a more rounded appearance compared to control cells, which is consistent with our previous observations in heat stressed and *t*BHP treated cells. These data suggest that simulated ischemia/reperfusion causes an increase in ROS generation in IVB cells.

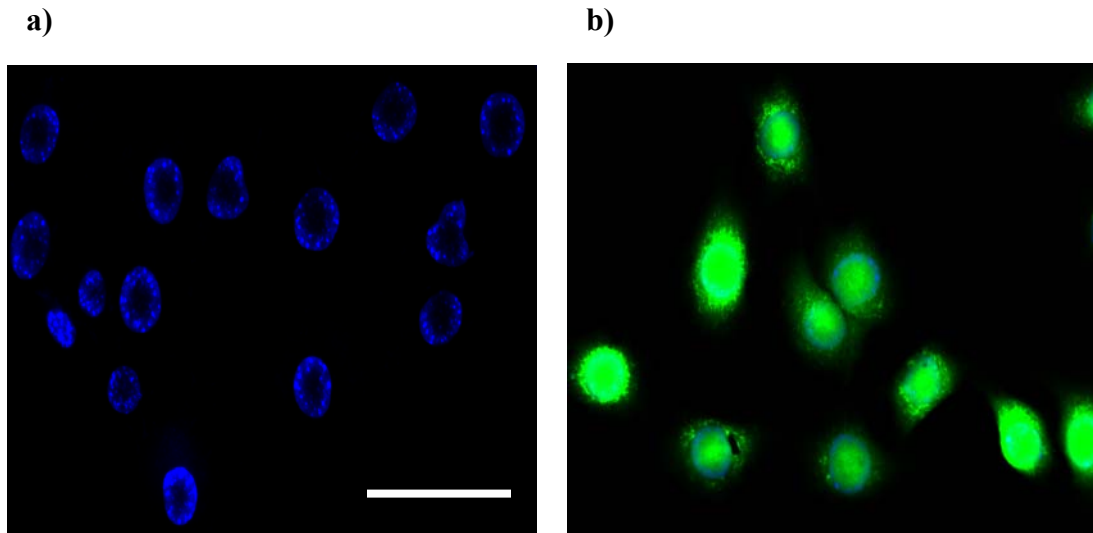


Figure 7. ROS generation in response to simulated ischemia/reperfusion in hypothalamus IVB cells. Cells were double labeled with a Hoescht stain (Excitation/Emission of 350/461 nm) which fluoresces blue inside the nucleus and a carboxy-H₂DCFDA stain (Excitation/Emission of 495/529 nm) which fluoresces green in the presence of ROS. a) Non-ischemic control cells. b) Cells subjected to 1 h simulated ischemia followed by 2 h reperfusion. Simulated ischemia/reperfusion caused an increase in ROS indicated by an increase in green fluorescence. All pictures are representative of 3 independent experiments. Scale bar = 35 micrometers.

Inhibition of NOX attenuates heat-induced oxidative stress in hypothalamus IVB

cells:

To determine the potential source(s) of heat stress-induced ROS generation in the hypothalamus IVB cells. IVB cells were pretreated with the mitochondrial complex I inhibitor, rotenone, or the NOX inhibitor, apocynin, and ROS generation measured using the Image-it Live Green ROS detection kit (Molecular Probes). For these experiments, IVB cells were treated with either apocynin (300 μ M), rotenone (100 nM) or their vehicle for one hour and then exposed to heat stress at 43°C for fifteen minutes followed by fifteen minutes recovery at 37°C. Inhibitor doses and time for exposure were based on previous studies [213]. In cells treated with vehicle, heat stress caused an increase in green fluorescence as previously observed (figure 8a). Treatment of control cells for one hour with either apocynin (300 μ M) or rotenone (100 nM) did not cause a change in fluorescence compared to vehicle-treated cells (data not shown). Treatment with apocynin but not rotenone prior to heat stress attenuated the increase in fluorescence compared to heat stress alone (figure 8b and 8c). These data suggest NOX is involved in heat-induced ROS generation in hypothalamus IVB cells.

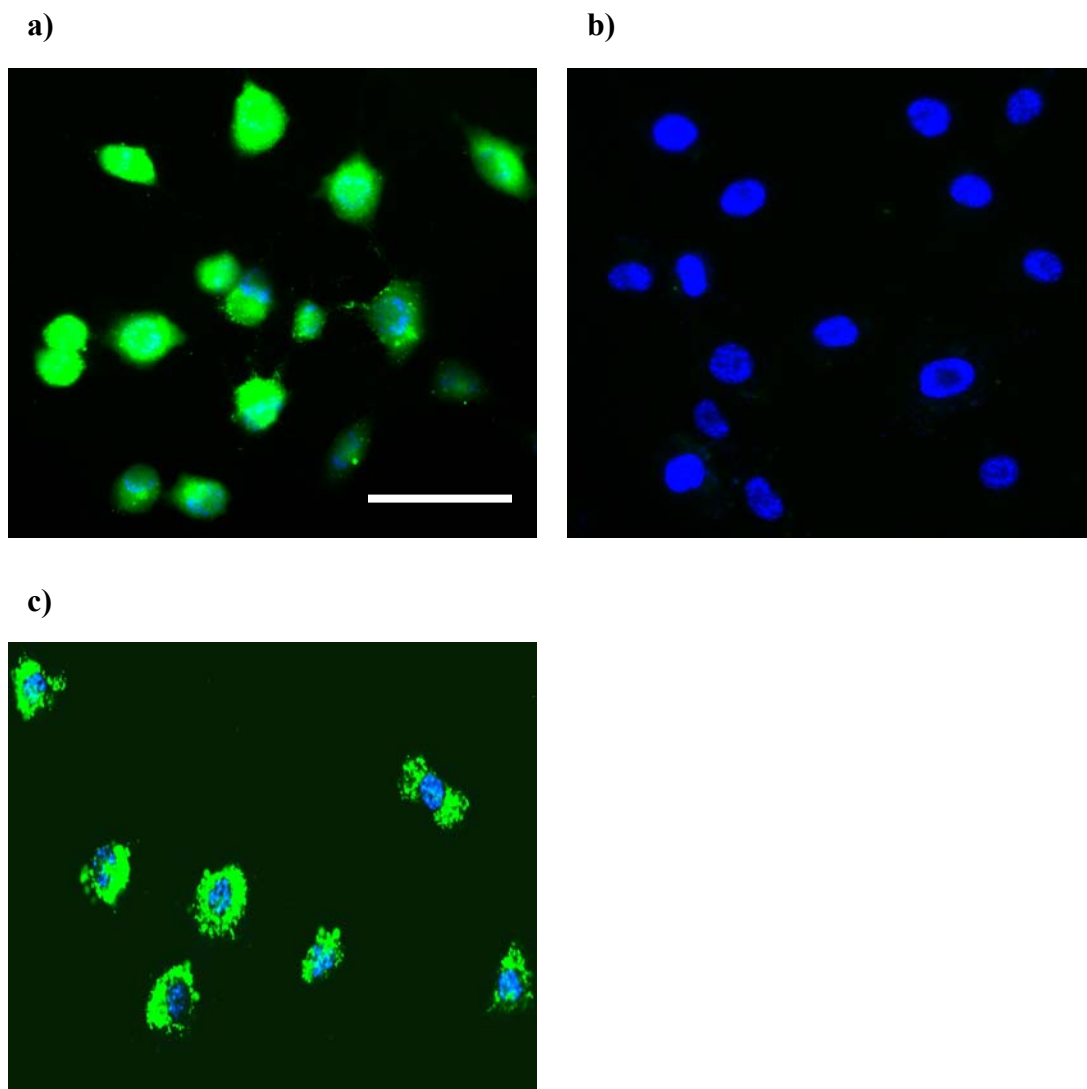


Figure 8. Apocynin inhibits heat-induced oxidative stress in hypothalamus IVB cells. Cells were double labeled with a Hoescht stain (Excitation/Emission of 350/461 nm) which fluoresces blue inside the nucleus and a carboxy-H₂DCFDA stain (Excitation/Emission of 495/529 nm) which fluoresces green in the presence of ROS. a) Cells heated for 15 min at 43°C followed by 15 min recovery at 37°C. b) Cells pretreated for 1 h with apocynin (300 μM) followed by heat stress. c) Cells pretreated for 1 h with rotenone (100 nM) followed by heat stress. Pretreatment with apocynin, but not rotenone inhibited ROS generated from heat stress to control levels. All pictures are representative of 3 independent experiments. Scale bar = 35 micrometers.

Inhibition of NOX attenuates simulated ischemia/reperfusion-induced oxidative stress in hypothalamus IVB cells:

In a similar fashion to heat stressed cells, we also sought to determine the site of ROS generation in IVB cells exposed to simulated ischemia/reperfusion. ROS was measured using the Image-it Live Green ROS detection kit (Molecular Probes). IVB cells were treated for one hour with apocynin (300 μ M) followed by exposure to simulated ischemia/reperfusion, as previously described. Apocynin pretreatment attenuated the increase in fluorescence in response to simulated ischemia/reperfusion compared to vehicle-treated cells (figure 9a and 9b). These data suggest that NOX is involved in simulated ischemia/reperfusion-induced ROS generation in hypothalamus IVB cells.

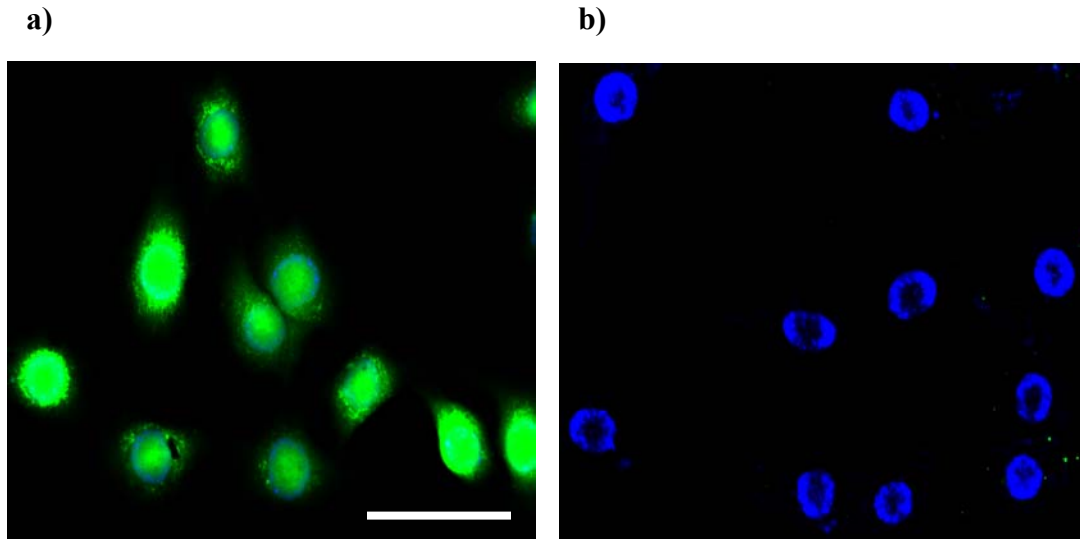


Figure 9. Apocynin inhibits simulated ischemia/reperfusion-induced oxidative stress in hypothalamus IVB cells. Cells were double labeled with a Hoescht stain (Excitation/Emission of 350/461 nm) which fluoresces blue inside the nucleus and a carboxy-H₂DCFDA stain (Excitation/Emission of 495/529 nm) which fluoresces green in the presence of ROS. a) Cells subjected to 1 h simulated ischemia followed by 2 h reperfusion. b) Cells pretreated for 1 h with apocynin (300 μ M) followed by simulated ischemia/reperfusion. Pretreatment with apocynin inhibited ROS generated from simulated ischemia/reperfusion to control levels. All pictures are representative of 3 independent experiments. Scale bar = 35 micrometers.

NOX activity increases in response to heat stress in hypothalamus IVB cells:

To further investigate the effect of heat stress on ROS generation, NOX activity was measured in IVB cells. The lucigenin-enhanced chemiluminescence assay was chosen for these experiments because it has been reported as a valid method for measuring ROS generation, specifically superoxide, as well as measuring NOX activity [137]. For these experiments, IVB cells were pretreated for one hour with the NOX inhibitors apocynin (300 μ M), diphenylene iodonium (DPI, 1 μ M) or their vehicle and exposed to either 37°C (control) or 43°C (heat stress) for fifteen minutes followed by fifteen minutes recovery in a 37°C cell culture incubator and NOX activity was measured. Baseline luminescence in the absence of NADPH was 0.50 ± 0.50 RLU/10⁵ cells (data not shown). NOX activity in non-heat stressed cells treated with vehicle was 5.01 ± 0.83 RLU/10⁵ cells (figure 10). Apocynin (300 μ M) pretreatment had no effect on NOX activity in control non-heat stressed cells. On the other hand, treatment with DPI (1 μ M) for one hour caused a decrease in NOX activity to 1.27 ± 0.34 RLU/10⁵ cells compared to vehicle-treated cells. Heat stress caused a significant increase in NOX activity to 20.9 ± 1.76 RLU/10⁵ cells compared to non-heated cells. The heat-induced increase in NOX activity was significantly reduced to 7.07 ± 0.81 RLU/10⁵ cells by one hour pretreatment with apocynin (300 μ M) and reduced to 0.52 ± 0.06 RLU/10⁵ cells by one hour pretreatment with DPI (1 μ M). These data suggest that heat stress causes an increase in NOX activity and this contributes to ROS accumulation in hypothalamic neurons.

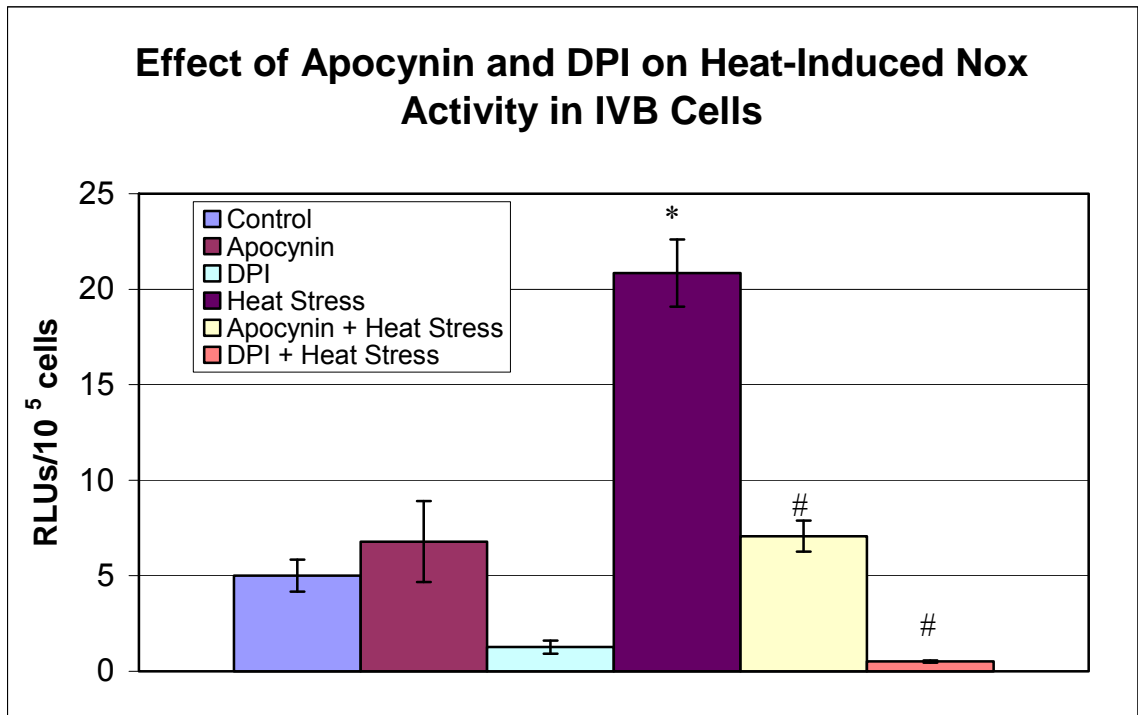


Figure 10. NOX activity in response to heat stress in hypothalamus IVB cells. The control bar represents NOX activity in non-heated vehicle-treated cells. The apocynin bar represents non-heated control cells treated for one hour with apocynin (300 μ M). The DPI bar represents non-heated control cells treated for one hour with DPI (1 μ M). The heat stress bar represents vehicle-treated cells treated for 15 minutes at 43°C followed by 15 minutes at 37°C. The apocynin + heat stress bar represents heat stressed cells pretreated for one hour with apocynin (300 μ M). The DPI + heat stress bar represents heat stressed cells pretreated for one hour with DPI (1 μ M). Values are means \pm standard error of three independent experiments. * indicates significantly different from control ($P < 0.05$). # indicates significantly different from heat stress ($P < 0.05$).

NOX activity increases in response to simulated ischemia/reperfusion in hypothalamus IVB cells:

To determine whether simulated ischemia/reperfusion produced a similar increase in NOX activity as found with heat stress, IVB cells were subjected to simulated ischemia/reperfusion and NOX activity was measured by chemiluminescence. IVB cells were pretreated for one hour with the NOX inhibitor apocynin (300 μM) and DPI (1 μM) and exposed to either control or one hour simulated ischemia followed by two hours reperfusion and NOX activity was measured. Control activity of NOX was 5.01 ± 0.83 RLUs/ 10^5 cells (figure 11). NOX activity in control cells was not affected by one hour treatment with the NOX inhibitor apocynin (300 μM) but was reduced by DPI (1 μM) to 1.27 ± 0.34 RLUs/ 10^5 cells. Simulated ischemia/reperfusion in vehicle-treated cells caused a significant increase in NOX activity to 13.3 ± 0.25 RLUs/ 10^5 cells. The simulated ischemia/reperfusion-induced increase in NOX activity was significantly reduced to 7.65 ± 1.09 RLUs/ 10^5 cells by one hour pretreatment with apocynin (300 μM) and to 0.91 ± 0.23 RLUs/ 10^5 cells by one hour pretreatment with DPI (1 μM). These data suggest that simulated ischemia/reperfusion causes an increase in NOX activity and this contributes to ROS accumulation in hypothalamic neurons.

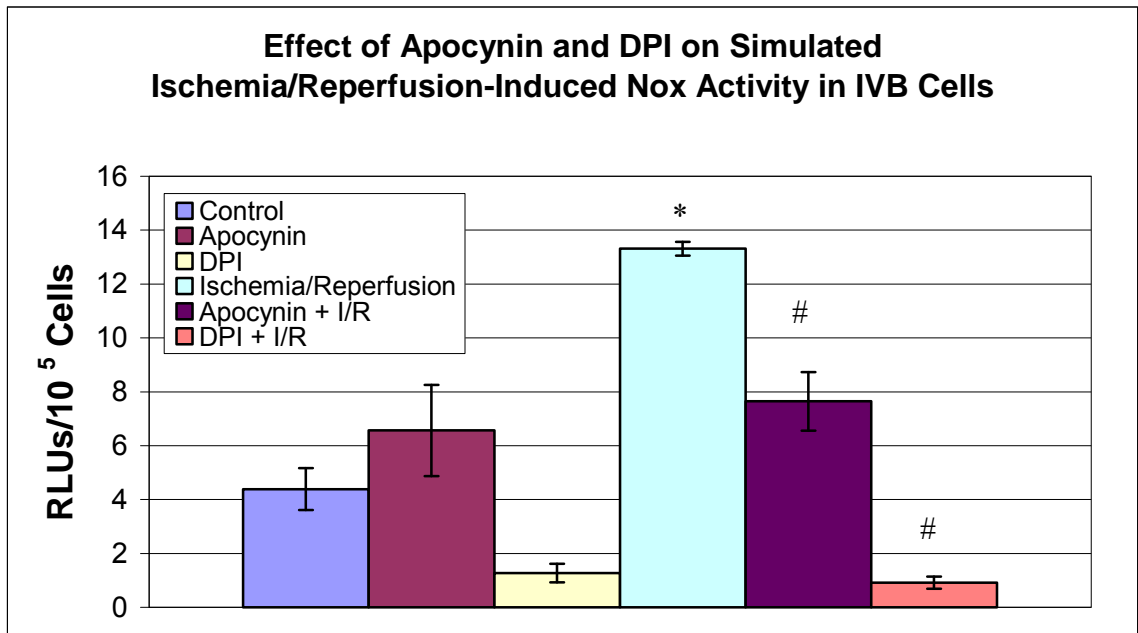


Figure 11. NOX activity in response to simulated ischemia/reperfusion in hypothalamus IVB cells. The control bar represents NOX activity in non-ischemic vehicle-treated cells. The apocynin bar represents non-ischemic control cells treated for one hour with apocynin (300 μ M). The DPI bar represents non-ischemic control cells treated for one hour with DPI (1 μ M). The ischemia/reperfusion bar represents vehicle-treated cells treated for one hour in ischemic media in a 37°C hypoxic chamber followed by two hours in reperfusion media in a 37°C incubator. The apocynin + ischemia/reperfusion bar represents simulated ischemia/reperfusion cells pretreated for one hour with apocynin (300 μ M). The DPI + ischemia/reperfusion bar represents simulated ischemia/reperfusion cells pretreated for one hour with DPI (1 μ M). Values are means \pm standard error of three independent experiments. * indicates significantly different from control ($P < 0.05$). # indicates significantly different from simulated ischemia/reperfusion ($P < 0.05$).

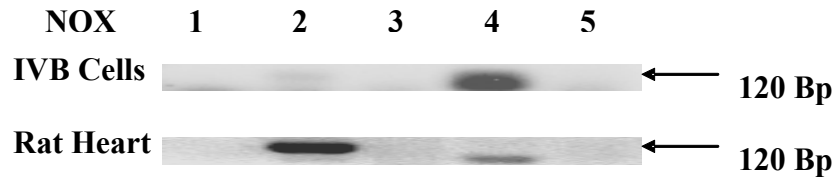
NOX gene and protein expression in hypothalamus IVB cells:

Following our findings that heat stress and simulated ischemia/reperfusion caused an increase in ROS generation and an increase in NOX activity, we wanted to determine the specific NOX isoform(s) involved in these responses. To determine the NOX isoforms expressed in hypothalamic neurons, we examined mRNA and protein expression of NOX in hypothalamus IVB cells. The NOX family of enzymes consists of seven different isoforms, but their expression in hypothalamic neurons has not been investigated. We tested the mRNA expression levels of NOX1-5, but did not test Duox1 and Duox2 because they are primarily found in the thyroid. We also tested the mRNA levels of the small GTPase Rac1 because Rac1 is a regulatory subunit of the NOX complex and has been shown to regulate ROS production in various cell types [137]. RNA was isolated from control IVB cells and rat hearts (positive control) and cDNA was synthesized using iScript cDNA synthesis kit (BioRad). Primers were designed using vector NTI software (Invitrogen) for NOX1-5 and Rac1 and RT-PCR was performed as described in section 5.2 of the methods. PCR analysis of the five NOX isoforms showed the presence of NOX2 and NOX4 isoforms in both IVB cells and rat heart (figure 12a). NOX1, NOX3 and NOX5 were not detected. Initially we saw a band for NOX2 in our IVB cells although it was faint and hard to visualize, therefore we performed another PCR on NOX2, NOX4 and the small GTPase Rac1 specifically. PCR analysis showed the presence of NOX4 and Rac1, but not NOX2 in IVB cells (figure 12b). To further analyze these findings, we cloned and sequenced the NOX2 and NOX4 PCR products and performed a BLAST search on the sequences. We found NOX2 did not match the sequence for NOX2 in the rat, suggesting NOX2 is not expressed in IVB cells. However,

NOX4 was 100% homologous with NOX4 in the rat suggesting NOX4 is the only isoform of NOX expressed in IVB cells. The mRNA expression levels of NOX1-5 did not change in response to heat stress or simulated ischemia/reperfusion as tested by real-time PCR.

Next we wanted to determine if protein expression of NOX4 matched the mRNA expression and confirm that NOX2 was not expressed in IVB cells. To determine the protein expression of NOX2 and NOX4, we performed western blots using rabbit polyclonal antibodies for NOX2 and NOX4 along with their blocking peptides (Santa Cruz Biotechnology) in control IVB cells. Rat brain was used as a control reference tissue. In rat brain, NOX2 and NOX4 immunoreactivity were detected (figure 13a), but only NOX4 immunoreactivity was detected in IVB cells (figure 13b). To determine the cellular location of NOX4, we performed differential centrifugation and collected nuclear, cytosolic and plasma membrane fractions and performed western blots using the rabbit polyclonal antibodies for NOX4 on each fraction. We found NOX4 immunoreactivity in each of the fractions tested with NOX4 showing the highest expression in the cytosol (figure 13c), which did not change following exposure to heat stress or simulated ischemia/reperfusion. Lamin A/C was used as the positive control for the nuclear fraction. These data suggest that NOX4 is the only NOX isoform expressed in the IVB cells and it resides in the cytoplasm, nucleus and membrane.

a)



b)

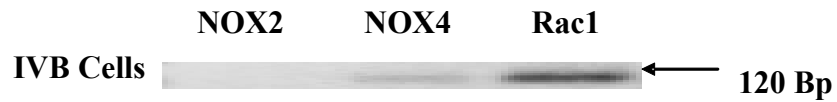
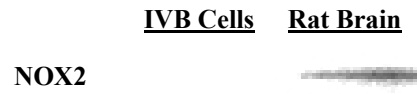
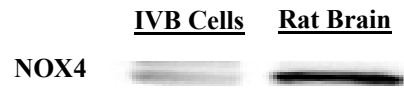


Figure 12. PCR analysis for NOX in control IVB cells and rat heart. a) NOX mRNA expression in control IVB cells and rat heart. One microgram of RNA isolated was reverse transcribed and used for PCR with primers specific for NOX1-5. Rat heart was used as reference tissue. b) NOX2, NOX4 and Rac1 mRNA expression in control IVB cells. Pictures are representative of 2 independent experiments.

a)



b)



c)

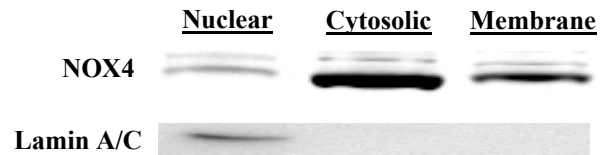


Figure 13. Western blots for NOX2 and NOX4 in IVB cells and rat brain. a) NOX2 Protein Expression. Control IVB cells and control rat brain protein expression was measured using western blot. Rat brain was used as reference tissue. b) NOX4 Protein Expression. c) NOX4 Protein Localization. Lamin A/C was used as the nuclear marker. Pictures are representative of 2 independent experiments.

Role of PKC in heat stress-induced oxidative stress in hypothalamus IVB cells:

PKC has been suggested to play a role in activating NOX by phosphorylating the cytosolic subunits (p47^{phox}, p40^{phox} and p67^{phox})[29,31]. To determine the mechanism of activation for NOX in response to heat stress, the PKC inhibitors Gö6976 (PKC α , PKC β _I and PKC μ inhibitor) and Ro-31-8220 (PKC α , PKC β _I, PKC β _{II}, PKC γ and PKC ϵ inhibitor) were used, and ROS generation was measured using fluorescence microscopy. IVB cells were grown on electrically charged coverslips and treated for one hour with Gö6976 (5 nM), Ro-31-8220 (5 nM) or their vehicle and exposed to control or heat stress conditions as previously described. The inhibitor concentrations were chosen based on published values of half maximal inhibition concentration (IC₅₀) for Gö6976 and Ro-31-8220 on PKC activity [205,341] shown in table 3. Treatment with Gö6976 (5 nM) or Ro-31-8220 (5 nM) did not alter fluorescence compared to control vehicle-treated cells. Treatment with either Gö6976 (5 nM) or Ro-31-8220 (5 nM) prior to heat stress attenuated heat-induced ROS generation to control levels (figure 14b and 14c). These data suggest PKC is involved in regulating ROS accumulation in response to heat stress in hypothalamus IVB cells.

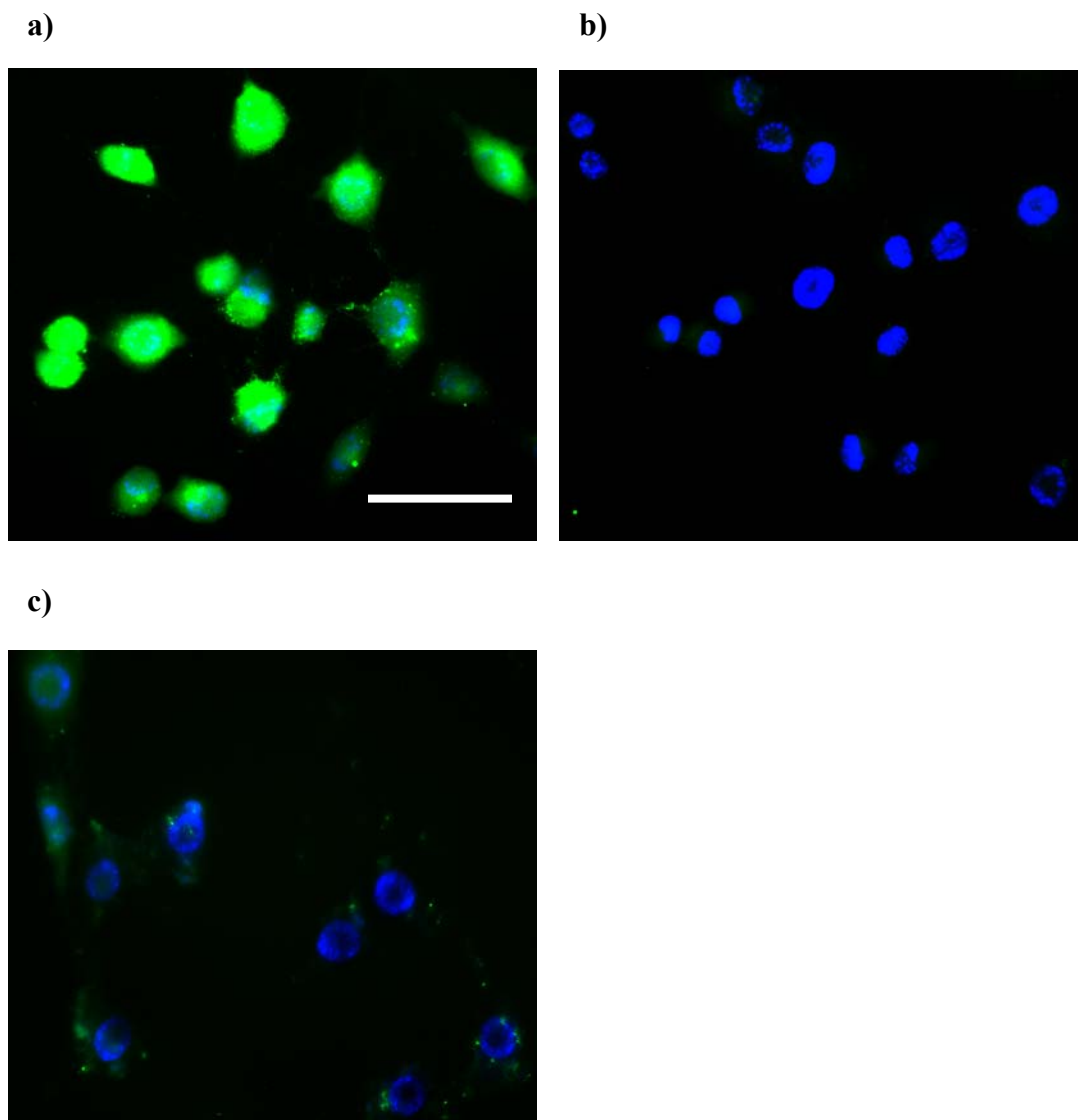


Figure 14. Effect of the PKC inhibitors Gö6976 and Ro-31-8220 on heat-induced ROS generation in hypothalamus IVB cells. Cells were double labeled with a Hoescht stain (Excitation/Emission of 350/461 nm) which fluoresces blue in the presence of nucleic acids and a carboxy-H₂DCFA stain (Excitation/Emission of 495/529 nm) which fluoresces green in the presence of ROS. a) Vehicle-treated cells heated for 15 minutes at 43°C followed by 15 minutes recovery at 37°C. b) Cells pretreated for one hour with Gö6976 (5 nM) followed by heat stress. c) Cells pretreated for one hour with Ro-31-8220 (5 nM) followed by heat stress. All pictures are representative of 3 independent experiments. Scale bar = 35 micrometers.

Role of PKC in simulated ischemia/reperfusion-induced oxidative stress in hypothalamus IVB cells:

To determine if the mechanism of activation for NOX in response to simulated ischemia/reperfusion was similar to heat stress, the PKC inhibitors Gö6976 (PKC α , PKC β _I and PKC μ inhibitor) and Ro-31-8220 (PKC α , PKC β _I, PKC β _{II}, PKC γ and PKC ϵ inhibitor) were used, and ROS generation was measured by fluorescence microscopy. IVB cells were grown on electrically charged coverslips and treated for one hour with Gö6976 (5 nM), Ro-31-8220 (5 nM) or their vehicle and subjected to control or simulated ischemia/reperfusion conditions as previously described. The inhibitor concentrations used were based on the previous experiments with heat stress. Gö6976 (5 nM) and Ro-31-8220 (5 nM) did not alter fluorescence in IVB cells compared to vehicle-treated control cells. In vehicle-treated cells, one hour ischemia followed by two hours reperfusion caused an increase in green fluorescence indicative of an increase in ROS generation (figure 15a). Treatment for one hour with either Gö6976 (5 nM) or Ro-31-8220 (5 nM) prior to simulated ischemia/reperfusion attenuated simulated ischemia/reperfusion-induced ROS generation to levels found in control cells (figure 15b and 15c). These data suggest PKC is involved in regulating ROS accumulation in response to simulated ischemia/reperfusion in hypothalamus IVB cells.

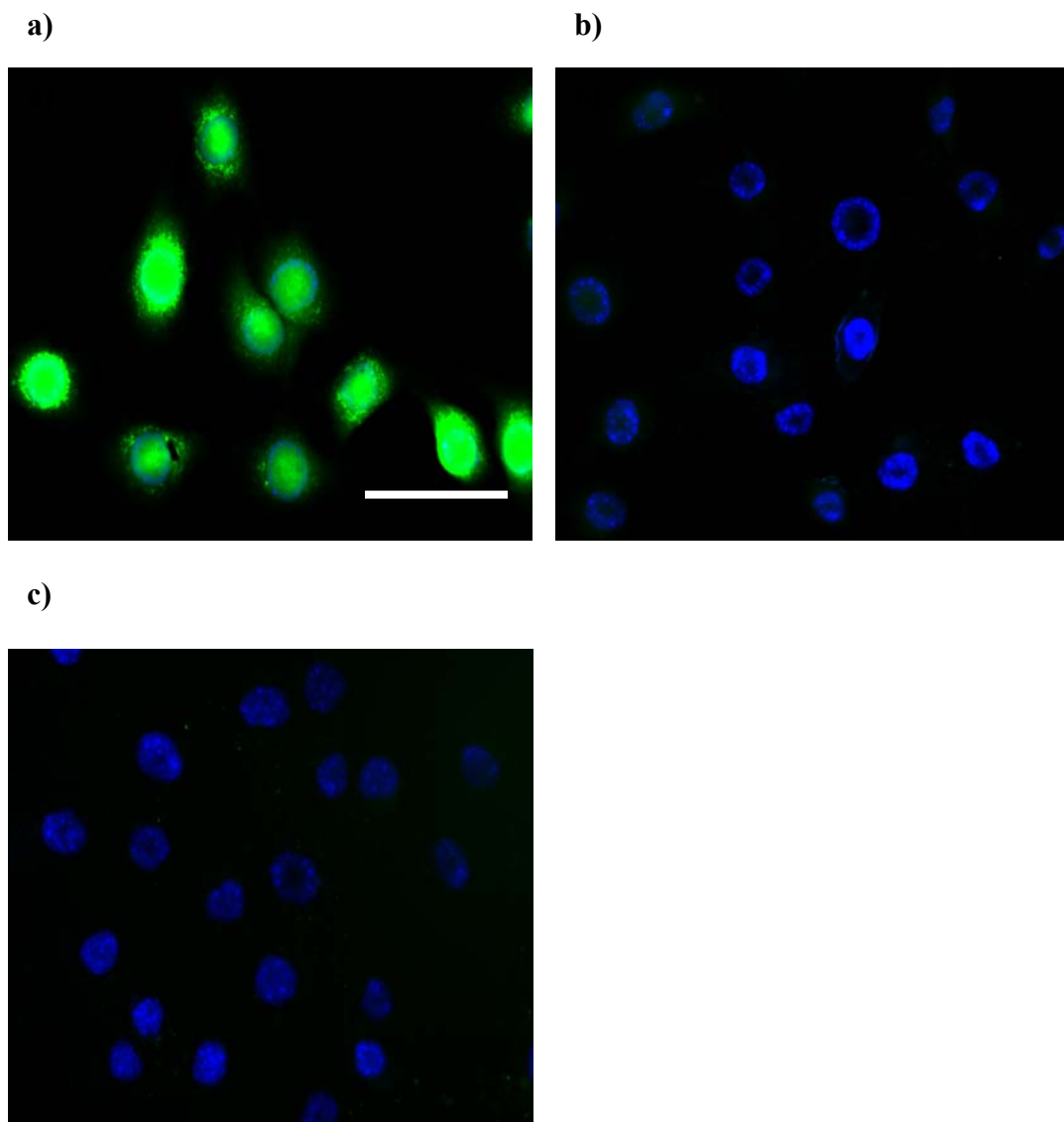


Figure 15. Effect of the PKC inhibitors Gö6976 and Ro-31-8220 on simulated ischemia/reperfusion-induced ROS generation in hypothalamus IVB cells. Cells were double labeled with a Hoescht stain (Excitation/Emission of 350/461 nm) which fluoresces blue in the presence of nucleic acids and a carboxy-H₂DCFA stain (Excitation/Emission of 495/529 nm) which fluoresces green in the presence of ROS. a) Vehicle-treated cells subjected to one hour simulated ischemia followed by two hours reperfusion. b) Cells pretreated for one hour with Gö6976 (5 nM) followed by simulated ischemia/reperfusion. c) Cells pretreated for one hour with Ro-31-8220 (5 nM) followed by simulated ischemia/reperfusion. All pictures are representative of 3 independent experiments.

Effect of PKC inhibitors on heat stress-induced NOX activity in hypothalamus IVB

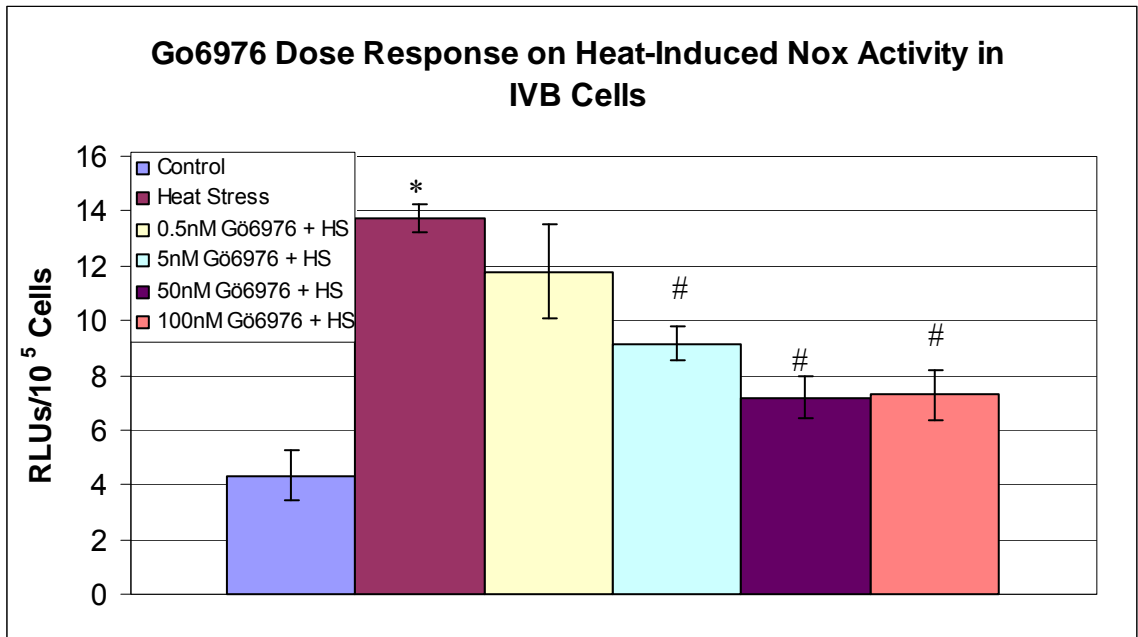
cells:

Following our findings that the PKC inhibitors Gö6976 and Ro-31-8220 inhibited heat-induced ROS generation, we wanted to determine if PKC mediated the increase in NOX activity in response to heat stress. To determine the effect of the PKC inhibitors on NOX activity, dose response curves were performed using the PKC inhibitors Gö6976 (0.5 nM – 100 nM), which inhibits PKC α , PKC β _I and PKC μ , and calphostin C (5 nM – 500 nM), which inhibits conventional and novel isoforms of PKC. IVB cells were treated for one hour with either Gö6976 (0.5 nM – 100 nM) or calphostin C (5 nM – 500 nM) and then exposed to heat stress as previously described. The PKC inhibitors had no effect on control NOX activity at any concentration (figure 16c). Heat stress caused a significant increase in NOX activity which was inhibited by the PKC inhibitors Gö6976 and calphostin C in a dose-dependent manner. The maximal inhibition of NOX activity by Gö6976 and calphostin C occurred at 50 nM (figure 16a and 16b). At this concentration heat-induced NOX activity was reduced to near control levels. Since treatment with Gö6976 at 5 nM and 50 nM appeared to have similar inhibitory efficiency at reducing heat-induced NOX activity 5 nM Gö6976 was chosen for the remaining experiments. Calphostin C was used at 50 nM for all remaining experiments.

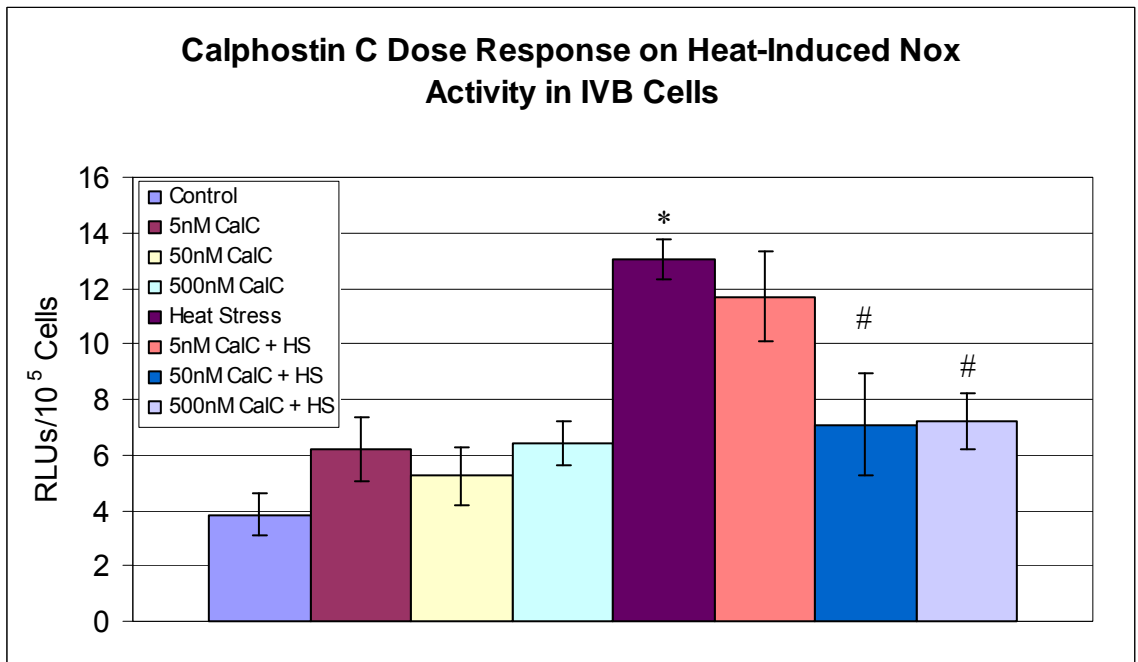
After performing the dose response curves for Gö6976 and calphostin C, we wanted to determine if the PKC inhibitor Ro-31-8220, which inhibits PKC α , PKC β _I, PKC β _{II}, PKC γ and PKC ϵ , also inhibited heat-induced NOX activation in the IVB cells. To test this, cells were treated for one hour with the PKC inhibitors Gö6976 (5 nM), Ro-31-8220 (5 nM) or calphostin C (50 nM) prior to heat stress and NOX activity was

measured. The PKC inhibitors Gö6976, Ro-31-8220 and calphostin C significantly reduced heat-induced NOX activation to control levels (figure 16c). These data suggest that PKC is involved in regulating NOX activation and ROS generation in response to heat stress in hypothalamus IVB cells.

a)



b)



c)

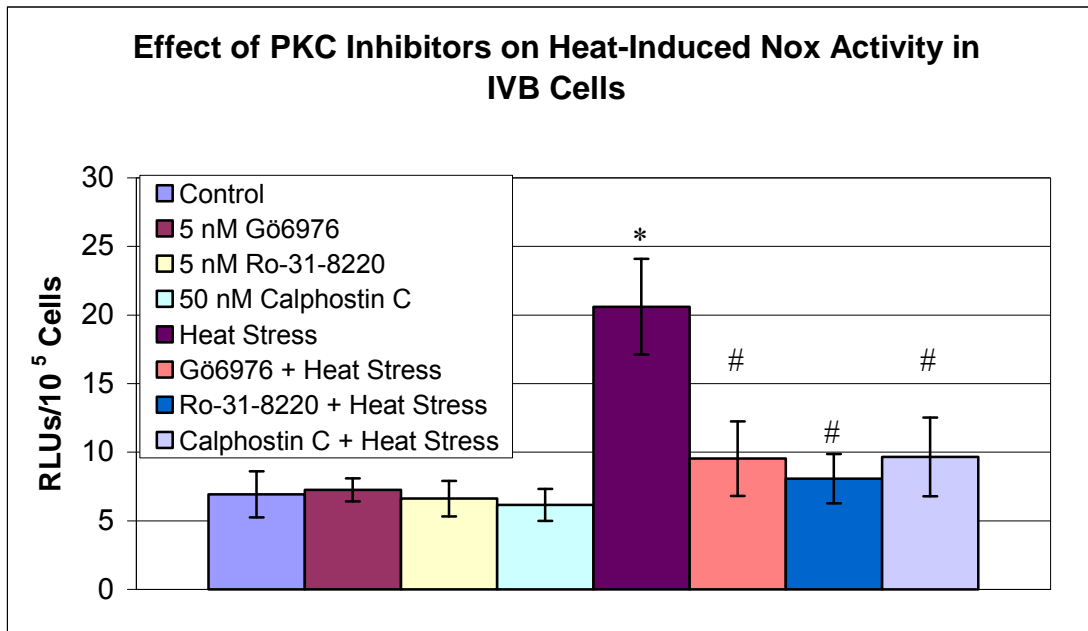


Figure 16. Effect of PKC inhibitors on heat-induced NOX activity. a) Gö6976 dose response curve in heat stressed IVB cells. The control bar represents NOX activity in non-heated vehicle-treated cells. The heat stress bar represents vehicle-treated cells treated for 15 minutes at 43°C followed by 15 minutes in a 37°C incubator. The 0.5 nM Gö6976 + heat stress bar represents heat stressed cells pretreated for one hour with Gö6976 (0.5 nM). The 5 nM Gö6976 + heat stress bar represents heat stressed cells pretreated for one hour with Gö6976 (5 nM). The 50 nM and 100 nM Gö6976 + heat stress bar represents heat stressed cells pretreated for one hour with Gö6976 (50 nM and 100 nM). b) Calphostin C dose response curve in heat stressed IVB cells. The 5, 50 and 100 nM calphostin C bars represent non-heated control cells treated for one hour with calphostin C at their respective concentrations. The heat stress bar represents vehicle-treated heat stressed IVB cells. The 5 nM calphostin C + heat stress bar represents heat stressed cells pretreated for one hour with calphostin C (5 nM). The 50 and 100 nM calphostin C + heat stress bars represent heat stressed cells pretreated for one hour with calphostin C (50 nM and 100 nM). c) The Gö6976, Ro-31-8220 and calphostin C bars represent non-heated control cells treated for one hour with Gö6976 (5 nM), Ro-31-8220 (5 nM) and calphostin C (50 nM). The heat stress bar represents vehicle-treated heat stressed IVB cells. The Gö6976, Ro-31-8220 and calphostin C + heat stress bars represent heat stressed cells pretreated for one hour with Gö6976 (5 nM), Ro-31-8220 (5 nM) and calphostin C (50 nM). Values are means ± standard error of three independent experiments. * indicates significantly different from control (P<0.05). # indicates significantly different from heat stress (P<0.05).

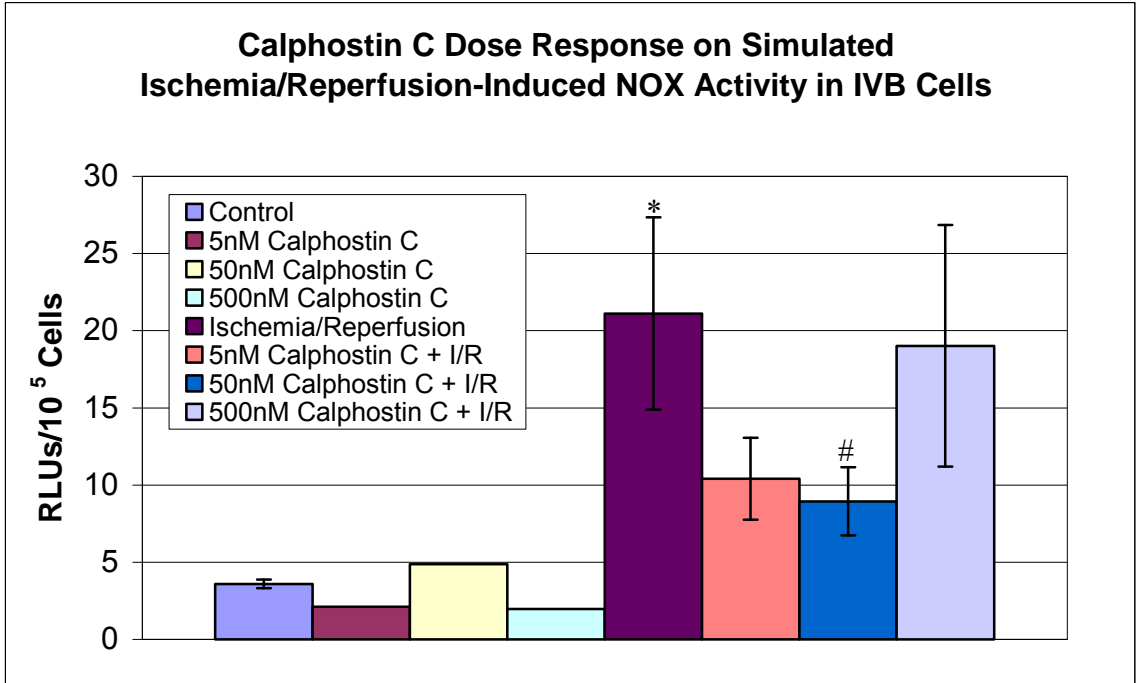
Effect of PKC inhibitors on simulated ischemia/reperfusion-induced NOX activity in hypothalamus IVB cells:

To determine if PKC was involved in the activation of NOX in response to simulated ischemia/reperfusion similar to heat stress, the PKC inhibitors Gö6976 (PKC α , PKC β _I and PKC μ inhibitor), rottlerin (PKC δ inhibitor), Ro-31-8220 (PKC α , PKC β _I, PKC β _{II}, PKC γ and PKC ϵ inhibitor) and calphostin C (general PKC inhibitor) were used, and NOX activity was measured using chemiluminescence. A dose response curve was performed for calphostin C (5 – 500 nM) to determine if there was a dose dependent inhibition of simulated ischemia/reperfusion-induced NOX activation (figure 17a). Since calphostin C is the general PKC inhibitor it was the only PKC inhibitor that we performed a dose response curve for to determine if PKC regulated NOX activation in cells exposed to simulated ischemia/reperfusion. Control NOX activity was 3.59 ± 0.28 RLU/10⁵ cells which was not changed in control cells treated for one hour with calphostin C at any concentration. Simulated ischemia/reperfusion caused a significant increase in NOX activity to 21.1 ± 6.23 RLU/10⁵ cells, which was significantly inhibited by the pretreatment for one hour with PKC inhibitor calphostin C (50 nM), but not 5 nM or 500 nM. The maximal inhibition of NOX activity by calphostin C was found at the concentration of 50 nM, which reduced simulated ischemia/reperfusion-induced NOX activity to 8.94 ± 2.20 RLU/10⁵ cells, but not to control levels. Based on these findings, the remainder of experiments were performed using 50 nM calphostin C.

Next, we wanted to determine the PKC isoforms involved in activating NOX in response to simulated ischemia/reperfusion by testing the PKC inhibitors Gö6976 (PKC α , PKC β _I and PKC μ inhibitor), rottlerin (PKC δ inhibitor) and Ro-31-8220 (PKC α , PKC β _I,

PKC β_{II} , PKC γ and PKC ϵ inhibitor) on NOX activity. Cells were treated with the PKC inhibitors Gö6976 (5 nM), Ro-31-8220 (5 nM) or calphostin C (50 nM) for one hour prior to simulated ischemia/reperfusion and NOX activity was measured. Control NOX activity was 4.52 ± 0.29 RLU/10⁵ cells (figure 17b). Gö6976 (5 nM), Ro-31-8220 (5 nM) and calphostin C (50 nM) did not cause a change in control NOX activity, whereas treatment for one hour with rottlerin (1 μ M) caused an increase in NOX activity to $9.35 \pm$ RLU/10⁵ cells. Simulated ischemia/reperfusion caused a significant increase in NOX activity to 21.7 ± 2.71 RLU/10⁵ cells compared to control. Pretreatment with the PKC inhibitors Gö6976 (5 nM), Ro-31-8220 (5 nM) and calphostin C (50 nM) for one hour prior to simulated ischemia/reperfusion significantly reduced simulated ischemia/reperfusion-induced NOX activation, but not to baseline levels. In the presence of the PKC inhibitors, NOX activity in response to simulated ischemia/reperfusion was significantly higher than baseline. Therefore, the PKC inhibitors did not completely inhibit simulated ischemia/reperfusion-induced NOX activation as they did with heat stress. These data suggest that simulated ischemia/reperfusion-induced NOX activation is both PKC-dependent and PKC-independent in hypothalamus IVB cells.

a)



b)

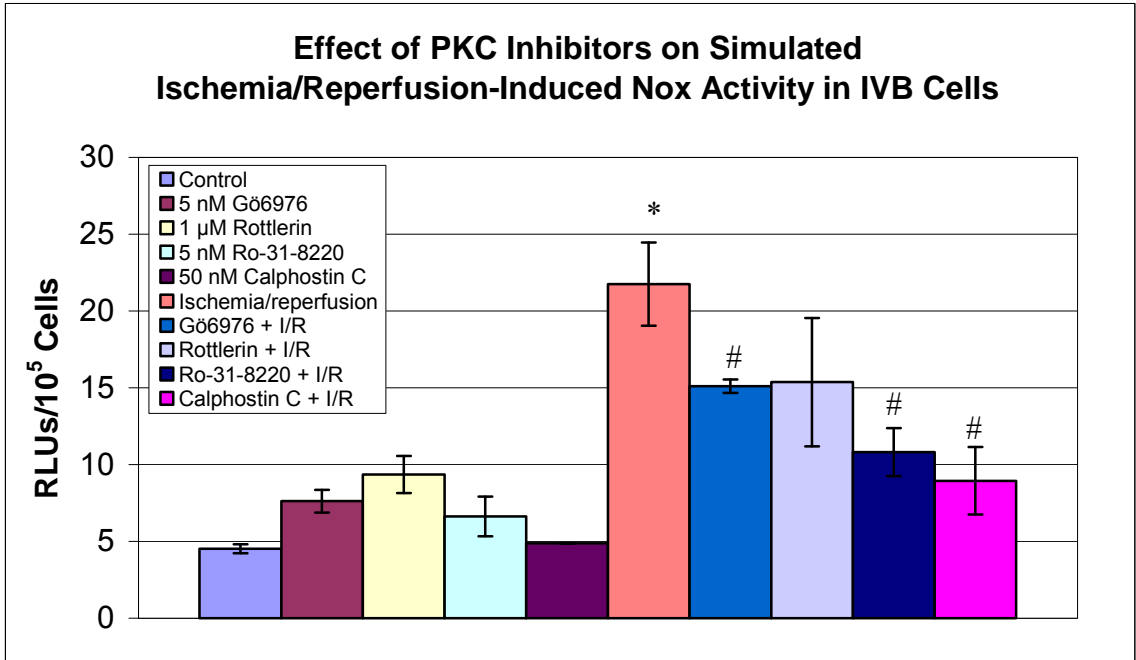


Figure 17. Effect of PKC inhibitors on simulated ischemia/reperfusion-induced NOX activity in hypothalamus IVB cells. a) Calphostin C dose response curve in simulated ischemia/reperfused IVB cells. The control bar represents NOX activity in non-ischemic vehicle-treated cells. The 5, 50 and 100 nM calphostin C bars represent non-ischemic control cells treated for one hour with calphostin C at their respective concentrations. The ischemia/reperfusion bar represents vehicle-treated cells treated for one hour in ischemic media in a 37°C hypoxic chamber followed by two hours in reperfusion media in a 37°C incubator. The 5 nM and 500 nM calphostin C + ischemia/reperfusion bars represent simulated ischemia/reperfused cells pretreated for one hour with calphostin C (5 nM or 500 nM). The 50 nM calphostin C + ischemia/reperfusion bar represent simulated ischemia/reperfused cells pretreated for one hour with calphostin C (50 nM). b) PKC inhibitors effect on simulated ischemia/reperfusion-induced NOX activity. The control bar represents NOX activity in non-ischemic vehicle-treated cells. The Gö6976, Ro-31-8220, and calphostin C bars represent non-ischemic control cells treated for one hour with Gö6976 (5 nM), Ro-31-8220 (5 nM) and calphostin C (50 nM). The rottlerin bar represents non-ischemic control cells treated for one hour with rottlerin (1 µM). The ischemia/reperfusion bar represents vehicle-treated cells exposed to simulated ischemia/reperfusion. The Gö6976 + ischemia/reperfusion bar represents simulated ischemia/reperfused cells pretreated for one hour with Gö6976 (5 nM). The rottlerin + ischemia/reperfusion bar represents simulated ischemia/reperfused cells pretreated for one hour with rottlerin (1 µM). The Ro-31-8220 + ischemia/reperfusion bar represents simulated ischemia/reperfused cells pretreated for one hour with Ro31-8220 (5 nM). The calphostin C + ischemia/reperfusion bar represents simulated ischemia/reperfused cells pretreated for one hour with calphostin C (50 nM). Values are means ± standard error of three independent experiments. * indicates significantly different from control (P<0.05). # indicates significantly different from simulated ischemia/reperfusion (P<0.05).

Effect of PKC and PI3 kinase inhibitors on heat- and simulated ischemia/reperfusion-induced NOX activation in hypothalamus IVB cells:

PI3 kinase regulates various cellular functions, mainly through activating Akt, including cell growth, proliferation, differentiation, motility, survival and intracellular trafficking [8,41,166,214]. PI3 kinase has also been linked to growth factor-induced ROS generation derived from NOX1 in nonphagocytic cells [245]. Therefore to determine if PI3 kinase was involved in the PKC-independent portion of NOX activation in response to simulated ischemia/reperfusion, the PI3 kinase inhibitor LY294002 was used along with the PKC inhibitor calphostin C and NOX activity was measured. We also tested the effects of LY294002 in combination with calphostin C in heat stressed cells to ensure PI3 kinase did not play a role in heat-induced NOX activation. Cells were treated for one hour in the presence of LY294002 (10 nM) alone or in combination with calphostin C (50 nM) and then exposed to heat stress or simulated ischemia/reperfusion and NOX activity was measured. Control NOX activity was 5.40 ± 0.90 RLU_s/10⁵ cells, which was not altered in control cells treated with either LY294002 (10 nM) or calphostin C (50 nM) (figure 18). Heat stress caused a significant increase in NOX activity to 18.9 ± 1.91 RLU_s/10⁵ cells, which did not change with one hour pretreatment with LY294002 (10 nM). Pretreatment of heat stressed cells for one hour with either calphostin C (50 nM) alone or in combination with LY294002 (10 nM) caused a significant decrease in heat-induced NOX activity to 8.72 ± 2.52 RLU_s/10⁵ cells. Simulated ischemia/reperfusion caused a significant increase in NOX activity to 17.8 ± 1.89 RLU_s/10⁵ cells. Cells pretreated for one hour with LY294002 (10 nM) or calphostin C (50 nM) alone showed a significant decrease in simulated ischemia/reperfusion-

induced NOX activity to 12.0 ± 1.46 RLU_s/10⁵ cells and 10.3 ± 0.77 RLU_s/10⁵ cells, respectively, but not to basal levels. However, cells pretreated for one hour with LY294002 (10 nM) and calphostin C (50 nM) together showed a significant decrease in simulated ischemia/reperfusion-induced NOX activity to 8.08 ± 1.09 RLU_s/10⁵ cells to near control levels. These data suggest simulated ischemia/reperfusion activates NOX through both PKC and PI3 kinase to produce ROS, whereas heat stress activates NOX solely through PKC in hypothalamus IVB cells.

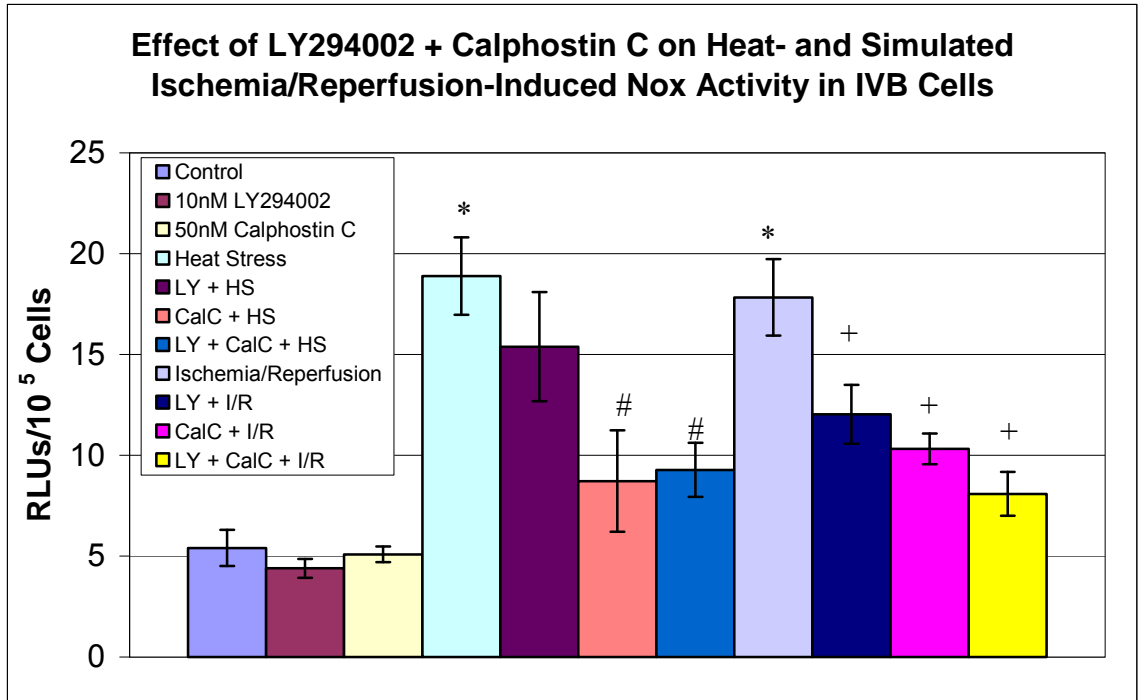


Figure 18. Effect of PKC and PI3 kinase inhibitors on heat- and simulated ischemia/reperfusion-induced NOX activity in hypothalamus IVB cells. The control bar represents NOX activity in vehicle-treated cells. The LY294002 and calphostin C bars represent control cells treated for one hour with the PI3 kinase inhibitor LY294002 (10 nM) or the PKC inhibitor calphostin C (50 nM). The heat stress bar represents vehicle-treated cells treated for 15 minutes at 43°C followed by 15 minutes in a 37°C incubator. The LY294002 + heat stress bar represents cells treated for one hour with LY294002 (10 nM) prior to exposure to heat stress. The calphostin C + heat stress and the LY294002 + calphostin C + heat stress bars represent heat stressed cells pretreated for one hour with either calphostin C (50 nM) alone or LY294002 (10 nM) and calphostin C (50 nM) combined. The ischemia/reperfusion bar represents vehicle-treated cells treated for one hour in ischemic media in a 37°C hypoxic chamber followed by two hours in reperfusion media in a 37°C incubator. The LY294002 + I/R and calphostin C + I/R bars represent simulated ischemia/reperfused cells that were pretreated for one hour with either LY294002 (10 nM) or calphostin C (50 nM). The LY294002 + calphostin C + I/R bar represents IVB cells treated for one hour with LY294002 (10 nM) and calphostin C (50 nM) combined prior to exposure to simulated ischemia/reperfusion. Values are means ± standard error of three independent experiments. * indicates significantly different from control (P<0.05). # indicates significantly different from heat stress (P<0.05). + indicates significantly different from simulated ischemia/reperfusion (P<0.05)

PMA activates NOX via PKC in hypothalamus IVB cells:

The phorbol ester phorbol-12-myristate-13-acetate (PMA) has been reported to increase NOX activity in various cell types and was used as a positive control for the NOX activity experiments. PMA is a widely used activator of both conventional and novel isoforms of PKC and was used with the selected PKC inhibitors to determine if PMA-induced NOX activation required PKC in IVB cells. We also tested the PI3 kinase inhibitor wortmannin to determine if PMA activated NOX through PKC and PI3 kinase, which we hypothesized; PMA would only activate PKC and not PI3 kinase. Cells were treated for thirty minutes with PMA (20 nM) and NOX activity was measured using chemiluminescence. Control NOX activity was 6.73 ± 0.52 RLU/10⁵ cells and PMA (20 nM) treatment caused a significant increase in NOX activity similar to heat stress and ischemia/reperfusion to 15.8 ± 0.52 RLU/10⁵ cells (figure 19). To determine if PMA activated NOX via PKC in IVB cells, cells were treated for one hour with Gö6976 (5 nM), Ro-31-8220 (5 nM) and calphostin C (50 nM) and then exposed to PMA (20 nM) for thirty minutes and NOX activity was measured. Treatment with Gö6976 (5 nM) for one hour prior to exposure to PMA (20 nM), did not cause a significant decrease in PMA-stimulated NOX activity (figure 19). On the other hand, treatment for one hour with either Ro-31-8220 (5 nM) or calphostin C (50 nM) prior to PMA (20 nM) exposure caused a significant decrease in NOX activity compared to PMA treatment. In the presence of Ro-31-8220 and calphostin C, PMA-induced NOX activity was still significantly elevated over baseline. To determine if PMA activated NOX through PKC and PI3 kinase in IVB cells, cells were treated for one hour with either wortmannin (100 nM) alone or in combination with calphostin C (50 nM) followed by thirty minutes of

PMA (20 nM) treatment and NOX activity was measured. Treatment for one hour with wortmannin (100 nM) had no effect on control NOX activity (figure 19), however treatment for one hour with wortmannin (100 nM) prior to exposure to PMA (20 nM) caused a significant decrease in NOX activity compared to PMA treatment. In the presence of wortmannin, PMA-induced NOX activity was still significantly elevated above baseline. However, treatment for one hour with both wortmannin (100 nM) and calphostin C (50 nM) combined, caused a significant decrease in PMA-induced NOX activation to near baseline (figure 19). These data suggest PMA stimulates NOX in IVB cells and the PMA-induced NOX activation appears to be mainly through PKC, but PI3 kinase plays a minor role in PMA-induced NOX activation in hypothalamus IVB cells.

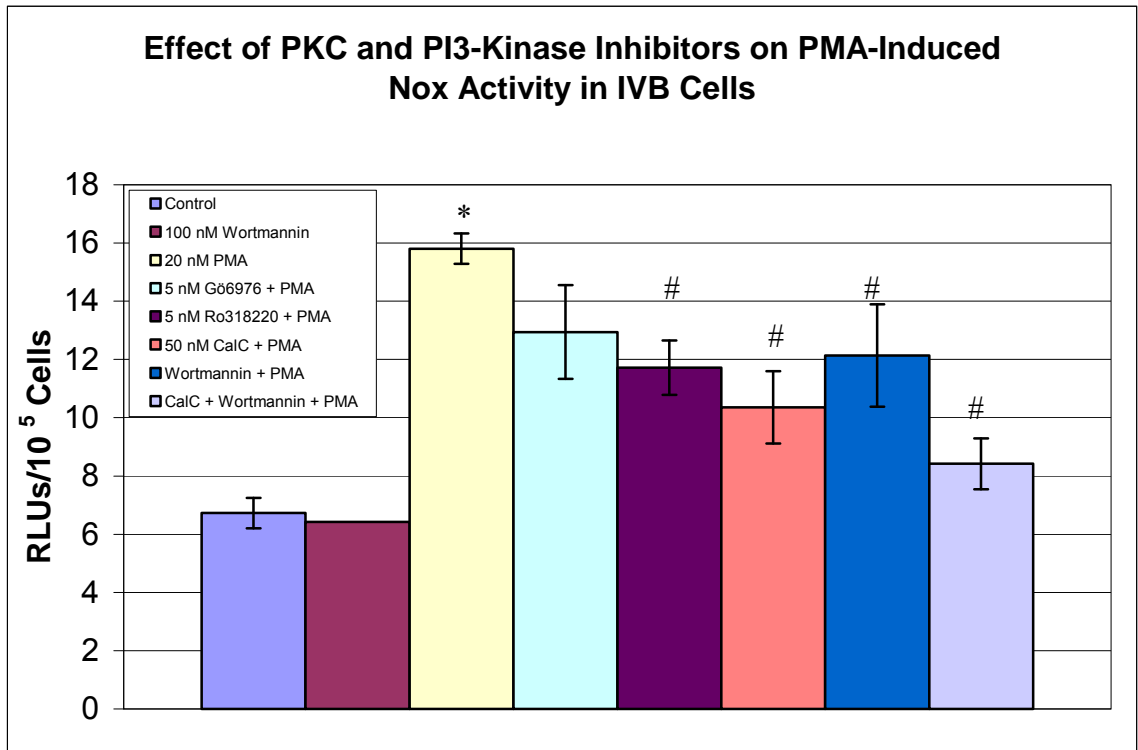


Figure 19. NOX activity in response to PMA in hypothalamus IVB cells. The control bar represents NOX activity in vehicle-treated cells. The wortmannin bar represents cells treated for one hour with wortmannin (100 nM). The PMA bar represents cells treated for thirty minutes with PMA (20 nM). The Gö6976 + PMA bar represents cells treated for one hour with Gö6976 (5 nM) followed by thirty minutes of PMA (20 nM). The Ro-31-8220 + PMA bar represents cells treated for one hour with Ro-31-8220 (5 nM) followed by thirty minutes of PMA (20 nM). The Calphostin C + PMA bar represents cells treated for one hour with calphostin C (50 nM) followed by thirty minutes of PMA (20 nM). The wortmannin + PMA bar represents cells treated for one hour with wortmannin (100 nM) prior to PMA (20 nM) exposure. The calphostin C + wortmannin + PMA bar represents cells treated for one hour with both calphostin C (50 nM) and wortmannin (100 nM) prior to PMA (20 nM) exposure. Values are means \pm standard error of three independent experiments. * indicates significantly different from control ($p < 0.05$). # indicates significantly different from PMA ($p < 0.05$)

PKC mRNA expression and protein expression in hypothalamus IVB cells:

To determine the specific PKC isoforms expressed in IVB cells, we examined the expression of various PKCs at the mRNA and protein levels. The PKC family consists of nearly twenty different homologues expressed throughout the body. We tested the mRNA expression levels of PKC α , PKC β , PKC δ , PKC ϵ , PKC ζ and PKC μ . RNA was isolated from control IVB cells and rat hearts (reference tissue) and cDNA was synthesized using iScript cDNA synthesis kit (BioRad). Primers were designed for PKC μ and PKC β using vector NTI software (Invitrogen) and the other primers were purchased from Sigma and PCR was performed as described in section 5.2 of the methods. PCR analysis of the six PKC isoforms tested showed the presence of all isoforms except PKC β (figure 20). PKC β was not detected in IVB cells, but was in reference tissue. To examine protein expression, we performed western blots using mouse monoclonal antibodies for PKC α , PKC δ , PKC ϵ , PKC ζ , PKC μ and PKC β (Transduction Laboratories, Lexington, KY). PKC α , PKC δ , PKC ϵ , PKC ζ , PKC μ immunoreactivity was detected in IVB cells, but PKC β was not detected (figure 21). These data suggest that heat- and simulated ischemia/reperfusion-induced NOX activation and ROS generation are regulated by PKC α in IVB cells.

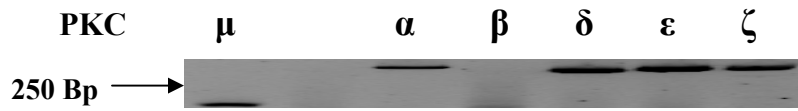


Figure 20. PKC μ , PKC α , PKC β , PKC δ , PKC ϵ and PKC ζ mRNA expression in control hypothalamus IVB cells. One microgram of RNA was reverse transcribed and used for PCR with primers specific for PKC μ , PKC α , PKC δ , PKC ϵ , PKC ζ and PKC β . Pictures are representative of 2 independent experiments.

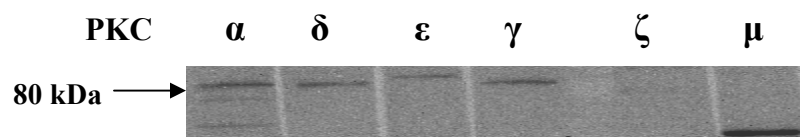


Figure 21. Western blot for PKC α , PKC δ , PKC ϵ , PKC γ , PKC ζ and PKC μ in IVB cells. Control IVB cells protein expression was measured using western blot. Pictures are representative of 2 independent experiments.

DISCUSSION

Ischemia/reperfusion-related injuries are associated with a wide range of diverse disorders including but not limited to aging, heat stroke, diabetes and Alzheimer's disease. Ischemia/reperfusion is known to cause oxidative stress through the generation of reactive oxygen species (ROS) and the resulting oxidative stress is thought to be a contributing factor in the progression of these neurological disorders [345]. In addition to ischemia/reperfusion injury, oxidative stress has also been reported to occur in response to heat stress in the brain and is thought to be one of the main contributors to the progression of heat-related illnesses [353]. In the present study, we examined whether simulated ischemia/reperfusion and mild heat stress increases ROS generation through similar mechanisms in cultured hypothalamic cells. Hypothalamus IVB cells were grown under normal culture conditions and either heat stressed at 43°C for 15 minutes followed by 15 minutes recovery or exposed to simulated ischemia/reperfusion by incubation for 1 hour in ischemic media in the absence of oxygen followed by 2 hours incubation in normal oxygenated media (reperfusion). Heat stress caused a significant increase in HSP70 and HO-1 gene expression as measured by real time RT-PCR. Heat stress also caused an increase in cytoplasmic HO-1 protein expression and nuclear translocation of HSF-1 as measured by western blot. Heat stress and simulated ischemia/reperfusion increased ROS generation as measured by the fluorescent indicator carboxy-H₂DCFDA. The increase in ROS was attenuated by pretreatment with the NOX inhibitor apocynin

and the PKC inhibitors Gö6976 and Ro-31-8220. To further investigate the generation of ROS, we measured NOX activity using chemiluminescence. Similar to what was seen with ROS generation, both mild heat stress and simulated ischemia/reperfusion increased NOX activity and these effects were blocked by apocynin, DPI, Gö6976, Ro-31-8220 and calphostin C. Furthermore, using RT-PCR and western blot analysis, NOX4 and PKC α were found to be expressed in IVB cells. These results suggest that both heat stress and simulated ischemia/reperfusion cause oxidative stress through PKC α -mediated NOX4 activation in hypothalamic IVB cells.

The hypothalamus is a part of the hypothalamic-pituitary-adrenal (HPA) axis, which controls cortisol or corticosterone levels released into the bloodstream in response to stressful stimuli. The hypothalamus secretes corticotrophin releasing hormone (CRH) which acts upon the pituitary to release ACTH into the blood. ACTH is then released into the blood stream where it stimulates the adrenal glands to release cortisol which signals to the body that it is in a state of stress and initiates a host of physiological responses. Therefore the hypothalamus is an important area of the brain for the study of the effects of heat stress and ischemia/reperfusion which both have been shown to cause increases in cortisol levels [288]. To study the effects of heat stress and simulated ischemia/reperfusion in hypothalamus, we obtained the rat hypothalamus IVB cell line as a generous gift from J.J. Mulcahey (University of Cincinnati, OH). IVB cells were developed from the hypothalamus of 19 day old embryonic rat pups [150]. These cells were immortalized by retrovirus-mediated transfer of the SV40 large T antigen gene and screened for expression of corticotrophin releasing hormone (CRH). The IVB clone cell line was used in this study because of its CRH-like immunoreactivity and expression of

CRH, CRH receptor, vasopressin (VP) and the neuronal marker, microtubule-associated protein-2 (MAP-2). The ability of the IVB cells to express CRH led us to believe that these cells represented a reasonably good model for studying stress in parvocellular neurons of the hypothalamus.

Heat shock proteins (HSPs) act as molecular chaperones through their binding to misfolded proteins and refolding them to their proper state, ultimately restoring their function [291]. The specific role of the antioxidant HO-1 is to catalyze the conversion of free heme to biliverdin, which is converted to the antioxidant bilirubin via biliverdin reductase, and carbon monoxide and iron [132]. To test the effects of heat stress in the hypothalamus IVB cells, real time RT-PCR analysis of HSP70 and HO-1 (HSP32) was performed. IVB cells were exposed to 43°C heat for 15 minutes and allowed to recover following a time course from 1 to 48 hours and RNA was collected at various times. Following RNA isolation, cDNA was synthesized and real time RT-PCR was performed using rat gene-specific primers for HSP70 and HO-1 and expression was normalized to the housekeeping genes GAPDH and Arbp. A major advantage of using real time RT-PCR is the ability to quantitatively examine increases or decrease in gene expression for a particular gene. We found that by 1 hour recovery following heat stress, HSP70 and HO-1 levels were significantly increased 15-fold and 20-fold higher than control, respectively. HO-1 and HSP70 expression remained elevated until 4 hours and 8 hours of recovery, respectively. These data suggest that exposure of IVB cells to a mild heat stress of 15 minutes at 43°C is sufficient for initiating HSP gene expression, which is indicative of the heat shock response [203,359].

HO-1 protein expression was examined following exposure to 43°C for 15 minutes followed by recovery following a time course from 1 hour to 48 hours. We examined HO-1 protein expression to determine whether the increases in HO-1 gene expression we had found correlated with increased protein levels. Total protein was collected at each respective measurement time and western blot analysis was performed. HO-1 immunoreactivity was significantly elevated by 2 hours and did not return to baseline until 8 hours into recovery. These data support our gene expression data and demonstrate that brief exposure to heat stress elevates HO-1 gene and protein levels in IVB cells. HO-1 is a HSP that is involved in not only the heat shock response [100], but has also been shown to increase in response to oxidative stress [85] and recently has emerged as an oxidative stress marker [222]. These findings suggest that heat stress may be directly causing an increase in HO-1 transcription and translation or that heat stress may cause oxidative stress in the IVB cells that directly affects the levels of HO-1 in the cell.

HSF-1 is a redox-sensitive and heat-sensitive transcription factor that regulates HSP gene expression by translocating from the cytoplasm to the nucleus where HSF-1 binds to the heat shock element (HSE) located upstream of the promoter region in all HSPs. Therefore to investigate the heat shock response in IVB cells, we measured HSF-1 translocation from the cytoplasm to the nucleus over a 4 hour time span after a mild heat stress. In non-heated cells, HSF-1 was primarily located in the cytoplasm. In heat stressed cells HSF-1 immunoreactivity shifted to the nucleus as early as 15 minutes into recovery and remained in the nuclear fraction for as long as 1 hour. HSF-1 levels increased in the cytoplasm by 1 hour and remained elevated at 4 hours recovery

suggesting heat stress increases HSF-1 translation at these times. These data also suggest that HSF-1 is involved in initiating the heat shock response by 15 minutes of recovery and is involved in initiation of HSP70 and HO-1 gene expression in the IVB cells. These findings led us to believe that our heat stress model (15 minutes 43°C followed by 15 minutes recovery at 37°C) was a good representation of the heat shock response in IVB cells and was therefore used for the remainder of our study. Our findings are also consistent with previous reports that a brief intense heat is able to initiate the heat shock response [243].

To date, little is known about the cellular effects of heat stress or ischemia/reperfusion on ROS generation in the hypothalamus. To determine whether heat stress and simulated ischemia/reperfusion caused an increase in ROS generation in the hypothalamus IVB cells we used the fluorescent dye carboxy-H₂DCFDA. This cell-permeable dye has been used extensively to measure ROS generation in live cells [210]. Upon entry into the cell, the dye is cleaved by cellular esterases to a non-permeant carboxy-DCFH. In the presence of nonspecific ROS the reduced fluorescein compound (carboxy-DCFH) is oxidized and emits a bright green fluorescence at an excitation/emission of 495/529 nanometers. We also used the blue fluorescent nuclear dye Hoechst 33342 to identify the nuclei of individual cells. Cellular fluorescence was viewed on a fluorescent microscope at emission/excitation of 350/461 nanometers. The advantages of using the carboxy-H₂DCFDA dye are its sensitivity to ROS, simplicity and ability to measure ROS generation in live cells rather than fixed cells. However carboxy-H₂DCFDA does not discriminate between the various types of ROS generated.

Therefore, we could determine whether heat stress and simulated ischemia/reperfusion increased ROS generation, but not the specific nature of the ROS generated.

Examination of ROS generation in IVB cells subjected to 43°C for 15 minutes followed by 15 minutes recovery or 1 hour simulated ischemia and 2 hours simulated reperfusion was measured using carboxy-H₂DCFDA. Control IVB cells displayed nuclei that fluoresced blue but showed little green fluorescence indicating low levels of ROS accumulation in control cells. There was a marked increase in cytoplasmic green fluorescence in response to both heat stress and simulated ischemia/reperfusion. The increase in green fluorescence found in response to heat stress and simulated ischemia/reperfusion was similar to our findings in cells exposed to *t*BHP, a known inducer of ROS. In addition to the increase in ROS, morphological changes were also observed in IVB cells exposed to heat stress, simulated ischemia/reperfusion as well as *t*BHP which we believe is due to ROS interactions with cytoskeletal proteins that have been previously documented [224]. The morphological changes observed were a more rounded appearance and an overall decrease in the cytosolic region of the cells. Our findings are in line with previous evidence of heat stress and ischemia/reperfusion causing oxidative stress in the brain that may lead to neuronal damage [147,183,262]. These data suggest that heat stress and simulated ischemia/reperfusion cause oxidative stress in hypothalamus IVB cells.

The source of ROS generation in response to heat stress has traditionally been attributed to mitochondrial generation, but recent evidence suggests that other ROS generating systems, such as NADPH oxidase (NOX), may be involved [286,292,332,360,366]. This led us to investigate the role of the mitochondria and/or

NOX in heat stress-induced ROS generation in IVB cells by using the mitochondrial inhibitor rotenone and the NOX inhibitor apocynin. IVB cells were treated for one hour with either apocynin (300 μ M) or rotenone (100 nM) prior to 15 minutes of 43°C heat exposure and ROS generation was measured using the carboxy-H₂DCFDA fluorescent dye. Apocynin (300 μ M) and rotenone (100 nM) alone did not cause a change in ROS generation in IVB cells. Pretreatment with apocynin (300 μ M), but not rotenone (100 nM) attenuated the increase in green fluorescence in response to heat stress. Cell morphology in heat stressed cells pretreated with apocynin mimicked non-heated cells with their stellate appearance, suggesting ROS generated by heat stress may play a role in cytoskeletal rearrangement consistent with a previous investigation [224]. Taken together, these data suggest that the increase in ROS accumulation in response to heat stress in IVB cells is mediated by NOX.

The involvement of NOX in the increase in ROS accumulation in response to simulated ischemia/reperfusion was also determined by examining the effects of apocynin on ROS generation in IVB cells following simulated ischemia/reperfusion. Similar to that seen with heat stress, treatment with the NOX inhibitor apocynin (300 μ M) reduced ROS generation in cells exposed to simulated ischemia/reperfusion. Evidence supporting our simulated ischemia/reperfusion data include a study performed by Wang *et al.* who reported that the NOX inhibitor apocynin protected gerbils from global ischemia/reperfusion-induced ROS generation in the hippocampus [330]. These data along with the heat stress data suggest that both heat stress and simulated ischemia/reperfusion appear to generate ROS through NOX in IVB cells.

NOX activity has traditionally been measured using the lucigenin-enhanced chemiluminescent assay [83]. Therefore, we used this assay to further examine the involvement of NOX in heat- and simulated ischemia/reperfusion-induced ROS generation. The chemiluminescent assay utilizes the exogenously added compound lucigenin and the substrate NADPH to measure NOX activity in whole cells. NOX produces superoxide in the presence of oxygen and NADPH and this assay measures NADPH-dependent superoxide generation as a measure of NOX activity. Lucigenin is a cell-permeable compound that binds specifically to superoxide releasing a photon. Photons are measured on a TD-20/20 luminometer and the amount of light generated is expressed as relative light units (RLUs). This method is considered a reliable and sensitive method for measuring NOX activity in cells and tissues [83].

NOX activity was measured in IVB cells exposed to heat stress and simulated ischemia/reperfusion. The measurement of NOX activity was carried out at exactly the same time following heat stress or simulated ischemia/reperfusion in every case. In these experiments, we were measuring basal NOX activity in either non-stimulated or heat stress and simulated ischemia/reperfusion exposed cells. To account for changes in cell number between samples, cells were counted on a hemocytometer following each assay and normalized to 10^5 cells. Chemiluminescence in IVB cells in the absence of lucigenin and NADPH was undetectable. Chemiluminescence in control IVB cells in the presence of NADPH and lucigenin was measurable and reproducible both within and between experiments and was used to define basal NOX activity. Exposure of IVB cells to heat stress and simulated ischemia/reperfusion caused a significant increase in chemiluminescence in the presence of NADPH compared to control cells.

Chemiluminescence was not different in control, heat stressed or simulated ischemia/reperfused cells prior to the addition of NADPH. These data suggest that heat stress and simulated ischemia/reperfusion increase NOX activity in IVB cells.

To help establish that the increase in chemiluminescence was due to an increase in NOX activity, the NOX inhibitors apocynin and diphenylene iodonium (DPI) were used. Apocynin (300 μ M) and DPI (1 μ M) have been previously shown to inhibit NOX at these concentrations [211,213]. Pretreatment with the NOX inhibitors apocynin (300 μ M) and DPI (1 μ M) significantly attenuated chemiluminescence in response to heat stress and simulated ischemia/reperfusion. Interestingly, treatment with DPI (1 μ M) alone or prior to heat stress and simulated ischemia/reperfusion reduced chemiluminescence to undetectable levels. Therefore, DPI appears to be a more potent nonspecific NOX oxidase inhibitor and has been reported to block an array of ROS generating enzymes other than NOX, including mitochondrial complex I [189], nitric oxide synthase [295], cyclooxygenase and xanthine oxidase [263]. Taken together, these data suggest that heat stress and simulated ischemia/reperfusion increase NOX activity that appears to be responsible for the increase in ROS generation.

The NOX family consists of seven homologues appropriately named NOX1-5 and Duox 1-2 that are involved in ROS generation in many tissues throughout the body [28,66], but their expression in hypothalamic neurons has not been investigated. Therefore, the gene expression of NOX1-5 and the NOX regulatory subunit Rac1 were examined in the IVB cells to identify the possible isoform(s) responsible for ROS generation in response to heat stress and simulated ischemia/reperfusion. Duox1 and Duox2 were not tested because they are primarily found in the thyroid where they have a

specialized role in maintaining normal thyroid function [218,323]. Rac1 is a small GTPase that is involved in regulating NOX activation and ROS generation [93]. Rac1 expression was examined in IVB cells to explore the possibility that Rac1 may be involved in regulating NOX activity in response to heat stress and simulated ischemia/reperfusion. To characterize the expression of the NOX1-5 in IVB cells, multiple rat gene-specific primers were designed for each NOX isoform and Rac1 using Vector NTI (Invitrogen) and were used with cDNA synthesized from control IVB total RNA to perform RT-PCR analysis. Rac1 is ubiquitously expressed [176] and was found to be expressed in our IVB cells. PCR analysis of NOX1-5 showed the presence of only NOX4 in IVB cells. NOX1, NOX3 and NOX5 were not detected. Initially a faint band for NOX2 was found in the IVB cells, but upon further RT-PCR analysis of NOX2 and NOX4, NOX2 was not found in the IVB cells. To ensure there was not a problem with the designed primers, RT-PCR analysis was also performed in rat hearts in which both NOX2 and NOX4 have been reported [184]. The presence of NOX2 and NOX4 was confirmed in rat hearts, but only NOX4 was detected in IVB cells.

The PCR product for NOX4 and from the faint band corresponding to NOX2 were also cloned and sequenced for verification of expression. The sequence analysis along with BLAST searches revealed the NOX2 band we had initially detected contained only vector sequence suggesting that NOX2 was not expressed in the IVB cells. The NOX4 sequence was 100% homologous with rat NOX4 (Accession # NM_053524) confirming that the gene for NOX4 is expressed in the IVB cells. NOX4 expression has been reported in brain and localized in neurons as detected by immunohistochemistry and RT-PCR [318]. Increases in ROS generation associated with NOX4 have been reported

to correlate with increases in NOX4 gene and protein expression [188] as well as increases in NOX activity in response to hypoxia [188], hyperoxia [224] and insulin [200]. However, we did not find changes in gene expression for any of the NOX isoforms in IVB cells exposed to heat stress and simulated ischemia/reperfusion when we examined this effect using real time RT-PCR. These results may be due to the acute stresses used in our study which were unable to alter NOX4 expression, but were able to cause increases in NOX4 activity. The lack of NOX2 expression in IVB cells was a bit of a surprise because the hypothalamus has been reported to express NOX1-3 [67,149] and neurons in areas of the brain other than the hypothalamus have been shown to express NOX1-4 [112]. However, studies in the hypothalamus only examined histological sections of the hypothalamus which contain neurons, astrocytes and endothelial cells and the observed NOX2 expression could arise from any one of these cell types.

The protein expression of NOX2 and NOX4 was also examined to further characterize NOX expression in IVB cells. Western blot analysis using NOX2 and NOX4 antibodies in IVB cells and rat brain was performed. Rat brain was used as a control reference tissue because it has been previously reported to express NOX1-4 [112]. In the rat brain, NOX2 and NOX4 immunoreactivity was detected at the appropriate molecular weights (91 kDa and 70 kDa, respectively) suggesting the antibodies for NOX2 and NOX4 were valid. In IVB cells, only NOX4 immunoreactivity was detected which supports our gene expression and sequencing data. These data show that NOX4 appears to be the only NOX isoform expressed in IVB cells. The prototypical

gp91^{phox} (Nox2) was not found to be expressed in these cells, which suggests a potentially specialized role for NOX4 in the IVB cells.

NOX4 expression has been reported to reside in the cytoplasm [206], perinuclear membrane, endoplasmic reticulum (ER) and plasma membrane in smooth muscle and endothelial cells [169,296]. Following the identification of the NOX4 protein, we also examined the cellular location of NOX4 in IVB cells. Nuclear, cytoplasmic and membrane fractions were isolated and NOX4 immunoreactivity was determined. NOX4 immunoreactivity was detected in all the fractions collected although it revealed the darkest band in the cytoplasmic fraction, which was not affected by heat stress or simulated ischemia/reperfusion exposure. Therefore NOX4 appears to have a wide distribution in hypothalamus IVB cells. This could be explained by the fact that NOX4 is the only isoform found in IVB cells and must be located in multiple compartments of the cell to generate ROS which perform specialized roles throughout the cell [18,140,278].

Recent evidence suggests a PKC-mediated mechanism for the activation of NOX in neuronal [56], endothelial [214], cardiac [270], vascular smooth muscle [175], and mesangial [308] cells in response to various stimuli. The PKC inhibitors Gö6976 and Ro-31-8220 were used to determine whether PKC was involved in ROS generation in response to heat stress and simulated ischemia/reperfusion. The PKC inhibitors used inhibit various isoforms of PKC shown in table 3 and were tested to narrow down the PKC isoform responsible for ROS generation following heat stress and simulated ischemia/reperfusion. We found Gö6976 (5 nM) and Ro-31-8220 (5 nM) inhibited heat- and simulated ischemia/reperfusion-induced ROS generation to near control levels. At these concentrations Gö6976 inhibits PKC α , PKC β and PKC μ and Ro-31-8220 inhibits

PKC α , PKC β , PKC ϵ and PKC γ . These experiments suggest that at least one isoform of PKC is responsible for ROS generation in response to heat stress and simulated ischemia/reperfusion in IVB cells. Heat stress and ischemia/reperfusion have been shown to activate PKC [47] and NOX [146] individually, but no one has examined whether there is a connection between PKC activation and NOX activation. In this study, we report that PKC is involved in ROS generation in response to heat stress and simulated ischemia/reperfusion in IVB cells. To further investigate the role of PKC in ROS generation, we tested the ability of the PKC inhibitors Gö6976, Ro-31-8220, rottlerin and calphostin C to inhibit heat- and simulated ischemia/reperfusion-induced NOX activation using chemiluminescence. PMA treatment was used as a positive control for these NOX activity studies. PMA has been reported to activate both the conventional and novel PKC isoforms that activate NOX [357]. Prior to testing Gö6976 and calphostin C, dose response curves were performed to identify the lowest concentration of inhibitor that would block NOX activity. We found that all the PKC inhibitors except rottlerin (1 μ M), which inhibits PKC δ , significantly inhibited heat- and simulated ischemia/reperfusion-induced NOX activity in hypothalamus IVB cells. The greatest inhibition we found was with calphostin c (50 nM), which inhibits both the conventional and novel PKC isoforms. These data suggest that PKC-regulated NOX activation found in response to heat stress and simulated ischemia/reperfusion involves conventional and/or novel PKC isoforms. Calphostin c (50 nM) was the only PKC inhibitor found to inhibit PMA-induced NOX activation as well, which was expected because PMA activates both conventional and novel PKC isoforms [258].

We found Gö6976 (5 nM) and Ro-31-8220 (5 nM) both caused a similar level of inhibition, suggesting the involvement of one or both of the common PKC isoforms these inhibitors block, PKC α and/or PKC β . The PKC inhibitors were able to inhibit heat-induced NOX activation to control levels, but were unable to inhibit simulated ischemia/reperfusion-induced NOX activation to control levels. These data suggest heat stress causes NOX activation in a PKC-dependent manner, whereas simulated ischemia/reperfusion causes NOX activation in a PKC-dependent and PKC-independent manner in hypothalamus IVB cells. PKC α has previously been reported to control NOX4 gene expression that caused increased ROS generation in response to PMA and VEGF suggesting a role for PKC in controlling NOX4 activity [346], but NOX4 activity was not directly measured. Here we suggest that PKC α and/or PKC β may be involved in regulating NOX4 activity in IVB cells in response to heat stress and simulated ischemia/reperfusion.

We examined the PKC isoforms expressed in control IVB cells to determine their involvement in NOX activation. RT-PCR and western blot were used to determine gene and protein expression of the PKC α , PKC β , PKC μ , PKC ϵ , PKC δ and PKC ζ in IVB cells. We found gene expression of all the isoforms tested except for PKC β . PKC β was found to be expressed in rat hearts that were used as our reference tissue. Western blot analysis of PKC α , PKC β , PKC μ , PKC ϵ , PKC δ , PKC γ and PKC ζ revealed immunoreactivity for all PKC isoforms except PKC β in the IVB cells, which was consistent with our gene expression studies. PKC ζ immunoreactivity was nearly undetectable in IVB cells, but there was a faint band detected at the correct molecular weight suggesting PKC ζ was expressed at low levels in IVB cells. Therefore, PKC α was the only isoform expressed in

the hypothalamic cells that was also inhibited by all the PKC inhibitors used. These data along with the PKC inhibitor data suggest that PKC α is responsible for NOX activation and ROS generation in response to heat stress and simulated ischemia/reperfusion.

PI3 kinase has been reported to activate NOX in phagocytes [350] and endothelial cells [82,91], but had not been tested in neurons. Heat stress and ischemia/reperfusion have been reported to activate PI3 kinase [82,191], but the role of PI3 kinase on NOX activation in response to these stressors was not examined. The PI3 kinase inhibitor LY294002 was used to determine the PKC-independent activation of NOX in response to simulated ischemia/reperfusion. IVB cells were treated for one hour with LY294002 (10 nM) alone or in combination with calphostin C (50 nM) prior to exposure to heat stress and simulated ischemia/reperfusion and NOX activity was measured. We found that LY294002 (10 nM) slightly inhibited simulated ischemia/reperfusion-induced NOX activity, while LY294002 (10 nM) in combination with the PKC inhibitor calphostin c (50 nM) blocked simulated ischemia/reperfusion-induced NOX activity. LY294002 (10 nM) had no effect on heat-induced NOX activation. Taken together, these data suggest that simulated ischemia/reperfusion, but not heat stress, requires both PKC and PI3 kinase for activation of NOX4 in IVB cells.

In summary, this study is the first to show NOX4 expression in hypothalamus IVB cells. NOX4 appears to be responsible for ROS generation in response to heat stress and simulated ischemia/reperfusion. Fluorescence microscopy and lucigenin-enhanced chemiluminescence analyses suggest that PKC is involved in the activation of NOX4 and ROS generation following heat stress and simulated ischemia/reperfusion. Gene and protein expression analyses along with our PKC inhibitor studies further suggest that

PKC α is involved in NOX4 activation in the IVB cells. Simulated ischemia/reperfusion was also found to require PI3 kinase for the full activation of NOX4, whereas heat stress appeared to be totally dependent on PKC for activation of NOX4. From these data it is concluded that ROS generated by heat stress and simulated ischemia/reperfusion is through PKC α -mediated NOX4 activation and simulated ischemia/reperfusion also requires PI3 kinase for complete activation of NOX4 in hypothalamus IVB cells.

CONCLUSION

From these data it is concluded that ROS generated by heat stress and simulated ischemia/reperfusion in hypothalamic neurons is through PKC α -mediated NOX4 activation. Along with PKC, simulated ischemia/reperfusion also requires PI3 kinase for complete activation of NOX4 and ROS generation. Further studies are necessary to confirm these findings and explore the PKC-dependent mechanism of NOX4 activation and the role of ROS generated from NOX in response to heat stress and simulated ischemia/reperfusion. However, our findings reveal a common mechanism for ROS generation in the hypothalamus that is a potential target for regulating oxidative stress caused by heat-related illnesses and stroke that can lead to neuronal dysfunction.

REFERENCES

- [1] Abdala-Valencia, H. and Cook-Mills, J.M., VCAM-1 signals activate endothelial cell protein kinase Calpha via oxidation, *J Immunol*, 177 (2006) 6379-87.
- [2] Abo, A., Pick, E., Hall, A., Totty, N., Teahan, C.G. and Segal, A.W., Activation of the NADPH oxidase involves the small GTP-binding protein p21rac1, *Nature*, 353 (1991) 668-70.
- [3] Abramov, A.Y., Canevari, L. and Duchen, M.R., Calcium signals induced by amyloid beta peptide and their consequences in neurons and astrocytes in culture, *Biochim Biophys Acta*, 1742 (2004) 81-7.
- [4] Abramov, A.Y. and Duchen, M.R., The role of an astrocytic NADPH oxidase in the neurotoxicity of amyloid beta peptides, *Philos Trans R Soc Lond B Biol Sci*, 360 (2005) 2309-14.
- [5] Abramov, A.Y., Jacobson, J., Wientjes, F., Hothersall, J., Canevari, L. and Duchen, M.R., Expression and modulation of an NADPH oxidase in mammalian astrocytes, *J Neurosci*, 25 (2005) 9176-84.
- [6] Abramov, A.Y., Scorziello, A. and Duchen, M.R., Three distinct mechanisms generate oxygen free radicals in neurons and contribute to cell death during anoxia and reoxygenation, *J Neurosci*, 27 (2007) 1129-38.
- [7] Adamczyk, A., Kazmierczak, A. and Strosznajder, J.B., Alpha-synuclein and its neurotoxic fragment inhibit dopamine uptake into rat striatal synaptosomes. Relationship to nitric oxide, *Neurochem Int*, 49 (2006) 407-12.
- [8] Adi, S., Wu, N.Y. and Rosenthal, S.M., Growth factor-stimulated phosphorylation of Akt and p70(S6K) is differentially inhibited by LY294002 and Wortmannin, *Endocrinology*, 142 (2001) 498-501.
- [9] Ago, T., Kitazono, T., Kuroda, J., Kumai, Y., Kamouchi, M., Ooboshi, H., Wakisaka, M., Kawahara, T., Rokutan, K., Ibayashi, S. and Iida, M., NAD(P)H oxidases in rat basilar arterial endothelial cells, *Stroke*, 36 (2005) 1040-6.
- [10] Al-Mehdi, A.B., Zhao, G., Dodia, C., Tozawa, K., Costa, K., Muzykantov, V., Ross, C., Blecha, F., Dinauer, M. and Fisher, A.B., Endothelial NADPH oxidase as the source of oxidants in lungs exposed to ischemia or high K⁺, *Circ Res*, 83 (1998) 730-7.
- [11] Alexandrova, M.L. and Bochev, P.G., Oxidative stress during the chronic phase after stroke, *Free Radic Biol Med*, 39 (2005) 297-316.
- [12] Alm, P., Sharma, H.S., Sjoquist, P.O. and Westman, J., A new antioxidant compound H-290/51 attenuates nitric oxide synthase and heme oxygenase expression following hyperthermic brain injury. An experimental study using immunohistochemistry in the rat, *Amino Acids*, 19 (2000) 383-94.

- [13] Amarenco, P., Benavente, O., Goldstein, L.B., Callahan, A., 3rd, Sillesen, H., Hennerici, M.G., Gilbert, S., Rudolph, A.E., Simunovic, L., Zivin, J.A. and Welch, K.M., Results of the Stroke Prevention by Aggressive Reduction in Cholesterol Levels (SPARCL) Trial by Stroke Subtypes, *Stroke* (2009).
- [14] Ambasta, R.K., Kumar, P., Griendling, K.K., Schmidt, H.H., Busse, R. and Brandes, R.P., Direct interaction of the novel Nox proteins with p22phox is required for the formation of a functionally active NADPH oxidase, *J Biol Chem*, 279 (2004) 45935-41.
- [15] Ando, M., Katagiri, K., Yamamoto, S., Wakamatsu, K., Kawahara, I., Asanuma, S., Usuda, M. and Sasaki, K., Age-related effects of heat stress on protective enzymes for peroxides and microsomal monooxygenase in rat liver, *Environ Health Perspect*, 105 (1997) 726-33.
- [16] Arbiser, J.L., Petros, J., Klafter, R., Govindajaran, B., McLaughlin, E.R., Brown, L.F., Cohen, C., Moses, M., Kilroy, S., Arnold, R.S. and Lambeth, J.D., Reactive oxygen generated by Nox1 triggers the angiogenic switch, *Proc Natl Acad Sci U S A*, 99 (2002) 715-20.
- [17] Asahi, M., Asahi, K., Wang, X. and Lo, E.H., Reduction of tissue plasminogen activator-induced hemorrhage and brain injury by free radical spin trapping after embolic focal cerebral ischemia in rats, *J Cereb Blood Flow Metab*, 20 (2000) 452-7.
- [18] Atkins, C.M. and Sweatt, J.D., Reactive oxygen species mediate activity-dependent neuron-glia signaling in output fibers of the hippocampus, *J Neurosci*, 19 (1999) 7241-8.
- [19] Baldino, F., Jr. and Geller, H.M., Electrophysiological analysis of neuronal thermosensitivity in rat preoptic and hypothalamic tissue cultures, *J Physiol*, 327 (1982) 173-84.
- [20] Banfi, B., Clark, R.A., Steger, K. and Krause, K.H., Two novel proteins activate superoxide generation by the NADPH oxidase NOX1, *J Biol Chem*, 278 (2003) 3510-3.
- [21] Banfi, B., Malgrange, B., Knisz, J., Steger, K., Dubois-Dauphin, M. and Krause, K.H., NOX3, a superoxide-generating NADPH oxidase of the inner ear, *J Biol Chem*, 279 (2004) 46065-72.
- [22] Banfi, B., Molnar, G., Maturana, A., Steger, K., Hegedus, B., Demarex, N. and Krause, K.H., A Ca(2+)-activated NADPH oxidase in testis, spleen, and lymph nodes, *J Biol Chem*, 276 (2001) 37594-601.
- [23] Banfi, B., Tirone, F., Durussel, I., Knisz, J., Moskwa, P., Molnar, G.Z., Krause, K.H. and Cox, J.A., Mechanism of Ca²⁺ activation of the NADPH oxidase 5 (NOX5), *J Biol Chem*, 279 (2004) 18583-91.
- [24] Barnett, M.E., Madgwick, D.K. and Takemoto, D.J., Protein kinase C as a stress sensor, *Cell Signal*, 19 (2007) 1820-9.
- [25] Barry-Lane, P.A., Patterson, C., van der Merwe, M., Hu, Z., Holland, S.M., Yeh, E.T. and Runge, M.S., p47phox is required for atherosclerotic lesion progression in ApoE(-/-) mice, *J Clin Invest*, 108 (2001) 1513-22.
- [26] Bautista, J., Corpas, R., Ramos, R., Cremades, O., Gutierrez, J.F. and Alegre, S., Brain mitochondrial complex I inactivation by oxidative modification, *Biochem Biophys Res Commun*, 275 (2000) 890-4.

- [27] Bayraktutan, U., Blayney, L. and Shah, A.M., Molecular characterization and localization of the NAD(P)H oxidase components gp91-phox and p22-phox in endothelial cells, *Arterioscler Thromb Vasc Biol*, 20 (2000) 1903-11.
- [28] Bedard, K. and Krause, K.H., The NOX family of ROS-generating NADPH oxidases: physiology and pathophysiology, *Physiol Rev*, 87 (2007) 245-313.
- [29] Benna, J.E., Dang, P.M., Gaudry, M., Fay, M., Morel, F., Hakim, J. and Gougerot-Pocidalo, M.A., Phosphorylation of the respiratory burst oxidase subunit p67(phox) during human neutrophil activation. Regulation by protein kinase C-dependent and independent pathways, *J Biol Chem*, 272 (1997) 17204-8.
- [30] Berendes, H., Bridges, R.A. and Good, R.A., A fatal granulomatosis of childhood: the clinical study of a new syndrome, *Minn Med*, 40 (1957) 309-12.
- [31] Bey, E.A., Xu, B., Bhattacharjee, A., Oldfield, C.M., Zhao, X., Li, Q., Subbulakshmi, V., Feldman, G.M., Wientjes, F.B. and Cathcart, M.K., Protein kinase C delta is required for p47phox phosphorylation and translocation in activated human monocytes, *J Immunol*, 173 (2004) 5730-8.
- [32] Bjorkman, U. and Ekholm, R., Generation of H₂O₂ in isolated porcine thyroid follicles, *Endocrinology*, 115 (1984) 392-8.
- [33] Block, M.L., Li, G., Qin, L., Wu, X., Pei, Z., Wang, T., Wilson, B., Yang, J. and Hong, J.S., Potent regulation of microglia-derived oxidative stress and dopaminergic neuron survival: substance P vs. dynorphin, *Faseb J*, 20 (2006) 251-8.
- [34] Bolander-Gouaille, C., [PS on homocysteine as a risk factor of cardiovascular disease], *Lakartidningen*, 97 (2000) 2786-7.
- [35] Borniquel, S., Valle, I., Cadenas, S., Lamas, S. and Monsalve, M., Nitric oxide regulates mitochondrial oxidative stress protection via the transcriptional coactivator PGC-1alpha, *Faseb J*, 20 (2006) 1889-91.
- [36] Boulant, J.A., Role of the preoptic-anterior hypothalamus in thermoregulation and fever, *Clin Infect Dis*, 31 Suppl 5 (2000) S157-61.
- [37] Boulant, J.A. and Demieville, H.N., Responses of thermosensitive preoptic and septal neurons to hippocampal and brain stem stimulation, *J Neurophysiol*, 40 (1977) 1356-68.
- [38] Boulant, J.A. and Gonzalez, R.R., The effect of skin temperature on the hypothalamic control of heat loss and heat production, *Brain Res*, 120 (1977) 367-72.
- [39] Brar, S.S., Corbin, Z., Kennedy, T.P., Hemendinger, R., Thornton, L., Bommarius, B., Arnold, R.S., Whorton, A.R., Sturrock, A.B., Huecksteadt, T.P., Quinn, M.T., Krenitsky, K., Ardie, K.G., Lambeth, J.D. and Hoidal, J.R., NOX5 NAD(P)H oxidase regulates growth and apoptosis in DU 145 prostate cancer cells, *Am J Physiol Cell Physiol*, 285 (2003) C353-69.
- [40] Brar, S.S., Kennedy, T.P., Sturrock, A.B., Huecksteadt, T.P., Quinn, M.T., Whorton, A.R. and Hoidal, J.R., An NAD(P)H oxidase regulates growth and transcription in melanoma cells, *Am J Physiol Cell Physiol*, 282 (2002) C1212-24.
- [41] Brunet, A., Datta, S.R. and Greenberg, M.E., Transcription-dependent and -independent control of neuronal survival by the PI3K-Akt signaling pathway, *Curr Opin Neurobiol*, 11 (2001) 297-305.

- [42] Burdon, R.H. and Rice-Evans, C., Free radicals and the regulation of mammalian cell proliferation, *Free Radic Res Commun*, 6 (1989) 345-58.
- [43] Burritt, J.B., Busse, S.C., Gizachew, D., Siemsen, D.W., Quinn, M.T., Bond, C.W., Dratz, E.A. and Jesaitis, A.J., Antibody imprint of a membrane protein surface. Phagocyte flavocytochrome b, *J Biol Chem*, 273 (1998) 24847-52.
- [44] Cai, Z. and Semenza, G.L., Phosphatidylinositol-3-kinase signaling is required for erythropoietin-mediated acute protection against myocardial ischemia/reperfusion injury, *Circulation*, 109 (2004) 2050-3.
- [45] Campese, V.M., Sindhu, R.K., Ye, S., Bai, Y., Vaziri, N.D. and Jabbari, B., Regional expression of NO synthase, NAD(P)H oxidase and superoxide dismutase in the rat brain, *Brain Res*, 1134 (2007) 27-32.
- [46] Cardell, M., Boris-Moller, F. and Wieloch, T., Hypothermia prevents the ischemia-induced translocation and inhibition of protein kinase C in the rat striatum, *J Neurochem*, 57 (1991) 1814-7.
- [47] Cardell, M. and Wieloch, T., Time course of the translocation and inhibition of protein kinase C during complete cerebral ischemia in the rat, *J Neurochem*, 61 (1993) 1308-14.
- [48] Carden, D.L. and Granger, D.N., Pathophysiology of ischaemia-reperfusion injury, *J Pathol*, 190 (2000) 255-66.
- [49] Carini, R., Grazia De Cesaris, M., Splendore, R., Baldanzi, G., Nitti, M.P., Alchera, E., Filigheddu, N., Domenicotti, C., Pronzato, M.A., Graziani, A. and Albano, E., Role of phosphatidylinositol 3-kinase in the development of hepatocyte preconditioning, *Gastroenterology*, 127 (2004) 914-23.
- [50] Caro, P., Gomez, J., Sanz, A., Portero-Otin, M., Pamplona, R. and Barja, G., Effect of graded corticosterone treatment on aging-related markers of oxidative stress in rat liver mitochondria, *Biogerontology* (2006).
- [51] Cartier, L., Hartley, O., Dubois-Dauphin, M. and Krause, K.H., Chemokine receptors in the central nervous system: role in brain inflammation and neurodegenerative diseases, *Brain Res Brain Res Rev*, 48 (2005) 16-42.
- [52] Ceolotto, G., Papparella, I., Lenzini, L., Sartori, M., Mazzoni, M., Iori, E., Franco, L., Gallo, A., de Kreutzenberg, S.V., Tiengo, A., Pessina, A.C., Avogaro, A. and Semplicini, A., Insulin generates free radicals in human fibroblasts ex vivo by a protein kinase C-dependent mechanism, which is inhibited by pravastatin, *Free Radic Biol Med*, 41 (2006) 473-83.
- [53] Cham, J.L. and Badoer, E., Exposure to a hot environment can activate rostral ventrolateral medulla-projecting neurones in the hypothalamic paraventricular nucleus in conscious rats, *Exp Physiol*, 93 (2008) 64-74.
- [54] Chamulitrat, W., Stremmel, W., Kawahara, T., Rokutan, K., Fujii, H., Wingler, K., Schmidt, H.H. and Schmidt, R., A constitutive NADPH oxidase-like system containing gp91phox homologs in human keratinocytes, *J Invest Dermatol*, 122 (2004) 1000-9.
- [55] Chan, P.H., Reactive oxygen radicals in signaling and damage in the ischemic brain, *J Cereb Blood Flow Metab*, 21 (2001) 2-14.
- [56] Chan, S.H., Wang, L.L., Tseng, H.L. and Chan, J.Y., Upregulation of AT1 receptor gene on activation of protein kinase C β /nicotinamide adenine dinucleotide diphosphate oxidase/ERK1/2/c-fos signaling cascade mediates long-

- term pressor effect of angiotensin II in rostral ventrolateral medulla, *J Hypertens*, 25 (2007) 1845-61.
- [57] Chandel, N.S., McClintock, D.S., Feliciano, C.E., Wood, T.M., Melendez, J.A., Rodriguez, A.M. and Schumacker, P.T., Reactive oxygen species generated at mitochondrial complex III stabilize hypoxia-inducible factor-1 α during hypoxia: a mechanism of O₂ sensing, *J Biol Chem*, 275 (2000) 25130-8.
- [58] Chandel, N.S. and Schumacker, P.T., Cellular oxygen sensing by mitochondria: old questions, new insight, *J Appl Physiol*, 88 (2000) 1880-9.
- [59] Chang, H.R., Tsao, D.A., Wang, S.R. and Yu, H.S., Expression of nitric oxide synthases in keratinocytes after UVB irradiation, *Arch Dermatol Res*, 295 (2003) 293-6.
- [60] Chen, J.X., Zeng, H., Lawrence, M.L., Blackwell, T.S. and Meyrick, B., Angiopoietin-1-induced angiogenesis is modulated by endothelial NADPH oxidase, *Am J Physiol Heart Circ Physiol*, 291 (2006) H1563-72.
- [61] Cheng, G., Cao, Z., Xu, X., van Meir, E.G. and Lambeth, J.D., Homologs of gp91phox: cloning and tissue expression of Nox3, Nox4, and Nox5, *Gene*, 269 (2001) 131-40.
- [62] Cheng, G. and Lambeth, J.D., Alternative mRNA splice forms of NOXO1: differential tissue expression and regulation of Nox1 and Nox3, *Gene*, 356 (2005) 118-26.
- [63] Chiu, W.T., Kao, T.Y. and Lin, M.T., Increased survival in experimental rat heatstroke by continuous perfusion of interleukin-1 receptor antagonist, *Neurosci Res*, 24 (1996) 159-63.
- [64] Choi, S.H., Lee, D.Y., Kim, S.U. and Jin, B.K., Thrombin-induced oxidative stress contributes to the death of hippocampal neurons in vivo: role of microglial NADPH oxidase, *J Neurosci*, 25 (2005) 4082-90.
- [65] Chrissobolis, S. and Faraci, F.M., The role of oxidative stress and NADPH oxidase in cerebrovascular disease, *Trends Mol Med*, 14 (2008) 495-502.
- [66] Clark, R.A., Epperson, T.K. and Valente, A.J., Mechanisms of activation of NADPH oxidases, *Jpn J Infect Dis*, 57 (2004) S22-3.
- [67] Cohen, A.C., Tong, M., Wands, J.R. and de la Monte, S.M., Insulin and insulin-like growth factor resistance with neurodegeneration in an adult chronic ethanol exposure model, *Alcohol Clin Exp Res*, 31 (2007) 1558-73.
- [68] Coyoy, A., Valencia, A., Guemez-Gamboa, A. and Moran, J., Role of NADPH oxidase in the apoptotic death of cultured cerebellar granule neurons, *Free Radic Biol Med*, 45 (2008) 1056-64.
- [69] Cui, X.L., Brockman, D., Campos, B. and Myatt, L., Expression of NADPH oxidase isoform 1 (Nox1) in human placenta: involvement in preeclampsia, *Placenta*, 27 (2006) 422-31.
- [70] Davidson, J.F. and Schiestl, R.H., Mitochondrial respiratory electron carriers are involved in oxidative stress during heat stress in *Saccharomyces cerevisiae*, *Mol Cell Biol*, 21 (2001) 8483-9.
- [71] De Deken, X., Wang, D., Many, M.C., Costagliola, S., Libert, F., Vassart, G., Dumont, J.E. and Miot, F., Cloning of two human thyroid cDNAs encoding new members of the NADPH oxidase family, *J Biol Chem*, 275 (2000) 23227-33.

- [72] de la Monte, S.M. and Wands, J.R., Molecular indices of oxidative stress and mitochondrial dysfunction occur early and often progress with severity of Alzheimer's disease, *J Alzheimers Dis*, 9 (2006) 167-81.
- [73] DeLeo, F.R., Burritt, J.B., Yu, L., Jesaitis, A.J., Dinauer, M.C. and Nauseef, W.M., Processing and maturation of flavocytochrome b558 include incorporation of heme as a prerequisite for heterodimer assembly, *J Biol Chem*, 275 (2000) 13986-93.
- [74] Dhaunsi, G.S., Paintlia, M.K., Kaur, J. and Turner, R.B., NADPH oxidase in human lung fibroblasts, *J Biomed Sci*, 11 (2004) 617-22.
- [75] Dinauer, M.C., Pierce, E.A., Bruns, G.A., Curnutte, J.T. and Orkin, S.H., Human neutrophil cytochrome b light chain (p22-phox). Gene structure, chromosomal location, and mutations in cytochrome-negative autosomal recessive chronic granulomatous disease, *J Clin Invest*, 86 (1990) 1729-37.
- [76] Doussiere, J. and Vignais, P.V., Diphenylene iodonium as an inhibitor of the NADPH oxidase complex of bovine neutrophils. Factors controlling the inhibitory potency of diphenylene iodonium in a cell-free system of oxidase activation, *Eur J Biochem*, 208 (1992) 61-71.
- [77] Droge, W., Free radicals in the physiological control of cell function, *Physiol Rev*, 82 (2002) 47-95.
- [78] Duong, T.T., Antao, S., Ellis, N.A., Myers, S.J. and Witting, P.K., Supplementation with a synthetic polyphenol limits oxidative stress and enhances neuronal cell viability in response to hypoxia-re-oxygenation injury, *Brain Res*, 1219 (2008) 8-18.
- [79] Dupuy, C., Ohayon, R., Valent, A., Noel-Hudson, M.S., Deme, D. and Virion, A., Purification of a novel flavoprotein involved in the thyroid NADPH oxidase. Cloning of the porcine and human cdnas, *J Biol Chem*, 274 (1999) 37265-9.
- [80] Dusi, S., Donini, M. and Rossi, F., Mechanisms of NADPH oxidase activation: translocation of p40phox, Rac1 and Rac2 from the cytosol to the membranes in human neutrophils lacking p47phox or p67phox, *Biochem J*, 314 (Pt 2) (1996) 409-12.
- [81] Edens, W.A., Sharling, L., Cheng, G., Shapira, R., Kinkade, J.M., Lee, T., Edens, H.A., Tang, X., Sullards, C., Flaherty, D.B., Benian, G.M. and Lambeth, J.D., Tyrosine cross-linking of extracellular matrix is catalyzed by Duox, a multidomain oxidase/oxidoreductase with homology to the phagocyte oxidase subunit gp91phox, *J Cell Biol*, 154 (2001) 879-91.
- [82] El-Assal, O.N. and Besner, G.E., HB-EGF enhances restitution after intestinal ischemia/reperfusion via PI3K/Akt and MEK/ERK1/2 activation, *Gastroenterology*, 129 (2005) 609-25.
- [83] Ellmark, S.H., Dusting, G.J., Fui, M.N., Guzzo-Pernell, N. and Drummond, G.R., The contribution of Nox4 to NADPH oxidase activity in mouse vascular smooth muscle, *Cardiovasc Res*, 65 (2005) 495-504.
- [84] Emmendorffer, A., Roesler, J., Elsner, J., Raeder, E., Lohmann-Matthes, M.L. and Meier, B., Production of oxygen radicals by fibroblasts and neutrophils from a patient with x-linked chronic granulomatous disease, *Eur J Haematol*, 51 (1993) 223-7.

- [85] Erdmann, K., Grosser, N. and Schroder, H., L-methionine reduces oxidant stress in endothelial cells: role of heme oxygenase-1, ferritin, and nitric oxide, *Aaps J*, 7 (2005) E195-200.
- [86] Etoh, T., Inoguchi, T., Kakimoto, M., Sonoda, N., Kobayashi, K., Kuroda, J., Sumimoto, H. and Nawata, H., Increased expression of NAD(P)H oxidase subunits, NOX4 and p22phox, in the kidney of streptozotocin-induced diabetic rats and its reversibility by interventional insulin treatment, *Diabetologia*, 46 (2003) 1428-37.
- [87] Fan, C.Y., Katsuyama, M. and Yabe-Nishimura, C., PKCdelta mediates up-regulation of NOX1, a catalytic subunit of NADPH oxidase, via transactivation of the EGF receptor: possible involvement of PKCdelta in vascular hypertrophy, *Biochem J*, 390 (2005) 761-7.
- [88] Fassbender, K., Schmidt, R., Mossner, R., Daffertshofer, M. and Hennerici, M., Pattern of activation of the hypothalamic-pituitary-adrenal axis in acute stroke. Relation to acute confusional state, extent of brain damage, and clinical outcome, *Stroke*, 25 (1994) 1105-8.
- [89] Flanagan, S.W., Moseley, P.L. and Buettner, G.R., Increased flux of free radicals in cells subjected to hyperthermia: detection by electron paramagnetic resonance spin trapping, *FEBS Lett*, 431 (1998) 285-6.
- [90] Forteza, R., Salathe, M., Miot, F., Forteza, R. and Conner, G.E., Regulated hydrogen peroxide production by Duox in human airway epithelial cells, *Am J Respir Cell Mol Biol*, 32 (2005) 462-9.
- [91] Frey, R.S., Gao, X., Javaid, K., Siddiqui, S.S., Rahman, A. and Malik, A.B., Phosphatidylinositol 3-kinase gamma signaling through protein kinase C ζ induces NADPH oxidase-mediated oxidant generation and NF-kappaB activation in endothelial cells, *J Biol Chem*, 281 (2006) 16128-38.
- [92] Friis, M.B., Vorum, K.G. and Lambert, I.H., Volume-sensitive NADPH oxidase activity and taurine efflux in NIH3T3 mouse fibroblasts, *Am J Physiol Cell Physiol*, 294 (2008) C1552-65.
- [93] Furst, R., Brueckl, C., Kuebler, W.M., Zahler, S., Krotz, F., Gorlach, A., Vollmar, A.M. and Kiemer, A.K., Atrial natriuretic peptide induces mitogen-activated protein kinase phosphatase-1 in human endothelial cells via Rac1 and NAD(P)H oxidase/Nox2-activation, *Circ Res*, 96 (2005) 43-53.
- [94] Gao, H.M., Liu, B. and Hong, J.S., Critical role for microglial NADPH oxidase in rotenone-induced degeneration of dopaminergic neurons, *J Neurosci*, 23 (2003) 6181-7.
- [95] Gao, H.M., Liu, B., Zhang, W. and Hong, J.S., Critical role of microglial NADPH oxidase-derived free radicals in the in vitro MPTP model of Parkinson's disease, *Faseb J*, 17 (2003) 1954-6.
- [96] Geiszt, M., Kopp, J.B., Varnai, P. and Leto, T.L., Identification of renox, an NAD(P)H oxidase in kidney, *Proc Natl Acad Sci U S A*, 97 (2000) 8010-4.
- [97] Geiszt, M., Lekstrom, K. and Leto, T.L., Analysis of mRNA transcripts from the NAD(P)H oxidase 1 (Nox1) gene. Evidence against production of the NADPH oxidase homolog-1 short (NOH-1S) transcript variant, *J Biol Chem*, 279 (2004) 51661-8.

- [98] Geiszt, M., Lekstrom, K., Witta, J. and Leto, T.L., Proteins homologous to p47phox and p67phox support superoxide production by NAD(P)H oxidase 1 in colon epithelial cells, *J Biol Chem*, 278 (2003) 20006-12.
- [99] Genova, M.L., Pich, M.M., Biondi, A., Bernacchia, A., Falasca, A., Bovina, C., Formiggini, G., Parenti Castelli, G. and Lenaz, G., Mitochondrial production of oxygen radical species and the role of Coenzyme Q as an antioxidant, *Exp Biol Med (Maywood)*, 228 (2003) 506-13.
- [100] Goldbaum, O. and Richter-Landsberg, C., Stress proteins in oligodendrocytes: differential effects of heat shock and oxidative stress, *J Neurochem*, 78 (2001) 1233-42.
- [101] Goldstein, B.J., Mahadev, K. and Wu, X., Redox paradox: insulin action is facilitated by insulin-stimulated reactive oxygen species with multiple potential signaling targets, *Diabetes*, 54 (2005) 311-21.
- [102] Gordon, C.J., Thermoregulatory aspects of environmental exposure to anticholinesterase agents, *Rev Environ Health*, 11 (1996) 101-17.
- [103] Gordon, C.J. and Leon, L.R., Thermal stress and the physiological response to environmental toxicants, *Rev Environ Health*, 20 (2005) 235-63.
- [104] Gorin, Y., Ricono, J.M., Kim, N.H., Bhandari, B., Choudhury, G.G. and Abboud, H.E., Nox4 mediates angiotensin II-induced activation of Akt/protein kinase B in mesangial cells, *Am J Physiol Renal Physiol*, 285 (2003) F219-29.
- [105] Goyal, P., Weissmann, N., Rose, F., Grimminger, F., Schafers, H.J., Seeger, W. and Hanze, J., Identification of novel Nox4 splice variants with impact on ROS levels in A549 cells, *Biochem Biophys Res Commun*, 329 (2005) 32-9.
- [106] Grandvaux, N., Grizot, S., Vignais, P.V. and Dagher, M.C., The Ku70 autoantigen interacts with p40phox in B lymphocytes, *J Cell Sci*, 112 (Pt 4) (1999) 503-13.
- [107] Griendling, K.K., Novel NAD(P)H oxidases in the cardiovascular system, *Heart*, 90 (2004) 491-3.
- [108] Griendling, K.K., Minieri, C.A., Ollerenshaw, J.D. and Alexander, R.W., Angiotensin II stimulates NADH and NADPH oxidase activity in cultured vascular smooth muscle cells, *Circ Res*, 74 (1994) 1141-8.
- [109] Groemping, Y., Lapouge, K., Smerdon, S.J. and Rittinger, K., Molecular basis of phosphorylation-induced activation of the NADPH oxidase, *Cell*, 113 (2003) 343-55.
- [110] Groemping, Y. and Rittinger, K., Activation and assembly of the NADPH oxidase: a structural perspective, *Biochem J*, 386 (2005) 401-16.
- [111] Gschwendt, M., Dieterich, S., Rennecke, J., Kittstein, W., Mueller, H.J. and Johannes, F.J., Inhibition of protein kinase C mu by various inhibitors. Differentiation from protein kinase c isoenzymes, *FEBS Lett*, 392 (1996) 77-80.
- [112] Guggilam, A., Haque, M., Kerut, E.K., McIlwain, E., Lucchesi, P., Seghal, I. and Francis, J., TNF-alpha blockade decreases oxidative stress in the paraventricular nucleus and attenuates sympathoexcitation in heart failure rats, *Am J Physiol Heart Circ Physiol*, 293 (2007) H599-609.
- [113] Guidi, I., Galimberti, D., Lonati, S., Novembrino, C., Bamonti, F., Tiriticco, M., Fenoglio, C., Venturelli, E., Baron, P., Bresolin, N. and Scarpini, E., Oxidative

- imbalance in patients with mild cognitive impairment and Alzheimer's disease, *Neurobiol Aging*, 27 (2006) 262-9.
- [114] Guzy, R.D., Hoyos, B., Robin, E., Chen, H., Liu, L., Mansfield, K.D., Simon, M.C., Hammerling, U. and Schumacker, P.T., Mitochondrial complex III is required for hypoxia-induced ROS production and cellular oxygen sensing, *Cell Metab*, 1 (2005) 401-8.
- [115] Han, C.H., Freeman, J.L., Lee, T., Motalebi, S.A. and Lambeth, J.D., Regulation of the neutrophil respiratory burst oxidase. Identification of an activation domain in p67(phox), *J Biol Chem*, 273 (1998) 16663-8.
- [116] Hanna, I.R., Hilenski, L.L., Dikalova, A., Taniyama, Y., Dikalov, S., Lyle, A., Quinn, M.T., Lassegue, B. and Griendling, K.K., Functional association of nox1 with p22phox in vascular smooth muscle cells, *Free Radic Biol Med*, 37 (2004) 1542-9.
- [117] Hanrott, K., Gudmunsen, L., O'Neill, M.J. and Wonnacott, S., 6-hydroxydopamine-induced apoptosis is mediated via extracellular auto-oxidation and caspase 3-dependent activation of protein kinase Cdelta, *J Biol Chem*, 281 (2006) 5373-82.
- [118] Harada, K., Maekawa, T., Abu Shama, K.M., Yamashima, T. and Yoshida, K., Translocation and down-regulation of protein kinase C-alpha, -beta, and -gamma isoforms during ischemia-reperfusion in rat brain, *J Neurochem*, 72 (1999) 2556-64.
- [119] Harikai, N., Tomogane, K., Miyamoto, M., Shimada, K., Onodera, S. and Tashiro, S., Dynamic responses to acute heat stress between 34 degrees C and 38.5 degrees C, and characteristics of heat stress response in mice, *Biol Pharm Bull*, 26 (2003) 701-8.
- [120] Harikai, N., Tomogane, K., Sugawara, T. and Tashiro, S., Differences in hypothalamic Fos expressions between two heat stress conditions in conscious mice, *Brain Res Bull*, 61 (2003) 617-26.
- [121] Hattori, Y., Akimoto, K., Gross, S.S., Hattori, S. and Kasai, K., Angiotensin-II-induced oxidative stress elicits hypoadiponectinaemia in rats, *Diabetologia*, 48 (2005) 1066-74.
- [122] He, L., Dinger, B., Sanders, K., Hoidal, J., Obeso, A., Stensaas, L., Fidone, S. and Gonzalez, C., Effect of p47phox gene deletion on ROS production and oxygen sensing in mouse carotid body chemoreceptor cells, *Am J Physiol Lung Cell Mol Physiol*, 289 (2005) L916-24.
- [123] Heumuller, S., Wind, S., Barbosa-Sicard, E., Schmidt, H.H., Busse, R., Schroder, K. and Brandes, R.P., Apocynin is not an inhibitor of vascular NADPH oxidases but an antioxidant, *Hypertension*, 51 (2008) 211-7.
- [124] Heymes, C., Bendall, J.K., Ratajczak, P., Cave, A.C., Samuel, J.L., Hasenfuss, G. and Shah, A.M., Increased myocardial NADPH oxidase activity in human heart failure, *J Am Coll Cardiol*, 41 (2003) 2164-71.
- [125] Higashi, M., Shimokawa, H., Hattori, T., Hiroki, J., Mukai, Y., Morikawa, K., Ichiki, T., Takahashi, S. and Takeshita, A., Long-term inhibition of Rho-kinase suppresses angiotensin II-induced cardiovascular hypertrophy in rats in vivo: effect on endothelial NAD(P)H oxidase system, *Circ Res*, 93 (2003) 767-75.

- [126] Hilenski, L.L., Clempus, R.E., Quinn, M.T., Lambeth, J.D. and Griendling, K.K., Distinct subcellular localizations of Nox1 and Nox4 in vascular smooth muscle cells, *Arterioscler Thromb Vasc Biol*, 24 (2004) 677-83.
- [127] Hoffmeyer, M.R., Jones, S.P., Ross, C.R., Sharp, B., Grisham, M.B., Laroux, F.S., Stalker, T.J., Scalia, R. and Lefer, D.J., Myocardial ischemia/reperfusion injury in NADPH oxidase-deficient mice, *Circ Res*, 87 (2000) 812-7.
- [128] Holmberg, C.I., Roos, P.M., Lord, J.M., Eriksson, J.E. and Sistonen, L., Conventional and novel PKC isoenzymes modify the heat-induced stress response but are not activated by heat shock, *J Cell Sci*, 111 (Pt 22) (1998) 3357-65.
- [129] Horowitz, M., From molecular and cellular to integrative heat defense during exposure to chronic heat, *Comp Biochem Physiol A Mol Integr Physiol*, 131 (2002) 475-83.
- [130] Hsueh, C.M., Kuo, J.S. and Chen, S.F., Ischemia/reperfusion-induced changes of hypothalamic-pituitary-adrenal (HPA) activity is opioid related in Sprague-Dawley rat, *Neurosci Lett*, 349 (2003) 155-8.
- [131] Hu, B.R., Yang, Y.B. and Wieloch, T., Heat-shock inhibits protein synthesis and eIF-2 activity in cultured cortical neurons, *Neurochem Res*, 18 (1993) 1003-7.
- [132] Huang, E., Ong, W.Y., Go, M.L. and Garey, L.J., Heme oxygenase-1 activity after excitotoxic injury: immunohistochemical localization of bilirubin in neurons and astrocytes and deleterious effects of heme oxygenase inhibition on neuronal survival after kainate treatment, *J Neurosci Res*, 80 (2005) 268-78.
- [133] Huang, J., Hitt, N.D. and Kleinberg, M.E., Stoichiometry of p22-phox and gp91-phox in phagocyte cytochrome b558, *Biochemistry*, 34 (1995) 16753-7.
- [134] Hwang, J., Ing, M.H., Salazar, A., Lassegue, B., Griendling, K., Navab, M., Sevastian, A. and Hsiai, T.K., Pulsatile versus oscillatory shear stress regulates NADPH oxidase subunit expression: implication for native LDL oxidation, *Circ Res*, 93 (2003) 1225-32.
- [135] Hwang, J., Kleinhenz, D.J., Lassegue, B., Griendling, K.K., Dikalov, S. and Hart, C.M., Peroxisome proliferator-activated receptor-gamma ligands regulate endothelial membrane superoxide production, *Am J Physiol Cell Physiol*, 288 (2005) C899-905.
- [136] Iaccio, A., Collinet, C., Gesualdi, N.M. and Ammendola, R., Protein kinase C-alpha and -delta are required for NADPH oxidase activation in WKYVM-stimulated IMR90 human fibroblasts, *Arch Biochem Biophys*, 459 (2007) 288-94.
- [137] Ibi, M., Katsuyama, M., Fan, C., Iwata, K., Nishinaka, T., Yokoyama, T. and Yabe-Nishimura, C., NOX1/NADPH oxidase negatively regulates nerve growth factor-induced neurite outgrowth, *Free Radic Biol Med*, 40 (2006) 1785-95.
- [138] Imajoh-Ohmi, S., Tokita, K., Ochiai, H., Nakamura, M. and Kanegasaki, S., Topology of cytochrome b558 in neutrophil membrane analyzed by anti-peptide antibodies and proteolysis, *J Biol Chem*, 267 (1992) 180-4.
- [139] Inoguchi, T., Sonta, T., Tsubouchi, H., Etoh, T., Kakimoto, M., Sonoda, N., Sato, N., Sekiguchi, N., Kobayashi, K., Sumimoto, H., Utsumi, H. and Nawata, H., Protein kinase C-dependent increase in reactive oxygen species (ROS) production in vascular tissues of diabetes: role of vascular NAD(P)H oxidase, *J Am Soc Nephrol*, 14 (2003) S227-32.

- [140] Irani, K., Oxidant signaling in vascular cell growth, death, and survival: a review of the roles of reactive oxygen species in smooth muscle and endothelial cell mitogenic and apoptotic signaling, *Circ Res*, 87 (2000) 179-83.
- [141] Jaattela, M., Heat shock proteins as cellular lifeguards, *Ann Med*, 31 (1999) 261-71.
- [142] Javesghani, D., Magder, S.A., Barreiro, E., Quinn, M.T. and Hussain, S.N., Molecular characterization of a superoxide-generating NAD(P)H oxidase in the ventilatory muscles, *Am J Respir Crit Care Med*, 165 (2002) 412-8.
- [143] Jesaitis, A.J., Buescher, E.S., Harrison, D., Quinn, M.T., Parkos, C.A., Livesey, S. and Linner, J., Ultrastructural localization of cytochrome b in the membranes of resting and phagocytosing human granulocytes, *J Clin Invest*, 85 (1990) 821-35.
- [144] Jiang, B., Xiao, W., Shi, Y., Liu, M. and Xiao, X., Heat shock pretreatment inhibited the release of Smac/DIABLO from mitochondria and apoptosis induced by hydrogen peroxide in cardiomyocytes and C2C12 myogenic cells, *Cell Stress Chaperones*, 10 (2005) 252-62.
- [145] Jones, S.A., O'Donnell, V.B., Wood, J.D., Broughton, J.P., Hughes, E.J. and Jones, O.T., Expression of phagocyte NADPH oxidase components in human endothelial cells, *Am J Physiol*, 271 (1996) H1626-34.
- [146] Joyeux, M., Baxter, G.F., Thomas, D.L., Ribouot, C. and Yellon, D.M., Protein kinase C is involved in resistance to myocardial infarction induced by heat stress, *J Mol Cell Cardiol*, 29 (1997) 3311-9.
- [147] Kahles, T., Luedike, P., Endres, M., Galla, H.J., Steinmetz, H., Busse, R., Neumann-Haefelin, T. and Brandes, R.P., NADPH oxidase plays a central role in blood-brain barrier damage in experimental stroke, *Stroke*, 38 (2007) 3000-6.
- [148] Kamsler, A. and Segal, M., Hydrogen peroxide as a diffusible signal molecule in synaptic plasticity, *Mol Neurobiol*, 29 (2004) 167-78.
- [149] Kang, Y.M., Ma, Y., Elks, C., Zheng, J.P., Yang, Z.M. and Francis, J., Cross-talk between cytokines and renin-angiotensin in hypothalamic paraventricular nucleus in heart failure: role of nuclear factor-kappaB, *Cardiovasc Res*, 79 (2008) 671-8.
- [150] Kasckow, J., Mulchahey, J.J., Aguilera, G., Pisarska, M., Nikodemova, M., Chen, H.C., Herman, J.P., Murphy, E.K., Liu, Y., Rizvi, T.A., Dautzenberg, F.M. and Sheriff, S., Corticotropin-releasing hormone (CRH) expression and protein kinase A mediated CRH receptor signalling in an immortalized hypothalamic cell line, *J Neuroendocrinol*, 15 (2003) 521-9.
- [151] Katoh, S., Mitsui, Y., Kitani, K. and Suzuki, T., Hyperoxia induces the neuronal differentiated phenotype of PC12 cells via a sustained activity of mitogen-activated protein kinase induced by Bcl-2, *Biochem J*, 338 (Pt 2) (1999) 465-70.
- [152] Katschinski, D.M., Boos, K., Schindler, S.G. and Fandrey, J., Pivotal role of reactive oxygen species as intracellular mediators of hyperthermia-induced apoptosis, *J Biol Chem*, 275 (2000) 21094-8.
- [153] Kawahara, T., Kohjima, M., Kuwano, Y., Mino, H., Teshima-Kondo, S., Takeya, R., Tsunawaki, S., Wada, A., Sumimoto, H. and Rokutan, K., Helicobacter pylori lipopolysaccharide activates Rac1 and transcription of NADPH oxidase Nox1 and its organizer NOXO1 in guinea pig gastric mucosal cells, *Am J Physiol Cell Physiol*, 288 (2005) C450-7.

- [154] Kawahara, T., Ritsick, D., Cheng, G. and Lambeth, J.D., Point mutations in the proline-rich region of p22phox are dominant inhibitors of Nox1- and Nox2-dependent reactive oxygen generation, *J Biol Chem*, 280 (2005) 31859-69.
- [155] Kawano, T., Kunz, A., Abe, T., Girouard, H., Anrather, J., Zhou, P. and Iadecola, C., iNOS-derived NO and nox2-derived superoxide confer tolerance to excitotoxic brain injury through peroxynitrite, *J Cereb Blood Flow Metab*, 27 (2007) 1453-62.
- [156] Keller, J.N., Kindy, M.S., Holtsberg, F.W., St Clair, D.K., Yen, H.C., Germeyer, A., Steiner, S.M., Bruce-Keller, A.J., Hutchins, J.B. and Mattson, M.P., Mitochondrial manganese superoxide dismutase prevents neural apoptosis and reduces ischemic brain injury: suppression of peroxynitrite production, lipid peroxidation, and mitochondrial dysfunction, *J Neurosci*, 18 (1998) 687-97.
- [157] Kikuchi, H., Hikage, M., Miyashita, H. and Fukumoto, M., NADPH oxidase subunit, gp91(phox) homologue, preferentially expressed in human colon epithelial cells, *Gene*, 254 (2000) 237-43.
- [158] Kim, S.H., Won, S.J., Sohn, S., Kwon, H.J., Lee, J.Y., Park, J.H. and Gwag, B.J., Brain-derived neurotrophic factor can act as a pronecrotic factor through transcriptional and translational activation of NADPH oxidase, *J Cell Biol*, 159 (2002) 821-31.
- [159] Kim, S.Y., Lee, H.G., Choi, E.J., Park, K.Y. and Yang, J.H., TCDD alters PKC signaling pathways in developing neuronal cells in culture, *Chemosphere*, 67 (2007) S421-7.
- [160] Kishida, K.T., Hoeffler, C.A., Hu, D., Pao, M., Holland, S.M. and Klann, E., Synaptic plasticity deficits and mild memory impairments in mouse models of chronic granulomatous disease, *Mol Cell Biol*, 26 (2006) 5908-20.
- [161] Kiss, P.J., Knisz, J., Zhang, Y., Baltrusaitis, J., Sigmund, C.D., Thalmann, R., Smith, R.J., Verpy, E. and Banfi, B., Inactivation of NADPH oxidase organizer 1 results in severe imbalance, *Curr Biol*, 16 (2006) 208-13.
- [162] Knapp, L.T. and Klann, E., Role of reactive oxygen species in hippocampal long-term potentiation: contributory or inhibitory? *J Neurosci Res*, 70 (2002) 1-7.
- [163] Kobayashi, S., Nojima, Y., Shibuya, M. and Maru, Y., Nox1 regulates apoptosis and potentially stimulates branching morphogenesis in sinusoidal endothelial cells, *Exp Cell Res*, 300 (2004) 455-62.
- [164] Kochhar, A., Saitoh, T. and Zivin, J., Reduced protein kinase C activity in ischemic spinal cord, *J Neurochem*, 53 (1989) 946-52.
- [165] Koga, H., Terasawa, H., Nunoi, H., Takeshige, K., Inagaki, F. and Sumimoto, H., Tetratricopeptide repeat (TPR) motifs of p67(phox) participate in interaction with the small GTPase Rac and activation of the phagocyte NADPH oxidase, *J Biol Chem*, 274 (1999) 25051-60.
- [166] Koliakos, G., Befani, C., Paletas, K. and Kaloyianni, M., Effect of endothelin on sodium/hydrogen exchanger activity of human monocytes and atherosclerosis-related functions, *Ann N Y Acad Sci*, 1095 (2007) 274-91.
- [167] Krijnen, P.A., Meischl, C., Hack, C.E., Meijer, C.J., Visser, C.A., Roos, D. and Niessen, H.W., Increased Nox2 expression in human cardiomyocytes after acute myocardial infarction, *J Clin Pathol*, 56 (2003) 194-9.

- [168] Kumagai, A., Kodama, H., Kumagai, J., Fukuda, J., Kawamura, K., Tanikawa, H., Sato, N. and Tanaka, T., Xanthine oxidase inhibitors suppress testicular germ cell apoptosis induced by experimental cryptorchidism, *Mol Hum Reprod*, 8 (2002) 118-23.
- [169] Kuroda, J., Nakagawa, K., Yamasaki, T., Nakamura, K., Takeya, R., Kuribayashi, F., Imajoh-Ohmi, S., Igarashi, K., Shibata, Y., Sueishi, K. and Sumimoto, H., The superoxide-producing NAD(P)H oxidase Nox4 in the nucleus of human vascular endothelial cells, *Genes Cells*, 10 (2005) 1139-51.
- [170] Kusaka, I., Kusaka, G., Zhou, C., Ishikawa, M., Nanda, A., Granger, D.N., Zhang, J.H. and Tang, J., Role of AT1 receptors and NAD(P)H oxidase in diabetes-aggravated ischemic brain injury, *Am J Physiol Heart Circ Physiol*, 286 (2004) H2442-51.
- [171] Lafeber, F.P., Beukelman, C.J., van den Worm, E., van Roy, J.L., Vianen, M.E., van Roon, J.A., van Dijk, H. and Bijlsma, J.W., Apocynin, a plant-derived, cartilage-saving drug, might be useful in the treatment of rheumatoid arthritis, *Rheumatology (Oxford)*, 38 (1999) 1088-93.
- [172] Lapouge, K., Smith, S.J., Walker, P.A., Gamblin, S.J., Smerdon, S.J. and Rittinger, K., Structure of the TPR domain of p67phox in complex with Rac.GTP, *Mol Cell*, 6 (2000) 899-907.
- [173] Lassegue, B., Sorescu, D., Szocs, K., Yin, Q., Akers, M., Zhang, Y., Grant, S.L., Lambeth, J.D. and Griendling, K.K., Novel gp91(phox) homologues in vascular smooth muscle cells: nox1 mediates angiotensin II-induced superoxide formation and redox-sensitive signaling pathways, *Circ Res*, 88 (2001) 888-94.
- [174] Lavigne, M.C., Malech, H.L., Holland, S.M. and Leto, T.L., Genetic requirement of p47phox for superoxide production by murine microglia, *Faseb J*, 15 (2001) 285-7.
- [175] Lavrentyev, E.N. and Malik, K.U., High glucose-induced Nox1-derived superoxides downregulate PKC- β II, which subsequently decreases ACE2 expression and ANG(1-7) formation in rat VSMCs, *Am J Physiol Heart Circ Physiol*, 296 (2009) H106-18.
- [176] Lee, M., You, H.J., Cho, S.H., Woo, C.H., Yoo, M.H., Joe, E.H. and Kim, J.H., Implication of the small GTPase Rac1 in the generation of reactive oxygen species in response to beta-amyloid in C6 astrogloma cells, *Biochem J*, 366 (2002) 937-43.
- [177] Lee, N.K., Choi, Y.G., Baik, J.Y., Han, S.Y., Jeong, D.W., Bae, Y.S., Kim, N. and Lee, S.Y., A crucial role for reactive oxygen species in RANKL-induced osteoclast differentiation, *Blood*, 106 (2005) 852-9.
- [178] Lenaz, G., The mitochondrial production of reactive oxygen species: mechanisms and implications in human pathology, *IUBMB Life*, 52 (2001) 159-64.
- [179] Leon, L.R., DuBose, D.A. and Mason, C.W., Heat stress induces a biphasic thermoregulatory response in mice, *Am J Physiol Regul Integr Comp Physiol*, 288 (2005) R197-204.
- [180] Leto, T.L., Adams, A.G. and de Mendez, I., Assembly of the phagocyte NADPH oxidase: binding of Src homology 3 domains to proline-rich targets, *Proc Natl Acad Sci U S A*, 91 (1994) 10650-4.

- [181] Leusen, J.H., Fluiter, K., Hilarius, P.M., Roos, D., Verhoeven, A.J. and Bolscher, B.G., Interactions between the cytosolic components p47phox and p67phox of the human neutrophil NADPH oxidase that are not required for activation in the cell-free system, *J Biol Chem*, 270 (1995) 11216-21.
- [182] Levy, R., Rotrosen, D., Nagauker, O., Leto, T.L. and Malech, H.L., Induction of the respiratory burst in HL-60 cells. Correlation of function and protein expression, *J Immunol*, 145 (1990) 2595-601.
- [183] Li, B., Guo, Y.S., Sun, M.M., Dong, H., Wu, S.Y., Wu, D.X. and Li, C.Y., The NADPH oxidase is involved in lipopolysaccharide-mediated motor neuron injury, *Brain Res*, 1226 (2008) 199-208.
- [184] Li, H., Hortmann, M., Daiber, A., Oelze, M., Ostad, M.A., Schwarz, P.M., Xu, H., Xia, N., Kleschyov, A.L., Mang, C., Warnholtz, A., Munzel, T. and Forstermann, U., Cyclooxygenase 2-selective and nonselective nonsteroidal anti-inflammatory drugs induce oxidative stress by up-regulating vascular NADPH oxidases, *J Pharmacol Exp Ther*, 326 (2008) 745-53.
- [185] Li, J., Baud, O., Vartanian, T., Volpe, J.J. and Rosenberg, P.A., Peroxynitrite generated by inducible nitric oxide synthase and NADPH oxidase mediates microglial toxicity to oligodendrocytes, *Proc Natl Acad Sci U S A*, 102 (2005) 9936-41.
- [186] Li, J.M. and Shah, A.M., Intracellular localization and preassembly of the NADPH oxidase complex in cultured endothelial cells, *J Biol Chem*, 277 (2002) 19952-60.
- [187] Li, N., Frigerio, F. and Maechler, P., The sensitivity of pancreatic beta-cells to mitochondrial injuries triggered by lipotoxicity and oxidative stress, *Biochem Soc Trans*, 36 (2008) 930-4.
- [188] Li, S., Tabar, S.S., Malec, V., Eul, B.G., Klepetko, W., Weissmann, N., Grimminger, F., Seeger, W., Rose, F. and Hanze, J., NOX4 regulates ROS levels under normoxic and hypoxic conditions, triggers proliferation, and inhibits apoptosis in pulmonary artery adventitial fibroblasts, *Antioxid Redox Signal*, 10 (2008) 1687-98.
- [189] Li, Y. and Trush, M.A., Diphenyleneiodonium, an NAD(P)H oxidase inhibitor, also potently inhibits mitochondrial reactive oxygen species production, *Biochem Biophys Res Commun*, 253 (1998) 295-9.
- [190] Li, Y., Zhu, H. and Trush, M.A., Detection of mitochondria-derived reactive oxygen species production by the chemilumigenic probes lucigenin and luminol, *Biochim Biophys Acta*, 1428 (1999) 1-12.
- [191] Lin, R.Z., Hu, Z.W., Chin, J.H. and Hoffman, B.B., Heat shock activates c-Src tyrosine kinases and phosphatidylinositol 3-kinase in NIH3T3 fibroblasts, *J Biol Chem*, 272 (1997) 31196-202.
- [192] Lindquist, S. and Craig, E.A., The heat-shock proteins, *Annu Rev Genet*, 22 (1988) 631-77.
- [193] Liu, P.G., He, S.Q., Zhang, Y.H. and Wu, J., Protective effects of apocynin and allopurinol on ischemia/reperfusion-induced liver injury in mice, *World J Gastroenterol*, 14 (2008) 2832-7.
- [194] Loehr, A., Willms, I. and Huchzermeyer, B., A regulatory effect of the electron transport chain on the ATP synthase, *Arch Biochem Biophys*, 236 (1985) 832-40.

- [195] Love, S., Oxidative stress in brain ischemia, *Brain Pathol*, 9 (1999) 119-31.
- [196] Luo, Y. and DeFranco, D.B., Opposing roles for ERK1/2 in neuronal oxidative toxicity: distinct mechanisms of ERK1/2 action at early versus late phases of oxidative stress, *J Biol Chem*, 281 (2006) 16436-42.
- [197] Lushchak, V.I. and Bagnyukova, T.V., Temperature increase results in oxidative stress in goldfish tissues. 1. Indices of oxidative stress, *Comp Biochem Physiol C Toxicol Pharmacol*, 143 (2006) 30-5.
- [198] Lushchak, V.I. and Bagnyukova, T.V., Temperature increase results in oxidative stress in goldfish tissues. 2. Antioxidant and associated enzymes, *Comp Biochem Physiol C Toxicol Pharmacol*, 143 (2006) 36-41.
- [199] Madden, K.P., Clark, W.M., Kochhar, A. and Zivin, J.A., Effect of protein kinase C modulation on outcome of experimental CNS ischemia, *Brain Res*, 547 (1991) 193-8.
- [200] Mahadev, K., Motoshima, H., Wu, X., Ruddy, J.M., Arnold, R.S., Cheng, G., Lambeth, J.D. and Goldstein, B.J., The NAD(P)H oxidase homolog Nox4 modulates insulin-stimulated generation of H₂O₂ and plays an integral role in insulin signal transduction, *Mol Cell Biol*, 24 (2004) 1844-54.
- [201] Mander, P. and Brown, G.C., Activation of microglial NADPH oxidase is synergistic with glial iNOS expression in inducing neuronal death: a dual-key mechanism of inflammatory neurodegeneration, *J Neuroinflammation*, 2 (2005) 20.
- [202] Maridonneau-Parini, I., Clerc, J. and Polla, B.S., Heat shock inhibits NADPH oxidase in human neutrophils, *Biochem Biophys Res Commun*, 154 (1988) 179-86.
- [203] Maroni, P., Bendinelli, P., Tiberio, L., Rovetta, F., Piccoletti, R. and Schiaffonati, L., In vivo heat-shock response in the brain: signalling pathway and transcription factor activation, *Brain Res Mol Brain Res*, 119 (2003) 90-9.
- [204] Marsden, P.A., Heng, H.H., Scherer, S.W., Stewart, R.J., Hall, A.V., Shi, X.M., Tsui, L.C. and Schappert, K.T., Structure and chromosomal localization of the human constitutive endothelial nitric oxide synthase gene, *J Biol Chem*, 268 (1993) 17478-88.
- [205] Martiny-Baron, G., Kazanietz, M.G., Mischak, H., Blumberg, P.M., Kochs, G., Hug, H., Marme, D. and Schachtele, C., Selective inhibition of protein kinase C isozymes by the indolocarbazole Go 6976, *J Biol Chem*, 268 (1993) 9194-7.
- [206] Martyn, K.D., Frederick, L.M., von Loehneysen, K., Dinauer, M.C. and Knaus, U.G., Functional analysis of Nox4 reveals unique characteristics compared to other NADPH oxidases, *Cell Signal*, 18 (2006) 69-82.
- [207] Massaro, M., Habib, A., Lubrano, L., Del Turco, S., Lazzerini, G., Bourcier, T., Weksler, B.B. and De Caterina, R., The omega-3 fatty acid docosahexaenoate attenuates endothelial cyclooxygenase-2 induction through both NADP(H) oxidase and PKC epsilon inhibition, *Proc Natl Acad Sci U S A*, 103 (2006) 15184-9.
- [208] Mathew, A. and Morimoto, R.I., Role of the heat-shock response in the life and death of proteins, *Ann N Y Acad Sci*, 851 (1998) 99-111.
- [209] Matsumoto, H., Hayashi, S., Hatashita, M., Ohnishi, K., Ohtsubo, T., Kitai, R., Shioura, H., Ohnishi, T. and Kano, E., Nitric oxide is an initiator of intercellular

- signal transduction for stress response after hyperthermia in mutant p53 cells of human glioblastoma, *Cancer Res*, 59 (1999) 3239-44.
- [210] Maurer, B.J., Metelitsa, L.S., Seeger, R.C., Cabot, M.C. and Reynolds, C.P., Increase of ceramide and induction of mixed apoptosis/necrosis by N-(4-hydroxyphenyl)-retinamide in neuroblastoma cell lines, *J Natl Cancer Inst*, 91 (1999) 1138-46.
- [211] Meier, B., Cross, A.R., Hancock, J.T., Kaup, F.J. and Jones, O.T., Identification of a superoxide-generating NADPH oxidase system in human fibroblasts, *Biochem J*, 275 (Pt 1) (1991) 241-5.
- [212] Michel, V., Peinnequin, A., Alonso, A., Buguet, A., Cespuglio, R. and Canini, F., Effect of glucocorticoid depletion on heat-induced Hsp70, IL-1beta and TNF-alpha gene expression, *Brain Res*, 1164 (2007) 63-71.
- [213] Miller, A.A., Drummond, G.R., Schmidt, H.H. and Sobey, C.G., NADPH oxidase activity and function are profoundly greater in cerebral versus systemic arteries, *Circ Res*, 97 (2005) 1055-62.
- [214] Min, J.K., Kim, Y.M., Kim, S.W., Kwon, M.C., Kong, Y.Y., Hwang, I.K., Won, M.H., Rho, J. and Kwon, Y.G., TNF-related activation-induced cytokine enhances leukocyte adhesiveness: induction of ICAM-1 and VCAM-1 via TNF receptor-associated factor and protein kinase C-dependent NF-kappaB activation in endothelial cells, *J Immunol*, 175 (2005) 531-40.
- [215] Min, K.J., Pyo, H.K., Yang, M.S., Ji, K.A., Jou, I. and Joe, E.H., Gangliosides activate microglia via protein kinase C and NADPH oxidase, *Glia*, 48 (2004) 197-206.
- [216] Moe, K.T., Aulia, S., Jiang, F., Chua, Y.L., Koh, T.H., Wong, M.C. and Dusting, G.J., Differential upregulation of Nox homologues of NADPH oxidase by tumor necrosis factor-alpha in human aortic smooth muscle and embryonic kidney cells, *J Cell Mol Med*, 10 (2006) 231-9.
- [217] Mollnau, H., Wendt, M., Szocs, K., Lassegue, B., Schulz, E., Oelze, M., Li, H., Bodenschatz, M., August, M., Kleschyov, A.L., Tsilimingas, N., Walter, U., Forstermann, U., Meinertz, T., Griendling, K. and Munzel, T., Effects of angiotensin II infusion on the expression and function of NAD(P)H oxidase and components of nitric oxide/cGMP signaling, *Circ Res*, 90 (2002) E58-65.
- [218] Morand, S., Chaaoui, M., Kaniewski, J., Deme, D., Ohayon, R., Noel-Hudson, M.S., Virion, A. and Dupuy, C., Effect of iodide on nicotinamide adenine dinucleotide phosphate oxidase activity and Duox2 protein expression in isolated porcine thyroid follicles, *Endocrinology*, 144 (2003) 1241-8.
- [219] Morand, S., Dos Santos, O.F., Ohayon, R., Kaniewski, J., Noel-Hudson, M.S., Virion, A. and Dupuy, C., Identification of a truncated dual oxidase 2 (DUOX2) messenger ribonucleic acid (mRNA) in two rat thyroid cell lines. Insulin and forskolin regulation of DUOX2 mRNA levels in FRTL-5 cells and porcine thyrocytes, *Endocrinology*, 144 (2003) 567-74.
- [220] Moreno, M.U., San Jose, G., Orbe, J., Paramo, J.A., Beloqui, O., Diez, J. and Zalba, G., Preliminary characterisation of the promoter of the human p22(phox) gene: identification of a new polymorphism associated with hypertension, *FEBS Lett*, 542 (2003) 27-31.

- [221] Morimoto, R.I. and Santoro, M.G., Stress-inducible responses and heat shock proteins: new pharmacologic targets for cytoprotection, *Nat Biotechnol*, 16 (1998) 833-8.
- [222] Morse, D. and Choi, A.M., Heme oxygenase-1: the "emerging molecule" has arrived, *Am J Respir Cell Mol Biol*, 27 (2002) 8-16.
- [223] Nakayama, M., Inoguchi, T., Sonta, T., Maeda, Y., Sasaki, S., Sawada, F., Tsubouchi, H., Sonoda, N., Kobayashi, K., Sumimoto, H. and Nawata, H., Increased expression of NAD(P)H oxidase in islets of animal models of Type 2 diabetes and its improvement by an AT1 receptor antagonist, *Biochem Biophys Res Commun*, 332 (2005) 927-33.
- [224] Natarajan, V., Pendyala, S., Gorshkova, I.A., Usatyuk, P., He, D., Pennathur, A., Lambeth, J.D. and Thannickal, V.J., Role Of Nox4 And Nox2 In Hyperoxia-Induced Reactive Oxygen Species Generation And Migration Of Human Lung Endothelial Cells, *Antioxid Redox Signal* (2008).
- [225] Nauseef, W.M., Assembly of the phagocyte NADPH oxidase, *Histochem Cell Biol*, 122 (2004) 277-91.
- [226] Newburger, P.E., Ezekowitz, R.A., Whitney, C., Wright, J. and Orkin, S.H., Induction of phagocyte cytochrome b heavy chain gene expression by interferon gamma, *Proc Natl Acad Sci U S A*, 85 (1988) 5215-9.
- [227] Nie, D. and Honn, K.V., Cyclooxygenase, lipoxygenase and tumor angiogenesis, *Cell Mol Life Sci*, 59 (2002) 799-807.
- [228] Nitti, M., Furfaro, A.L., Traverso, N., Odetti, P., Storace, D., Cottalasso, D., Pronzato, M.A., Marinari, U.M. and Domenicotti, C., PKC delta and NADPH oxidase in AGE-induced neuronal death, *Neurosci Lett*, 416 (2007) 261-5.
- [229] Niu, K.C., Lin, M.T. and Chang, C.P., Hyperbaric oxygen improves survival in heatstroke rats by reducing multiorgan dysfunction and brain oxidative stress, *Eur J Pharmacol*, 569 (2007) 94-102.
- [230] Noh, K.M. and Koh, J.Y., Induction and activation by zinc of NADPH oxidase in cultured cortical neurons and astrocytes, *J Neurosci*, 20 (2000) RC111.
- [231] Nunoi, H., Rotrosen, D., Gallin, J.I. and Malech, H.L., Two forms of autosomal chronic granulomatous disease lack distinct neutrophil cytosol factors, *Science*, 242 (1988) 1298-301.
- [232] Ohshiro, Y., Ma, R.C., Yasuda, Y., Hiraoka-Yamamoto, J., Clermont, A.C., Isshiki, K., Yagi, K., Arikawa, E., Kern, T.S. and King, G.L., Reduction of diabetes-induced oxidative stress, fibrotic cytokine expression, and renal dysfunction in protein kinase Cbeta-null mice, *Diabetes*, 55 (2006) 3112-20.
- [233] Ohta, Y., Matura, T., Kitagawa, A., Tokunaga, K. and Yamada, K., Xanthine oxidase-derived reactive oxygen species contribute to the development of D-galactosamine-induced liver injury in rats, *Free Radic Res*, 41 (2007) 135-44.
- [234] Olivetta, E., Pietraforte, D., Schiavoni, I., Minetti, M., Federico, M. and Sanchez, M., HIV-1 Nef regulates the release of superoxide anions from human macrophages, *Biochem J*, 390 (2005) 591-602.
- [235] Olsson, T., Marklund, N., Gustafson, Y. and Nasman, B., Abnormalities at different levels of the hypothalamic-pituitary-adrenocortical axis early after stroke, *Stroke*, 23 (1992) 1573-6.

- [236] Orlando, G.F., Wolf, G. and Engelmann, M., Role of neuronal nitric oxide synthase in the regulation of the neuroendocrine stress response in rodents: insights from mutant mice, *Amino Acids*, 35 (2008) 17-27.
- [237] Ott, M., Gogvadze, V., Orrenius, S. and Zhivotovsky, B., Mitochondria, oxidative stress and cell death, *Apoptosis*, 12 (2007) 913-22.
- [238] Pacher, P., Nivorozhkin, A. and Szabo, C., Therapeutic effects of xanthine oxidase inhibitors: renaissance half a century after the discovery of allopurinol, *Pharmacol Rev*, 58 (2006) 87-114.
- [239] Paffenholz, R., Bergstrom, R.A., Pasutto, F., Wabnitz, P., Munroe, R.J., Jagla, W., Heinzmann, U., Marquardt, A., Bareiss, A., Laufs, J., Russ, A., Stumm, G., Schimenti, J.C. and Bergstrom, D.E., Vestibular defects in head-tilt mice result from mutations in Nox3, encoding an NADPH oxidase, *Genes Dev*, 18 (2004) 486-91.
- [240] Pagano, P.J., Chanock, S.J., Siwik, D.A., Colucci, W.S. and Clark, J.K., Angiotensin II induces p67phox mRNA expression and NADPH oxidase superoxide generation in rabbit aortic adventitial fibroblasts, *Hypertension*, 32 (1998) 331-7.
- [241] Pairet, M. and Engelhardt, G., Distinct isoforms (COX-1 and COX-2) of cyclooxygenase: possible physiological and therapeutic implications, *Fundam Clin Pharmacol*, 10 (1996) 1-17.
- [242] Pao, M., Wiggs, E.A., Anastacio, M.M., Hyun, J., DeCarlo, E.S., Miller, J.T., Anderson, V.L., Malech, H.L., Gallin, J.I. and Holland, S.M., Cognitive function in patients with chronic granulomatous disease: a preliminary report, *Psychosomatics*, 45 (2004) 230-4.
- [243] Park, H.G., Han, S.I., Oh, S.Y. and Kang, H.S., Cellular responses to mild heat stress, *Cell Mol Life Sci*, 62 (2005) 10-23.
- [244] Park, H.S., Jung, H.Y., Park, E.Y., Kim, J., Lee, W.J. and Bae, Y.S., Cutting edge: direct interaction of TLR4 with NAD(P)H oxidase 4 isozyme is essential for lipopolysaccharide-induced production of reactive oxygen species and activation of NF-kappa B, *J Immunol*, 173 (2004) 3589-93.
- [245] Park, H.S., Lee, S.H., Park, D., Lee, J.S., Ryu, S.H., Lee, W.J., Rhee, S.G. and Bae, Y.S., Sequential activation of phosphatidylinositol 3-kinase, beta Pix, Rac1, and Nox1 in growth factor-induced production of H₂O₂, *Mol Cell Biol*, 24 (2004) 4384-94.
- [246] Park, L., Anrather, J., Zhou, P., Frys, K., Pitstick, R., Younkin, S., Carlson, G.A. and Iadecola, C., NADPH-oxidase-derived reactive oxygen species mediate the cerebrovascular dysfunction induced by the amyloid beta peptide, *J Neurosci*, 25 (2005) 1769-77.
- [247] Parkos, C.A., Allen, R.A., Cochrane, C.G. and Jesaitis, A.J., Purified cytochrome b from human granulocyte plasma membrane is comprised of two polypeptides with relative molecular weights of 91,000 and 22,000, *J Clin Invest*, 80 (1987) 732-42.
- [248] Parkos, C.A., Dinauer, M.C., Walker, L.E., Allen, R.A., Jesaitis, A.J. and Orkin, S.H., Primary structure and unique expression of the 22-kilodalton light chain of human neutrophil cytochrome b, *Proc Natl Acad Sci U S A*, 85 (1988) 3319-23.

- [249] Pawate, S., Shen, Q., Fan, F. and Bhat, N.R., Redox regulation of glial inflammatory response to lipopolysaccharide and interferongamma, *J Neurosci Res*, 77 (2004) 540-51.
- [250] Pedruzzi, E., Guichard, C., Ollivier, V., Driss, F., Fay, M., Prunet, C., Marie, J.C., Pouzet, C., Samadi, M., Elbim, C., O'Dowd, Y., Bens, M., Vandewalle, A., Gougerot-Pocidalo, M.A., Lizard, G. and Ogier-Denis, E., NAD(P)H oxidase Nox-4 mediates 7-ketocholesterol-induced endoplasmic reticulum stress and apoptosis in human aortic smooth muscle cells, *Mol Cell Biol*, 24 (2004) 10703-17.
- [251] Pendyala, S., Usatyuk, P., Gorshkova, I.A., Garcia, J.G. and Natarajan, V., Regulation of NADPH Oxidase in Vascular Endothelium: The Role of Phospholipases, Protein Kinases, and Cytoskeletal Proteins, *Antioxid Redox Signal* (2008).
- [252] Perner, A., Andresen, L., Pedersen, G. and Rask-Madsen, J., Superoxide production and expression of NAD(P)H oxidases by transformed and primary human colonic epithelial cells, *Gut*, 52 (2003) 231-6.
- [253] Pi, J., Bai, Y., Zhang, Q., Wong, V., Floering, L.M., Daniel, K., Reece, J.M., Deeney, J.T., Andersen, M.E., Corkey, B.E. and Collins, S., Reactive oxygen species as a signal in glucose-stimulated insulin secretion, *Diabetes*, 56 (2007) 1783-91.
- [254] Piccoli, C., Ria, R., Scrima, R., Cela, O., D'Aprile, A., Boffoli, D., Falzetti, F., Tabilio, A. and Capitanio, N., Characterization of mitochondrial and extra-mitochondrial oxygen consuming reactions in human hematopoietic stem cells. Novel evidence of the occurrence of NAD(P)H oxidase activity, *J Biol Chem*, 280 (2005) 26467-76.
- [255] Pidgeon, G.P., Lysaght, J., Krishnamoorthy, S., Reynolds, J.V., O'Byrne, K., Nie, D. and Honn, K.V., Lipoxygenase metabolism: roles in tumor progression and survival, *Cancer Metastasis Rev*, 26 (2007) 503-24.
- [256] Pignatelli, P., Di Santo, S., Buchetti, B., Sanguigni, V., Brunelli, A. and Violi, F., Polyphenols enhance platelet nitric oxide by inhibiting protein kinase C-dependent NADPH oxidase activation: effect on platelet recruitment, *Faseb J*, 20 (2006) 1082-9.
- [257] Qin, B., Cartier, L., Dubois-Dauphin, M., Li, B., Serrander, L. and Krause, K.H., A key role for the microglial NADPH oxidase in APP-dependent killing of neurons, *Neurobiol Aging*, 27 (2006) 1577-87.
- [258] Raad, H., Pacllet, M.H., Boussetta, T., Kroviarski, Y., Morel, F., Quinn, M.T., Gougerot-Pocidalo, M.A., Dang, P.M. and El-Benna, J., Regulation of the phagocyte NADPH oxidase activity: phosphorylation of gp91phox/NOX2 by protein kinase C enhances its diaphorase activity and binding to Rac2, p67phox, and p47phox, *Faseb J* (2008).
- [259] Rao, G.N. and Berk, B.C., Active oxygen species stimulate vascular smooth muscle cell growth and proto-oncogene expression, *Circ Res*, 70 (1992) 593-9.
- [260] Reinehr, R., Becker, S., Eberle, A., Grether-Beck, S. and Haussinger, D., Involvement of NADPH oxidase isoforms and Src family kinases in CD95-dependent hepatocyte apoptosis, *J Biol Chem*, 280 (2005) 27179-94.

- [261] Reinehr, R., Gorg, B., Becker, S., Qvarthava, N., Bidmon, H.J., Selbach, O., Haas, H.L., Schliess, F. and Haussinger, D., Hypoosmotic swelling and ammonia increase oxidative stress by NADPH oxidase in cultured astrocytes and vital brain slices, *Glia*, 55 (2007) 758-71.
- [262] Riedel, W., Lang, U., Oetjen, U., Schlapp, U. and Shibata, M., Inhibition of oxygen radical formation by methylene blue, aspirin, or alpha-lipoic acid, prevents bacterial-lipopolysaccharide-induced fever, *Mol Cell Biochem*, 247 (2003) 83-94.
- [263] Rieger, J.M., Shah, A.R. and Gidday, J.M., Ischemia-reperfusion injury of retinal endothelium by cyclooxygenase- and xanthine oxidase-derived superoxide, *Exp Eye Res*, 74 (2002) 493-501.
- [264] Riganti, C., Costamagna, C., Bosia, A. and Ghigo, D., The NADPH oxidase inhibitor apocynin (acetovanillone) induces oxidative stress, *Toxicol Appl Pharmacol*, 212 (2006) 179-87.
- [265] Rinckel, L.A., Faris, S.L., Hitt, N.D. and Kleinberg, M.E., Rac1 disrupts p67phox/p40phox binding: a novel role for Rac in NADPH oxidase activation, *Biochem Biophys Res Commun*, 263 (1999) 118-22.
- [266] Robinson, J.M., Ohira, T. and Badwey, J.A., Regulation of the NADPH-oxidase complex of phagocytic leukocytes. Recent insights from structural biology, molecular genetics, and microscopy, *Histochem Cell Biol*, 122 (2004) 293-304.
- [267] Romero, J.J., Clement, P.F. and Belden, C., Neuropsychological sequelae of heat stroke: report of three cases and discussion, *Mil Med*, 165 (2000) 500-3.
- [268] Rossi, F. and Zatti, M., Biochemical aspects of phagocytosis in polymorphonuclear leucocytes. NADH and NADPH oxidation by the granules of resting and phagocytizing cells, *Experientia*, 20 (1964) 21-3.
- [269] Rouhanizadeh, M., Hwang, J., Clempus, R.E., Marcu, L., Lassegue, B., Sevanian, A. and Hsiai, T.K., Oxidized-1-palmitoyl-2-arachidonoyl-sn-glycero-3-phosphorylcholine induces vascular endothelial superoxide production: implication of NADPH oxidase, *Free Radic Biol Med*, 39 (2005) 1512-22.
- [270] Rude, M.K., Duhaney, T.A., Kuster, G.M., Judge, S., Heo, J., Colucci, W.S., Siwik, D.A. and Sam, F., Aldosterone stimulates matrix metalloproteinases and reactive oxygen species in adult rat ventricular cardiomyocytes, *Hypertension*, 46 (2005) 555-61.
- [271] Ruiz-Gines, J.A., Lopez-Ongil, S., Gonzalez-Rubio, M., Gonzalez-Santiago, L., Rodriguez-Puyol, M. and Rodriguez-Puyol, D., Reactive oxygen species induce proliferation of bovine aortic endothelial cells, *J Cardiovasc Pharmacol*, 35 (2000) 109-13.
- [272] Saeed, S.A., Shad, K.F., Saleem, T., Javed, F. and Khan, M.U., Some new prospects in the understanding of the molecular basis of the pathogenesis of stroke, *Exp Brain Res*, 182 (2007) 1-10.
- [273] Safiulina, V.F., Afzalov, R., Khiroug, L., Cherubini, E. and Giniatullin, R., Reactive oxygen species mediate the potentiating effects of ATP on GABAergic synaptic transmission in the immature hippocampus, *J Biol Chem*, 281 (2006) 23464-70.

- [274] Salles, N., Szanto, I., Herrmann, F., Armenian, B., Stumm, M., Stauffer, E., Michel, J.P. and Krause, K.H., Expression of mRNA for ROS-generating NADPH oxidases in the aging stomach, *Exp Gerontol*, 40 (2005) 353-7.
- [275] Salo, D.C., Donovan, C.M. and Davies, K.J., HSP70 and other possible heat shock or oxidative stress proteins are induced in skeletal muscle, heart, and liver during exercise, *Free Radic Biol Med*, 11 (1991) 239-46.
- [276] Santoro, M.G., Heat shock factors and the control of the stress response, *Biochem Pharmacol*, 59 (2000) 55-63.
- [277] Sauer, H., Rahimi, G., Hescheler, J. and Wartenberg, M., Effects of electrical fields on cardiomyocyte differentiation of embryonic stem cells, *J Cell Biochem*, 75 (1999) 710-23.
- [278] Sauer, H., Wartenberg, M. and Hescheler, J., Reactive oxygen species as intracellular messengers during cell growth and differentiation, *Cell Physiol Biochem*, 11 (2001) 173-86.
- [279] Segal, A.W., Jones, O.T., Webster, D. and Allison, A.C., Absence of a newly described cytochrome b from neutrophils of patients with chronic granulomatous disease, *Lancet*, 2 (1978) 446-9.
- [280] Serrano, F., Kolluri, N.S., Wientjes, F.B., Card, J.P. and Klann, E., NADPH oxidase immunoreactivity in the mouse brain, *Brain Res*, 988 (2003) 193-8.
- [281] Shan, X., Chi, L., Ke, Y., Luo, C., Qian, S., Gozal, D. and Liu, R., Manganese superoxide dismutase protects mouse cortical neurons from chronic intermittent hypoxia-mediated oxidative damage, *Neurobiol Dis*, 28 (2007) 206-15.
- [282] Sharma, H.S., Drieu, K., Alm, P. and Westman, J., Role of nitric oxide in blood-brain barrier permeability, brain edema and cell damage following hyperthermic brain injury. An experimental study using EGB-761 and Gingkolide B pretreatment in the rat, *Acta Neurochir Suppl*, 76 (2000) 81-6.
- [283] Shi, Y., Mosser, D.D. and Morimoto, R.I., Molecular chaperones as HSF1-specific transcriptional repressors, *Genes Dev*, 12 (1998) 654-66.
- [284] Shiemke, A.K., Arp, D.J. and Sayavedra-Soto, L.A., Inhibition of membrane-bound methane monooxygenase and ammonia monooxygenase by diphenyliodonium: implications for electron transfer, *J Bacteriol*, 186 (2004) 928-37.
- [285] Shimohama, S., Tanino, H., Kawakami, N., Okamura, N., Kodama, H., Yamaguchi, T., Hayakawa, T., Nunomura, A., Chiba, S., Perry, G., Smith, M.A. and Fujimoto, S., Activation of NADPH oxidase in Alzheimer's disease brains, *Biochem Biophys Res Commun*, 273 (2000) 5-9.
- [286] Shin, M.H., Moon, Y.J., Seo, J.E., Lee, Y., Kim, K.H. and Chung, J.H., Reactive oxygen species produced by NADPH oxidase, xanthine oxidase, and mitochondrial electron transport system mediate heat shock-induced MMP-1 and MMP-9 expression, *Free Radic Biol Med*, 44 (2008) 635-45.
- [287] Shiose, A., Kuroda, J., Tsuruya, K., Hirai, M., Hirakata, H., Naito, S., Hattori, M., Sakaki, Y. and Sumimoto, H., A novel superoxide-producing NAD(P)H oxidase in kidney, *J Biol Chem*, 276 (2001) 1417-23.
- [288] Shoja, M.M., Tubbs, R.S., Shokouhi, G., Loukas, M., Ghabili, K. and Ansarin, K., The potential role of carbon dioxide in the neuroimmunoendocrine changes following cerebral ischemia, *Life Sci*, 83 (2008) 381-7.

- [289] Simon, H.B., Hyperthermia, *N Engl J Med*, 329 (1993) 483-7.
- [290] Simon, H.B., Hyperthermia and heatstroke, *Hosp Pract (Off Ed)*, 29 (1994) 65-8, 73, 78-80.
- [291] Soti, C., Nagy, E., Giricz, Z., Vigh, L., Csermely, P. and Ferdinandy, P., Heat shock proteins as emerging therapeutic targets, *Br J Pharmacol*, 146 (2005) 769-80.
- [292] Starkie, R.L., Hargreaves, M., Rolland, J. and Febbraio, M.A., Heat stress, cytokines, and the immune response to exercise, *Brain Behav Immun*, 19 (2005) 404-12.
- [293] Stolk, J., Hiltermann, T.J., Dijkman, J.H. and Verhoeven, A.J., Characteristics of the inhibition of NADPH oxidase activation in neutrophils by apocynin, a methoxy-substituted catechol, *Am J Respir Cell Mol Biol*, 11 (1994) 95-102.
- [294] Strong, K., Mathers, C. and Bonita, R., Preventing stroke: saving lives around the world, *Lancet Neurol*, 6 (2007) 182-7.
- [295] Stuehr, D.J., Fasehun, O.A., Kwon, N.S., Gross, S.S., Gonzalez, J.A., Levi, R. and Nathan, C.F., Inhibition of macrophage and endothelial cell nitric oxide synthase by diphenyleioidonium and its analogs, *Faseb J*, 5 (1991) 98-103.
- [296] Sturrock, A., Huecksteadt, T.P., Norman, K., Sanders, K., Murphy, T.M., Chitano, P., Wilson, K., Hoidal, J.R. and Kennedy, T.P., Nox4 mediates TGF-beta1-induced retinoblastoma protein phosphorylation, proliferation, and hypertrophy in human airway smooth muscle cells, *Am J Physiol Lung Cell Mol Physiol*, 292 (2007) L1543-55.
- [297] Suh, S.W., Shin, B.S., Ma, H., Van Hoecke, M., Brennan, A.M., Yenari, M.A. and Swanson, R.A., Glucose and NADPH oxidase drive neuronal superoxide formation in stroke, *Ann Neurol*, 64 (2008) 654-63.
- [298] Suh, Y.A., Arnold, R.S., Lassegue, B., Shi, J., Xu, X., Sorescu, D., Chung, A.B., Griendling, K.K. and Lambeth, J.D., Cell transformation by the superoxide-generating oxidase Mox1, *Nature*, 401 (1999) 79-82.
- [299] Suliman, H.B., Ali, M. and Piantadosi, C.A., Superoxide dismutase-3 promotes full expression of the EPO response to hypoxia, *Blood*, 104 (2004) 43-50.
- [300] Sun, C., Sellers, K.W., Sumners, C. and Raizada, M.K., NAD(P)H oxidase inhibition attenuates neuronal chronotropic actions of angiotensin II, *Circ Res*, 96 (2005) 659-66.
- [301] Szanto, I., Rubbia-Brandt, L., Kiss, P., Steger, K., Banfi, B., Kovari, E., Herrmann, F., Hadengue, A. and Krause, K.H., Expression of NOX1, a superoxide-generating NADPH oxidase, in colon cancer and inflammatory bowel disease, *J Pathol*, 207 (2005) 164-76.
- [302] Szocs, K., Lassegue, B., Sorescu, D., Hilenski, L.L., Valppu, L., Couse, T.L., Wilcox, J.N., Quinn, M.T., Lambeth, J.D. and Griendling, K.K., Upregulation of Nox-based NAD(P)H oxidases in restenosis after carotid injury, *Arterioscler Thromb Vasc Biol*, 22 (2002) 21-7.
- [303] Takeya, R., Ueno, N., Kami, K., Taura, M., Kohjima, M., Izaki, T., Nunoi, H. and Sumimoto, H., Novel human homologues of p47phox and p67phox participate in activation of superoxide-producing NADPH oxidases, *J Biol Chem*, 278 (2003) 25234-46.

- [304] Tammariello, S.P., Quinn, M.T. and Estus, S., NADPH oxidase contributes directly to oxidative stress and apoptosis in nerve growth factor-deprived sympathetic neurons, *J Neurosci*, 20 (2000) RC53.
- [305] Tang, X.Q., Yu, H.M., Zhi, J.L., Cui, Y., Tang, E.H., Feng, J.Q. and Chen, P.X., Inducible nitric oxide synthase and cyclooxygenase-2 mediate protection of hydrogen peroxide preconditioning against apoptosis induced by oxidative stress in PC12 cells, *Life Sci*, 79 (2006) 870-6.
- [306] Teahan, C., Rowe, P., Parker, P., Totty, N. and Segal, A.W., The X-linked chronic granulomatous disease gene codes for the beta-chain of cytochrome b-245, *Nature*, 327 (1987) 720-1.
- [307] Tejada-Simon, M.V., Serrano, F., Villasana, L.E., Kanterewicz, B.I., Wu, G.Y., Quinn, M.T. and Klann, E., Synaptic localization of a functional NADPH oxidase in the mouse hippocampus, *Mol Cell Neurosci*, 29 (2005) 97-106.
- [308] Thallas-Bonke, V., Thorpe, S.R., Coughlan, M.T., Fukami, K., Yap, F.Y., Sourris, K.C., Penfold, S.A., Bach, L.A., Cooper, M.E. and Forbes, J.M., Inhibition of NADPH oxidase prevents advanced glycation end product-mediated damage in diabetic nephropathy through a protein kinase C-alpha-dependent pathway, *Diabetes*, 57 (2008) 460-9.
- [309] Thiels, E. and Klann, E., Hippocampal memory and plasticity in superoxide dismutase mutant mice, *Physiol Behav*, 77 (2002) 601-5.
- [310] Thiels, E., Urban, N.N., Gonzalez-Burgos, G.R., Kanterewicz, B.I., Barrionuevo, G., Chu, C.T., Oury, T.D. and Klann, E., Impairment of long-term potentiation and associative memory in mice that overexpress extracellular superoxide dismutase, *J Neurosci*, 20 (2000) 7631-9.
- [311] Tojo, T., Ushio-Fukai, M., Yamaoka-Tojo, M., Ikeda, S., Patrushev, N. and Alexander, R.W., Role of gp91phox (Nox2)-containing NAD(P)H oxidase in angiogenesis in response to hindlimb ischemia, *Circulation*, 111 (2005) 2347-55.
- [312] Touyz, R.M., Chen, X., Tabet, F., Yao, G., He, G., Quinn, M.T., Pagano, P.J. and Schiffrin, E.L., Expression of a functionally active gp91phox-containing neutrophil-type NAD(P)H oxidase in smooth muscle cells from human resistance arteries: regulation by angiotensin II, *Circ Res*, 90 (2002) 1205-13.
- [313] Tsai, N.W., Chang, W.N., Shaw, C.F., Jan, C.R., Chang, H.W., Huang, C.R., Chen, S.D., Chuang, Y.C., Lee, L.H., Wang, H.C., Lee, T.H. and Lu, C.H., Levels and value of platelet activation markers in different subtypes of acute non-cardio-embolic ischemic stroke, *Thromb Res* (2009).
- [314] Tsay, H.J., Li, H.Y., Lin, C.H., Yang, Y.L., Yeh, J.Y. and Lin, M.T., Heatstroke induces c-fos expression in the rat hypothalamus, *Neurosci Lett*, 262 (1999) 41-4.
- [315] Ueno, N., Takeya, R., Miyano, K., Kikuchi, H. and Sumimoto, H., The NADPH oxidase Nox3 constitutively produces superoxide in a p22phox-dependent manner: its regulation by oxidase organizers and activators, *J Biol Chem*, 280 (2005) 23328-39.
- [316] Ueyama, T., Geiszt, M. and Leto, T.L., Involvement of Rac1 in activation of multicomponent Nox1- and Nox3-based NADPH oxidases, *Mol Cell Biol*, 26 (2006) 2160-74.

- [317] Valko, M., Leibfritz, D., Moncol, J., Cronin, M.T., Mazur, M. and Telser, J., Free radicals and antioxidants in normal physiological functions and human disease, *Int J Biochem Cell Biol*, 39 (2007) 44-84.
- [318] Vallet, P., Charnay, Y., Steger, K., Ogier-Denis, E., Kovari, E., Herrmann, F., Michel, J.P. and Szanto, I., Neuronal expression of the NADPH oxidase NOX4, and its regulation in mouse experimental brain ischemia, *Neuroscience*, 132 (2005) 233-8.
- [319] Van Buul, J.D., Fernandez-Borja, M., Anthony, E.C. and Hordijk, P.L., Expression and localization of NOX2 and NOX4 in primary human endothelial cells, *Antioxid Redox Signal*, 7 (2005) 308-17.
- [320] Vandesompele, J., De Preter, K., Pattyn, F., Poppe, B., Van Roy, N., De Paepe, A. and Speleman, F., Accurate normalization of real-time quantitative RT-PCR data by geometric averaging of multiple internal control genes, *Genome Biol*, 3 (2002) RESEARCH0034.
- [321] Venugopal, S.K., Devaraj, S., Yang, T. and Jialal, I., Alpha-tocopherol decreases superoxide anion release in human monocytes under hyperglycemic conditions via inhibition of protein kinase C-alpha, *Diabetes*, 51 (2002) 3049-54.
- [322] Vidal, C., Gomez-Hernandez, A., Sanchez-Galan, E., Gonzalez, A., Ortega, L., Gomez-Gerique, J.A., Tunon, J. and Egido, J., Licofelone, a balanced inhibitor of cyclooxygenase and 5-lipoxygenase, reduces inflammation in a rabbit model of atherosclerosis, *J Pharmacol Exp Ther*, 320 (2007) 108-16.
- [323] Vigone, M.C., Fugazzola, L., Zamproni, I., Passoni, A., Di Candia, S., Chiumello, G., Persani, L. and Weber, G., Persistent mild hypothyroidism associated with novel sequence variants of the DUOX2 gene in two siblings, *Hum Mutat*, 26 (2005) 395.
- [324] Vilhardt, F., Plastre, O., Sawada, M., Suzuki, K., Wiznerowicz, M., Kiyokawa, E., Trono, D. and Krause, K.H., The HIV-1 Nef protein and phagocyte NADPH oxidase activation, *J Biol Chem*, 277 (2002) 42136-43.
- [325] Volpp, B.D., Nauseef, W.M. and Clark, R.A., Two cytosolic neutrophil oxidase components absent in autosomal chronic granulomatous disease, *Science*, 242 (1988) 1295-7.
- [326] Walder, C.E., Green, S.P., Darbonne, W.C., Mathias, J., Rae, J., Dinauer, M.C., Curnutte, J.T. and Thomas, G.R., Ischemic stroke injury is reduced in mice lacking a functional NADPH oxidase, *Stroke*, 28 (1997) 2252-8.
- [327] Wallach, T.M. and Segal, A.W., Analysis of glycosylation sites on gp91phox, the flavocytochrome of the NADPH oxidase, by site-directed mutagenesis and translation in vitro, *Biochem J*, 321 (Pt 3) (1997) 583-5.
- [328] Wang, D., De Deken, X., Milenkovic, M., Song, Y., Pirson, I., Dumont, J.E. and Miot, F., Identification of a novel partner of duox: EFP1, a thioredoxin-related protein, *J Biol Chem*, 280 (2005) 3096-103.
- [329] Wang, J.Y., Wen, L.L., Huang, Y.N., Chen, Y.T. and Ku, M.C., Dual effects of antioxidants in neurodegeneration: direct neuroprotection against oxidative stress and indirect protection via suppression of glia-mediated inflammation, *Curr Pharm Des*, 12 (2006) 3521-33.

- [330] Wang, Q., Tompkins, K.D., Simonyi, A., Korthuis, R.J., Sun, A.Y. and Sun, G.Y., Apocynin protects against global cerebral ischemia-reperfusion-induced oxidative stress and injury in the gerbil hippocampus, *Brain Res*, 1090 (2006) 182-9.
- [331] Wartenberg, M., Diederhagen, H., Hescheler, J. and Sauer, H., Growth stimulation versus induction of cell quiescence by hydrogen peroxide in prostate tumor spheroids is encoded by the duration of the Ca(2+) response, *J Biol Chem*, 274 (1999) 27759-67.
- [332] Wartenberg, M., Gronczynska, S., Bekhite, M.M., Saric, T., Niedermeier, W., Hescheler, J. and Sauer, H., Regulation of the multidrug resistance transporter P-glycoprotein in multicellular prostate tumor spheroids by hyperthermia and reactive oxygen species, *Int J Cancer*, 113 (2005) 229-40.
- [333] Wei, H. and Vander Heide, R.S., Heat stress activates AKT via focal adhesion kinase-mediated pathway in neonatal rat ventricular myocytes, *Am J Physiol Heart Circ Physiol*, 295 (2008) H561-8.
- [334] Wei, X.F., Zhou, Q.G., Hou, F.F., Liu, B.Y. and Liang, M., Advanced oxidation protein products induce mesangial cells perturbation through PKC-dependent activation of NADPH oxidase, *Am J Physiol Renal Physiol* (2008).
- [335] Westerheide, S.D. and Morimoto, R.I., Heat shock response modulators as therapeutic tools for diseases of protein conformation, *J Biol Chem*, 280 (2005) 33097-100.
- [336] White, C.W., Commentary on "Hypoxia, hypoxic signaling, tissue damage, and detection of reactive oxygen species (ROS)", *Free Radic Biol Med*, 40 (2006) 923-7.
- [337] White, M.G., Luca, L.E., Nonner, D., Saleh, O., Hu, B., Barrett, E.F. and Barrett, J.N., Cellular mechanisms of neuronal damage from hyperthermia, *Prog Brain Res*, 162 (2007) 347-71.
- [338] Wieloch, T., Cardell, M., Bingren, H., Zivin, J. and Saitoh, T., Changes in the activity of protein kinase C and the differential subcellular redistribution of its isozymes in the rat striatum during and following transient forebrain ischemia, *J Neurochem*, 56 (1991) 1227-35.
- [339] Wientjes, F.B., Hsuan, J.J., Totty, N.F. and Segal, A.W., p40phox, a third cytosolic component of the activation complex of the NADPH oxidase to contain src homology 3 domains, *Biochem J*, 296 (Pt 3) (1993) 557-61.
- [340] Wilkinson, B., Koenigsknecht-Talboo, J., Grommes, C., Lee, C.Y. and Landreth, G., Fibrillar beta-amyloid-stimulated intracellular signaling cascades require Vav for induction of respiratory burst and phagocytosis in monocytes and microglia, *J Biol Chem*, 281 (2006) 20842-50.
- [341] Wilkinson, S.E., Parker, P.J. and Nixon, J.S., Isoenzyme specificity of bisindolylmaleimides, selective inhibitors of protein kinase C, *Biochem J*, 294 (Pt 2) (1993) 335-7.
- [342] Wingler, K., Wunsch, S., Kreutz, R., Rothermund, L., Paul, M. and Schmidt, H.H., Upregulation of the vascular NAD(P)H-oxidase isoforms Nox1 and Nox4 by the renin-angiotensin system in vitro and in vivo, *Free Radic Biol Med*, 31 (2001) 1456-64.
- [343] Wu, C., Heat shock transcription factors: structure and regulation, *Annu Rev Cell Dev Biol*, 11 (1995) 441-69.

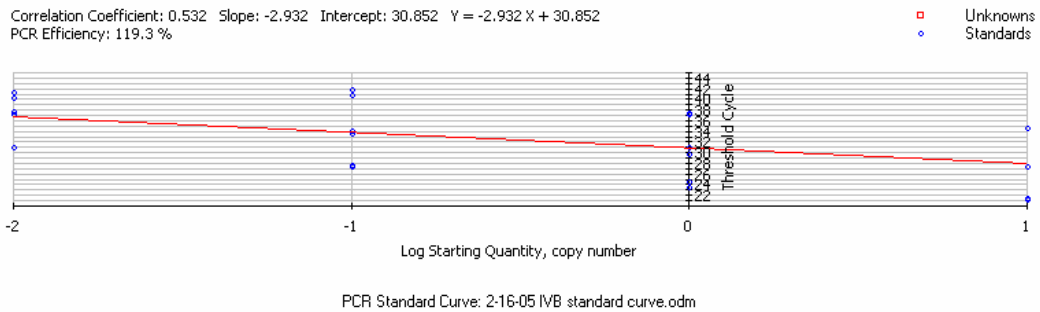
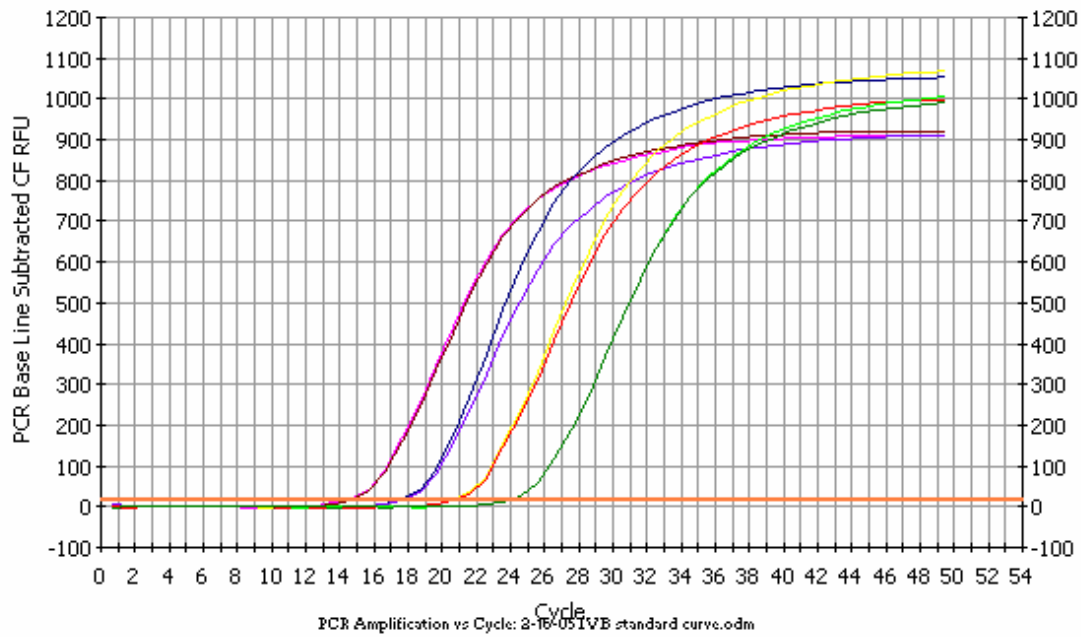
- [344] Wu, J.M., Xiao, L., Cheng, X.K., Cui, L.X., Wu, N.H. and Shen, Y.F., PKC epsilon is a unique regulator for hsp90 beta gene in heat shock response, *J Biol Chem*, 278 (2003) 51143-9.
- [345] Xia, C.F., Smith, R.S., Jr., Shen, B., Yang, Z.R., Borlongan, C.V., Chao, L. and Chao, J., Postischemic brain injury is exacerbated in mice lacking the kinin B2 receptor, *Hypertension*, 47 (2006) 752-61.
- [346] Xu, H., Goettsch, C., Xia, N., Horke, S., Morawietz, H., Forstermann, U. and Li, H., Differential roles of PKCalpha and PKCepsilon in controlling the gene expression of Nox4 in human endothelial cells, *Free Radic Biol Med*, 44 (2008) 1656-67.
- [347] Yaksh, T.L. and Myers, R.D., Hypothalamic "coding" in the unanesthetized monkey of noradrenergic sites mediating feeding and thermoregulation, *Physiol Behav*, 8 (1972) 251-7.
- [348] Yaksh, T.L. and Myers, R.D., Neurohumoral substances released from hypothalamus of the monkey during hunger and satiety, *Am J Physiol*, 222 (1972) 503-15.
- [349] Yamaguchi, T., Miki, Y. and Yoshida, K., Protein kinase C delta activates IkkappaB-kinase alpha to induce the p53 tumor suppressor in response to oxidative stress, *Cell Signal*, 19 (2007) 2088-97.
- [350] Yamamori, T., Inanami, O., Nagahata, H. and Kuwabara, M., Phosphoinositide 3-kinase regulates the phosphorylation of NADPH oxidase component p47(phox) by controlling cPKC/PKCdelta but not Akt, *Biochem Biophys Res Commun*, 316 (2004) 720-30.
- [351] Yamato, M., Egashira, T. and Utsumi, H., Application of in vivo ESR spectroscopy to measurement of cerebrovascular ROS generation in stroke, *Free Radic Biol Med*, 35 (2003) 1619-31.
- [352] Yan, Y.E., Zhao, Y.Q., Wang, H. and Fan, M., Pathophysiological factors underlying heatstroke, *Med Hypotheses*, 67 (2006) 609-17.
- [353] Yang, C.Y. and Lin, M.T., Oxidative stress in rats with heatstroke-induced cerebral ischemia, *Stroke*, 33 (2002) 790-4.
- [354] Yang, S., Madyastha, P., Bingel, S., Ries, W. and Key, L., A new superoxide-generating oxidase in murine osteoclasts, *J Biol Chem*, 276 (2001) 5452-8.
- [355] Yoo, B.K., Choi, J.W., Shin, C.Y., Jeon, S.J., Park, S.J., Cheong, J.H., Han, S.Y., Ryu, J.R., Song, M.R. and Ko, K.H., Activation of p38 MAPK induced peroxynitrite generation in LPS plus IFN-gamma-stimulated rat primary astrocytes via activation of iNOS and NADPH oxidase, *Neurochem Int*, 52 (2008) 1188-97.
- [356] Zalba, G., San Jose, G., Moreno, M.U., Fortuno, M.A., Fortuno, A., Beaumont, F.J. and Diez, J., Oxidative stress in arterial hypertension: role of NAD(P)H oxidase, *Hypertension*, 38 (2001) 1395-9.
- [357] Zawalich, W.S., Zawalich, K.C., Ganesan, S., Calle, R. and Rasmussen, H., Effects of the phorbol ester phorbol 12-myristate 13-acetate (PMA) on islet-cell responsiveness, *Biochem J*, 278 (Pt 1) (1991) 49-56.
- [358] Zekry, D., Epperson, T.K. and Krause, K.H., A role for NOX NADPH oxidases in Alzheimer's disease and other types of dementia? *IUBMB Life*, 55 (2003) 307-13.

- [359] Zhang, H.J., Doctrow, S.R., Oberley, L.W. and Kregel, K.C., Chronic antioxidant enzyme mimetic treatment differentially modulates hyperthermia-induced liver HSP70 expression with aging, *J Appl Physiol*, 100 (2006) 1385-91.
- [360] Zhang, H.J., Xu, L., Drake, V.J., Xie, L., Oberley, L.W. and Kregel, K.C., Heat-induced liver injury in old rats is associated with exaggerated oxidative stress and altered transcription factor activation, *Faseb J*, 17 (2003) 2293-5.
- [361] Zhang, W., Wang, T., Qin, L., Gao, H.M., Wilson, B., Ali, S.F., Zhang, W., Hong, J.S. and Liu, B., Neuroprotective effect of dextromethorphan in the MPTP Parkinson's disease model: role of NADPH oxidase, *Faseb J*, 18 (2004) 589-91.
- [362] Zhao, Q.L., Fujiwara, Y. and Kondo, T., Mechanism of cell death induction by nitroxide and hyperthermia, *Free Radic Biol Med*, 40 (2006) 1131-43.
- [363] Zhu, D.Y., Liu, S.H., Sun, H.S. and Lu, Y.M., Expression of inducible nitric oxide synthase after focal cerebral ischemia stimulates neurogenesis in the adult rodent dentate gyrus, *J Neurosci*, 23 (2003) 223-9.
- [364] Zimmerman, M.C., Dunlay, R.P., Lazartigues, E., Zhang, Y., Sharma, R.V., Engelhardt, J.F. and Davisson, R.L., Requirement for Rac1-dependent NADPH oxidase in the cardiovascular and dipsogenic actions of angiotensin II in the brain, *Circ Res*, 95 (2004) 532-9.
- [365] Zimmerman, M.C., Lazartigues, E., Lang, J.A., Sinnayah, P., Ahmad, I.M., Spitz, D.R. and Davisson, R.L., Superoxide mediates the actions of angiotensin II in the central nervous system, *Circ Res*, 91 (2002) 1038-45.
- [366] Zuo, L., Christofi, F.L., Wright, V.P., Liu, C.Y., Merola, A.J., Berliner, L.J. and Clanton, T.L., Intra- and extracellular measurement of reactive oxygen species produced during heat stress in diaphragm muscle, *Am J Physiol Cell Physiol*, 279 (2000) C1058-66.
- [367] Zuo, L., Pasniciuc, S., Wright, V.P., Merola, A.J. and Clanton, T.L., Sources for superoxide release: lessons from blockade of electron transport, NADPH oxidase, and anion channels in diaphragm, *Antioxid Redox Signal*, 5 (2003) 667-75.

APPENDICES

Appendix B. Real-time PCR standard curves for HSP70, HO-1, GAPDH, Arbp. The primer efficiency was determined by a standard curve of 10-fold serial dilutions of IVB cDNA. The top graph is the real-time PCR quantification graph for HSP70. The orange line is the cycle threshold (C_t), which indicates the beginning of gene copy number increasing. Each curve represents a reaction with a certain dilution of cDNA in duplicate. The curves with the lowest C_t , represent the highest concentration of cDNA. The lower graph and subsequent graphs are standard curves with cDNA concentration on the X axis and C_t on the Y axis. Each standard curve has a PCR efficiency used by the gene expression macro, and is calculated from the standard curve.

HSP70



HO-1

Correlation Coefficient: 0.758 Slope: -3.318 Intercept: 15.246 $Y = -3.318 X + 15.246$
PCR Efficiency: 100.2 %

Unknowns
Standards



Arbp

Correlation Coefficient: 0.988 Slope: -3.559 Intercept: 21.127 $Y = -3.559 X + 21.127$
PCR Efficiency: 91.0 %

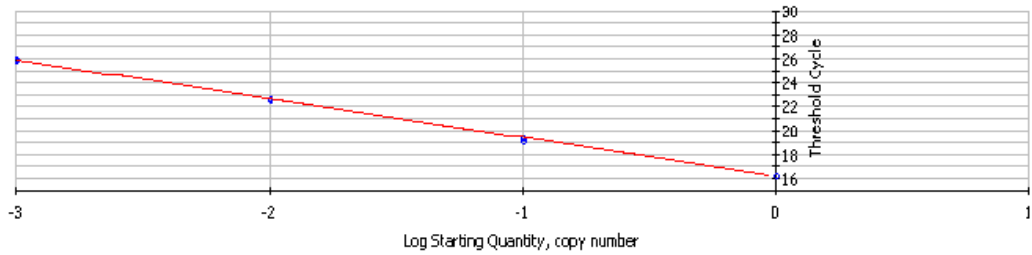
Unknowns
Standards



GAPDH

Correlation Coefficient: 0.999 Slope: -3.245 Intercept: 16.163 $Y = -3.245 X + 16.163$
PCR Efficiency: 103.3 %

Unknowns
Standards



Appendix C. Melt curve for HSP70. The single peak represents one amplicon with a distinct melting temperature T_m .

